Ocean Modelling 2 (2000) 123–192

Ocean Modelling

www.elsevier.com/locate/omodol

Developments in ocean climate modelling

Stephen M. Griffies [a,*], Claus Böning [b], Frank O. Bryan [c], Eric P. Chassignet [d], Rüdiger Gerdes [e], Hiroyasu Hasumi [f], Anthony Hirst [g], Anne-Marie Treguier [h], David Webb [i]

[a] *NOAA/GFDL, P.O. Box 308, Princeton, NJ 08542, USA*
[b] *Institut für Meereskunde an der Universität Kiel, Kiel, Germany*
[c] *National Center for Atmospheric Research, Boulder, USA*
[d] *RSMAS/MPO, University of Miami, Miami, USA*
[e] *Alfred-Wegener-Institut, Bremerhaven, Germany*
[f] *Center for Climate System Research, University of Tokyo, Tokyo, Japan*
[g] *CSIRO Atmospheric Research, Aspendale, Australia*
[h] *Laboratoire de Physique des Oceans, IFREMER, Plouzané, France*
[i] *Southampton Oceanography Centre, Southampton, UK*

Received 23 August 2000; received in revised form 2 November 2000; accepted 2 November 2000

Abstract

This paper presents some research developments in primitive equation ocean models which could impact the ocean component of realistic global coupled climate models aimed at large-scale, low frequency climate simulations and predictions. It is written primarily to an audience of modellers concerned with the ocean component of climate models, although not necessarily experts in the design and implementation of ocean model algorithms. © 2001 Elsevier Science Ltd. All rights reserved.

1. Introduction

The purpose of this paper is to present some developments in *primitive equation* ocean models which could impact the ocean component of realistic global climate models aimed at large-scale, low frequency climate simulations and predictions. It is written primarily to an audience of

* Corresponding author.
E-mail addresses: smg@gfdl.gov (S.M. Griffies), boening@ifm.uni-kiel.de (C. Böning), bryan@ncar.ucar.edu (F.O. Bryan), echassignet@rsmas.miami.edu (E.P. Chassignet), rgerdes@awi-bremerhaven.de (R. Gerdes), hasumi@ccsr.u-tokyo.ac.jp (H. Hasumi), ach@atmos.dar.csiro.au (A. Hirst), treguier@ifremer.fr (A.-M. Treguier), david.webb@soc.soton.ac.uk (D. Webb).

1463-5003/00/$ - see front matter © 2001 Elsevier Science Ltd. All rights reserved.
PII: S1463-5003(00)00014-7

modellers concerned with the ocean component of climate models, although not necessarily experts in the design and implementation of ocean model algorithms.

The authors of this paper comprise the World Climate Research Programme (WCRP)/World Ocean Circulation Experiment (WOCE) Working Group on Ocean Model Development (WGOMD) (see `http://www.ifremer.fr/lpo/WGOMD/` for details). There are various "Terms of Reference" for this working group, of which the following three provide motivation for the preparation of this document: (1) To stimulate the development of ocean models for research in climate and related fields, with a focus on decadal and longer timescales at mid- and high-latitudes. (2) To encourage investigations of the effects of model formulation on the results of ocean models, making use of sensitivity studies and intercomparisons. (3) To publicize developments in ocean models amongst the climate modelling community.

Given these mandates, we aim with this document to provide a readable account of what the authors consider to be a selected number of "Best Practices" in ocean climate modelling. We have attempted to be fair, thorough, and objective in our presentation. Given our limitations, we certainly will fail in some aspects. It is our hope that this paper will nonetheless be of use for a broad range of climate modellers, including those with minimal knowledge of ocean modelling. Quite generally, we feel it to be vital for the development of sound climate models that such efforts at communication between the various climate sub-fields be encouraged and fostered.

1.1. Representation and parameterization

Ocean climate models are tools used to numerically simulate the large space-time scales which characterize the ocean climate system. Realizing simulations of physical integrity requires both an ability to accurately *represent* the various phenomena which are resolved, and an ability to *parameterize* those scales of variability which are not resolved. For example, the representation of transport falls under the class of problems addressed by numerical advection schemes, whereas parameterizing sub-grid-scale transport is linked to turbulence closure considerations. Although there are often areas of overlap between representation and parameterization, the distinction is useful to make and it generally lies at the heart of various model development issues.

1.2. Vertical coordinates

A key characteristic of rotating and stratified fluids, such as the ocean, is the dominance of lateral over vertical transport. Hence, it is traditional in ocean modelling to orient the two horizontal coordinates orthogonal to the local vertical direction as determined by gravity. The more difficult choice is how to specify the vertical coordinate. Indeed, as noted by various ocean modelling studies such as DYNAMO (DYNAMO Group, 1997; Willebrand et al., 2000) and DAMÉE (Chassignet and Malanotte-Rizzoli, 2000; Chassignet et al., 2000), the choice of vertical coordinate system is the single most important aspect of an ocean model's design. The practical issues of representation and parameterization are often directly linked to the vertical coordinate choice. It is here where details are crucial. Currently, there are three main vertical coordinates in use, none of which provide universal utility. Hence, many developers have been motivated to pursue research into hybrid approaches, some of which are mentioned in this paper.

1.3. Contents

This paper starts in Section 2 with an overview of vertical coordinates and introduces some advantages and disadvantages of the different choices. We then discuss further numerical and physical issues of importance to ocean climate modelling. In particular, Section 3 discusses horizontal coordinates (spherical and/or generalized orthogonal), horizontal grids (Arakawa A, B, C, D, or E), and time stepping schemes in use amongst the various models. The time stepping schemes are closely tied to the discretized barotropic dynamics, which are presented in Section 4. Section 5 summarizes some developments in parameterizing the planetary boundary layer (PBL). Section 6 presents advances in representing bottom topography in z-coordinate models. Section 7 discusses the crucial problem of representing and parameterizing overflow processes in climate models. Section 8 highlights issues relevant for incorporating a realistic equation of state. Section 9 comments on the difficulties of faithfully simulating tracer transport in the ocean interior with non-isopycnal models. Section 10 points out some issues with discretizing momentum transport. Section 11 comments on research aimed at parameterizing mesoscale eddies in coarse resolution models. Section 12 summarizes the various methods used to dissipate linear momentum. Finally, Section 13 offers some closing remarks regarding trends and the need to employ higher resolution for climate modelling.

1.4. Limitations

As mentioned above, we have aimed here to present a fair treatment of the many diverse areas of activity ongoing in the ocean climate modelling community. Unfortunately, various limitations kept us from doing justice to all developments. Notably, we have chosen to focus on ocean model developments alone; the formidable issues of coupling to other component models, initialization, data assimilation, forcing, etc., are beyond our scope. Additionally, we concentrate on issues central to decadal to centennial problems, although many of the topics will be of interest for high resolution modelling as well as ocean models for coupled seasonal to interannual forecasting. Finally, we fail to provide a thorough discussion of developments with terrain following σ-coordinate models. The central reason is the absence of examples of global climate models in use with a σ-coordinate ocean. Further elaboration is given in Section 2.

As we hope to show, the field of ocean climate modelling is currently in a healthy stage of adolescence. The maturation of a field is arguably paralleled by the publication of textbooks which help to establish an intellectual base. Some books are highlighted here as they provide added discussions of many points which we can only touch on the surface. The numerical geophysical fluids book by Durran (1999) and the numerical ocean modelling books by Kowalik and Murty (1993) and Haidvogel and Beckmann (1999) are recommended for a more detailed overview of numerical modelling. Additionally, the books edited by O'Brien (1986) and Chassignet and Verron (1998) provide valuable sources of pedagogical articles on various fundamental and applied aspects of ocean climate modelling and parameterization. Finally, the recent publication of the massive two volume series by Kantha and Clayson (2000a,b) provide a significant and valuable contribution to the field.

Even with omissions and partial treatments, this paper is quite long and dense with information. To help alleviate the burden on the reader, each section is generally independent, save for a common dependence on the vertical coordinate Section 2. Additionally, the conclusion of each section provides an itemized summary of its main points. The accumulation of these summary items, as well as the points highlighted in Section 2, can serve as an "executive summary" for the document.

2. Vertical coordinate

Fig. 1 illustrates the three regimes of the ocean germane to the considerations of an appropriate vertical coordinate. First, there is the surface mixed layer. This is a region which is generally turbulent and dominated by transfers of momentum, heat, freshwater, and tracers with the overlying atmosphere, sea ice, rivers, etc., which makes it of prime importance for climate system modelling. It is typically very well-mixed in the vertical through three-dimensional convective/turbulent processes. These processes involve non-hydrostatic physics which requires very high horizontal and vertical resolution (i.e., a vertical to horizontal grid aspect ratio near unity) to explicitly represent. A parameterization of these processes is therefore necessary in primitive equation ocean models. In contrast, tracer transport processes in the ocean interior predominantly occur along constant density directions (more precisely, along neutral directions as described by McDougall, 1987a). Therefore, water mass properties in the interior tend to be preserved over large space and time scales (e.g., basin and decade scales). The ocean's bottom topography acts as a strong forcing on the overlying currents and so directly influences dynamical balances. In an unstratified ocean, the flow generally follows lines of constant f/H, where f is the Coriolis parameter and H ocean depth. In a stratified ocean the effective vertical scale is reduced (see Hogg, 1973), and so control over the dynamics is also reduced. Finally, there are several regions where density driven currents (overflows) and turbulent bottom boundary layer (BBL) processes act as a strong determinant of water mass characteristics. Many such processes are crucial for the formation of deep water properties in the World Ocean.

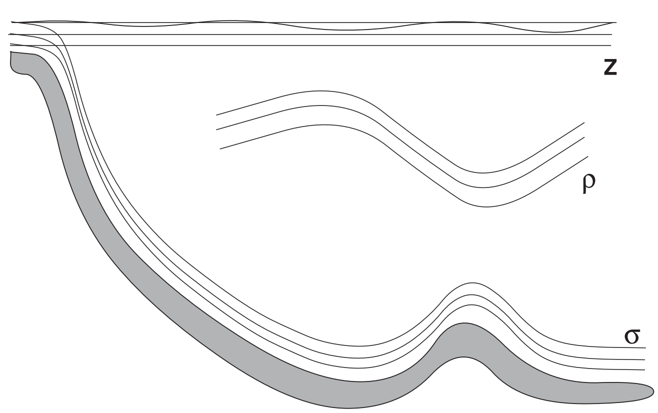

Fig. 1. Schematic of an ocean basin illustrating the three regimes of the ocean germane to the considerations of an appropriate vertical coordinate. The surface mixed layer is naturally represented using z-coordinates; the interior is naturally represented using isopycnal ρ-coordinates; and the bottom boundary is naturally represented using terrain following σ-coordinates.

Fig. 1 represents an idealization. For example, in continental shelf regions and in the vicinity of islands, the distinction between the three regimes is blurred. Nonetheless, this picture provides a useful conceptual basis from which to formulate the dynamical equations describing the ocean, and hence to design ocean models.

Another general consideration relevant to coordinate choice relates to the importance of the hydrostatic and geostrophic balances for geophysical fluids. For numerical accuracy and analytic simplicity, it is useful to describe these balances with a convenient set of coordinates. In particular, measuring vertical distances in the direction parallel to gravity, and horizontal distances perpendicular to gravity, yields simple equations. Ocean models based on z, σ and ρ vertical coordinates are canonical examples. These three choices represent specific *generalized vertical coordinate systems*, which are discussed by Starr (1945), Sutcliffe, 1947, Phillips (1957), Bleck (1978), Haltiner and Williams (1980) and others (see in particular the appendix to McDougall, 1995). An alternative approach is to make "vertical" measurements perpendicular to surfaces of the constant generalized vertical coordinate (i.e., perpendicular to σ or ρ surfaces). The result, however, is a cumbersome set of dynamical equations which are not used in practice for large-scale ocean models.

2.1. Z-models

The simplest choice of vertical coordinate is z, which represents the vertical distance from a resting [1] ocean surface at $z = 0$, with z positive upwards and $z = -H(x, y)$ the topography. Z-models have been around for many decades, with the pioneering work of Bryan (1969a), and then Semtner (1974) and Cox (1984) leading to the development of the first ocean model used for studies of global climate (e.g., Bryan, 1969b; Bryan et al., 1975). The latest incarnation in this lineage is version 3 of the GFDL Modular Ocean Model (MOM), which is extensively documented in the MOM manual of Pacanowski and Griffies (1999). Southampton Oceanography Centre's MOMA (Webb, 1996) and ocean circulation and climate advanced modelling project (OCCAM) (Webb et al., 1997, 1998a), their derivative SEA (The Southampton-East Anglia Parallel Ocean Circulation Model), the Los Alamos Parallel Ocean Program (POP; Smith et al., 1992; Dukowicz and Smith, 1994), and the Hadley Centre's ocean model (Gordon et al., 2000) are also directly linked to the Bryan–Cox–Semtner model. Other z-models less directly tied to this lineage include the Canadian CANDIE model (Sheng et al., 1998; Lu et al., 2000), which is a modification of the DieCAST model of Dietrich et al. (1987), the Center for Climate System Research (Tokyo) Ocean COmponent (COCO) model (Hasumi, 2000), the Goddard Institute for Space Studies (GISS) model (Russell et al., 1995), the Hamburg Ocean Primitive Equation (HOPE) model (Wolff et al., 1997), the LODYC's OPA model (Madec et al., 1998), and the MIT model (Marshall et al., 1997a,b). The MIT model is notable for its hydrostatic and non-hydrostatic capabilities, thus allowing for systematic tests of the validity of the hydrostatic approximation for climate modelling. Table 1 provides a summary of these models and how they can be accessed.

[1] That is, a static ocean under hydrostatic balance.

Table 1
Summary of z-coordinate ocean models currently developed and supported with applications to climate related studies[a]

Model/Institute/Language	Documentation	Web site
CANDIE/Dalhousie/F77	Sheng et al. (1998), Lu et al. (2000)	www.phys.ocean.dal.ca/programs/CANDIE
COCO/CCSR/F77	Hasumi (2000)	www.ccsr.u-tokyo.ac.jp/~hasumi/COCO/
GISS/GISS/F77	Russell et al. (1995)	www.giss.nasa.gov/gpol/abstracts/1995.RussellMiller.html
Hadley/Hadley/F77	Gordon et al. (2000)	
HOPE/DKRZ/F77	Wolff et al. (1997)	www.dkrz.de/forschung/reports.html
MIT/MIT/F77	Marshall et al. (1997a,b)	mitgcm.lcs.mit.edu
MOM/GFDL/F77-F90	Pacanowski and Griffies (1999)	www.gfdl.gov/MOM.html
MOMA/SOC/F77	Webb et al. (1997, 1998a)	www.mth.uea.ac.uk/ocean/SEA
SEA/EA/F77	Webb (1996)	www.mth.uea.ac.uk/ocean/SEA
OCCAM/SOC/F77	Webb et al. (1997, 1998a)	www.soc.soton.ac.uk/JRD/OCCAM/
OPA/LODYC/F77	Madec et al. (1998)	www.ipsl.jussieu.fr/~gmlod/OPA_web
POP/LANL/F90	Smith et al. (1992)	www.acl.lanl.gov/climate/models/pop

[a] Given here are the model names, their main supporting institutions, their computer language (F77 = Fortran 77, F90 = Fortran 90), their documentation source, and a web site describing how to obtain the code. Acronyms represent the following: CANDIE = Canadian DieCAST ocean model, DieCAST = Dietrich/Center for Air-Sea Technology, Dalhousie = Dalhousie University (Halifax, Canada), COCO = CCSR Ocean COmponent model, CCSR = Center for Climate System Research (Tokyo), GISS = Goddard Institute for Space Sciences, Hadley = Hadley Centre, HOPE = Hamburg Ocean Primitive Equation, DKRZ = Deutsche Klimarechenzentrum, MIT = Massachusetts Institute of Technology, MOM = Modular Ocean Model, GFDL = Geophysical Fluid Dynamics Laboratory, MOMA = Modular Ocean Model-Array processor version, SEA = The Southampton-East Anglia Parallel Ocean Circulation Model, EA = University of East Anglia, OCCAM = Ocean Circulation and Climate Advanced Modelling Project, SOC = Southampton Oceanography Centre, OPA = Océan PArallélisé, LODYC = Laboratoire d' Océanographie Dynamique et de Climatologie, POP = Parallel Ocean Program, LANL = Los Alamos National Laboratory.

Some key advantages of z-models are the following:

- The simplest of numerical discretization approaches have been used, to some success, in this framework. This has allowed z-models to be used for climate purposes soon after their initial development, thus providing valuable years of experience with this class of model.
- For a Boussinesq fluid, the horizontal pressure gradient can be easily represented.
- The equation of state for ocean water, which is highly non-linear and important for determining water mass properties, can be cleanly and accurately represented.
- The surface mixed layer is naturally parameterized using a z-coordinate. In general, a z-coordinate provides a useful framework for representing diabatic processes.

Some of the disadvantages are

- The representation of tracer advection and diffusion along inclined density surfaces in the ocean interior is cumbersome.
- Representation and parameterization of the BBL is unnatural.
- Representation of bottom topography is difficult.

These aspects of z-models will be discussed at more length in the following sections. As might be expected, much of the research into z-model development has focused on remedying the cumbersome aspects.

2.2. ρ-models

Another choice for vertical coordinate is the potential density ρ referenced to a given pressure. This coordinate is a close analog to the atmosphere's entropy or potential temperature. In a stably stratified adiabatic ocean, potential density is materially conserved and defines a monotonic layering of the ocean fluid. Examples of isopycnal ocean models are the Miami Isopycnal Coordinate Model (MICOM; Bleck et al., 1992), the Hallberg Isopycnal Model (HIM; Hallberg, 1995, 1997), the OPYC (Oberhuber, 1993) from the Max Planck Institute in Hamburg, and the Parallel Oregon State University Model (POSUM). Two hybrid models which share much in common with isopycnal models are HYCOM, which is a pressure–density hybrid originating from MICOM, and POSEIDON (Schopf and Loughe, 1995), which is a generalized vertical coordinate model that combines an explicit turbulent mixed layer, a sigma-based buffer layer, and a quasi-isopycnal interior. Table 2 summarizes the ρ-models currently supported and developed for purposes of regional and/or global climate related studies. Although used extensively for coupled climate simulations (e.g., Lunkeit et al., 1996; Roeckner et al., 1996; Timmermann et al., 1999), the OPYC model is no longer supported, hence its absence from this table.

Some key advantages of ρ-models are the following:

- Tracer transport in the ocean interior has a strong tendency to occur along directions defined by locally referenced potential density (i.e., neutral directions), rather than across. Hence, ρ-models are well suited for representing the dynamics in this regime, so long as isopycnals are reasonably parallel to neutral directions.
- The bottom topography is represented in a piecewise linear fashion, hence avoiding the need to distinguish bottom from side as traditionally done with z-models.
- Current research into the physics of overflows suggests that the ρ-models may provide some advantage over z-models in the representation of these processes.

Table 2
Summary of ρ-coordinate ocean models currently developed and supported[a]

Model/Institute/Language	Documentation	Web site
HIM/GFDL/C	Hallberg (1995, 1997)	`www.gfdl.gov/~rwh/HIM/HIM.html`
MICOM (HYCOM)/Miami, LANL, Stennis/F77	Bleck et al. (1992)	`panoramix.rsmas.miami.edu/micom/`
POSEIDON/COLA, George Mason/F90-F95	Schopf and Loughe (1995)	`grads.iges.org/poseidon`
POSUM/Oregon State/F77	de Szoeke & Springer	`posum.oce.orst.edu/`

[a] Some have been used for climate related studies, although such is generally at its early stages relative to z-coordinate models. Given here are the model names, their main supporting institutions, their computer language (F77 = Fortran 77, F90 = Fortran 90, F95 = Fortran 95, C = C), their documentation source, and a web site describing how to obtain the code. Acronyms represent the following: HIM = Hallberg Isopycnal Model, GFDL = Geophysical Fluid Dynamics Laboratory, MICOM = Miami Isopycnal Coordinate Ocean Model, NRL-Stennis = Naval Research Laboratory, Stennis Space Center, Mississippi, COLA = Center for Ocean, Land, and Atmospheres, Geogre Mason = George Mason University, HYCOM = HYbrid Coordinate Ocean Model. Note that HYCOM is a hybrid pressure–density model and POSEIDON is written in generalized vertical coordinates; their inclusion in this table arises from their having much in common with other isopycnal models.

- For an adiabatic fluid, the horizontal pressure gradient can be easily represented.
- For an adiabatic fluid, the volume (for a Boussinesq fluid) or mass (for a non-Boussinesq fluid) between isopycnals is conserved.

Some of the disadvantages are

- Representing the effects of a realistic (non-linear) equation of state is cumbersome.
- A ρ-coordinate is an inappropriate framework for representing the surface mixed layer or BBL, since these boundary layers are mostly unstratified.

These aspects of ρ-models will be discussed at more length in the following sections. As with the z-models, much of the research into ρ-model development has focused on remedying its cumbersome aspects.

2.3. σ-models

A terrain following σ-coordinate was introduced to the atmospheric modelling community by Phillips (1957). For ocean modelling, it is usually defined as

$$\sigma = \frac{z - \eta}{H + \eta}, \tag{1}$$

where $\eta(x, y, t)$ is the displacement of the ocean surface from its resting position $z = 0$, and $z = -H(x, y)$ is the ocean bottom. Note that $\sigma = 0$ at the ocean surface and $\sigma = -1$ at the bottom. σ is monotonic, and so the relation (1) defines a unique mapping between depth z and σ, thus allowing for σ to be a valid vertical coordinate. The Princeton Ocean Model (POM) has traditionally employed a sigma-coordinate as its vertical coordinate, and it has been used extensively for coastal engineering applications, prediction (see the review by Greatbatch and Mellor (1999) for coastal prediction models), as well as regional and basin-wide studies. Other σ-models include those developed by the Rutgers-UCLA groups (e.g., SPEM, ROMS, and relatives), with many variants in use. Table 3 summarizes the σ-models currently supported and developed for purposes of regional studies.

Some key advantages of σ-models are the following:

- They provide a smooth representation of the ocean bottom topography, with coordinate isolines concentrated in regions where BBL processes are most important. Hence, they allow for a natural framework to parameterize BBL processes.
- Thermodynamic effects associated with the equation of state are well represented.

Table 3
Summary of σ-coordinate ocean models currently developed and supported[a]

Model/Institute/Language	Documentation	Web site
POM/Princeton, GFDL/F77	Blumberg and Mellor (1987)	`www.aos.princeton.edu/WWW-PUBLIC/htdocs.pom`
SPEM (ROMS)/Rutgers, UCLA/F77	Haidvogel et al.	`marine.rutgers.edu/po/`

[a] Most applications are for coastal and regional modelling, with no examples of global σ-models. Given here are the model names, their main supporting institutions, their computer language (F77 = Fortran 77), their documentation source, and a web site describing how to obtain the code. Acronyms represent the following: POM = Princeton Ocean Model, GFDL = Geophysical Fluid Dynamics Laboratory, SPEM = S-coordinate Primitive Equation Model, ROMS = Regional Ocean Modelling System.

Some of the disadvantages are

- The surface mixed layer can be less well represented using σ than with the z-coordinate. The reason is that the vertical distance between grid points generally increases upon moving away from the continental shelf regions, hence leaving the surface layer with potentially less than ideal vertical resolution in the middle of an ocean basin (e.g., see Fig. 4.2 of Haidvogel and Beckmann, 1999). This problem is overcome via a variant of the σ coordinate, commonly called the s-coordinate, in which resolution in the mixed layer away from coasts can be maintained (e.g., Song and Haidvogel, 1994; Mellor et al., 2000; Haidvogel and Beckmann, 1999; Haidvogel et al., 2000).
- As with the z-models, the representation of advection and diffusion along inclined density surfaces in the ocean interior is cumbersome. Additionally, the ability of z-models to "reorient" the sub-grid-scale physics to lie along neutral directions, as explained in Section 9, is more difficult. The reason is that σ coordinate surfaces can cross neutral directions at large angles when topography is steep. In contrast, neutral and z surfaces are typically quite close within the ocean interior, where neutral slopes relative to the horizontal typically do not reach much above 1/100.
- σ-models have difficulty accurately representing the horizontal pressure gradient (e.g., Janjić, 1977; Mesinger, 1982; Beckmann and Haidvogel, 1993; Mellor et al., 1994, 1998; Chu and Fan, 1997; Song and Wright, 1998a,b,c). Because the surfaces of constant sigma are not generally horizontal, the horizontal pressure gradient, which is perpendicular to the local vertical direction as defined by gravity, will have a projection along and across sigma surfaces. The result is a horizontal pressure gradient consisting of two terms

$$\begin{aligned} \nabla p &= (\nabla_\sigma - \nabla_\sigma z\, \partial_z) p, \\ &= \nabla_\sigma p + \rho g \nabla_\sigma z, \end{aligned} \tag{2}$$

where the hydrostatic balance $\partial_z p = -\rho g$ was used to reach the second relation. In these equations, ∇p the horizontal pressure gradient taken along surfaces of constant depth z, $\nabla_\sigma p$ the pressure gradient along surfaces of constant σ, and $\nabla_\sigma z$ is the slope of the sigma surface relative to the constant depth surfaces. In the ocean, especially next to the continental shelves, the slope of sigma surfaces can reach 1/100 to 1/10, at which point the "sigma coordinate correction term" $\rho g \nabla_\sigma z$ can be on the order of $\nabla_\sigma p$. In this case, the horizontal pressure force becomes the result of two sizable terms, each having separate numerical errors that generally do not cancel. The result can be spurious pressure forces that drive non-trivial unphysical currents.

Although there are encouraging research efforts aimed at resolving the problematic issues (e.g., see Song and Wright, 1998a,b,c for advances in representing the horizontal pressure gradient), and regional models are now more common with σ-models (e.g., Ezer and Mellor, 1997; Barnier et al., 1998; Marchesiello et al., 1998; Ezer, 1999; Beckmann et al., 1999; Hakkinen, 1999, 2000), there are presently no published global σ-models in use for climate modelling purposes. Given the limitations inherent in any paper, and our aim to focus on global ocean climate modelling, we limit the discussion in the following to developments in z- and ρ-models.

2.4. Computer language and computational platforms

The previous tables also indicate the computer language used in the various codes. Notably, HIM is the *only* model written in C, whereas all others are written in Fortran. Most of the Fortran models use Fortran 77, though some use mixtures of Fortran 77/90 or Fortran 90/95. Most models have been run on both vector and parallel machines, although some have run only on one or the other. Further details about platform dependencies are best found by going to the respective web site.

2.5. Summary items

The main points from this section include the following:

- The depth or z-coordinate provides the simplest and most established framework for ocean climate modelling. It is well suited for situations with strong vertical/diapycnal mixing and/or low stratification, yet is cumbersome in the ocean interior and bottom.
- The density or ρ-coordinate is less well established for climate modelling applications, but it has strong foundations in idealized configurations. It is well suited to modelling the observed tendency for tracer transport to be along neutral directions. Significant advances are being made which show promise for future climate models, especially when used within a hybrid coordinate approach.
- The terrain following or σ-coordinate provides a suitable framework in situations where capturing the dynamical and/or boundary layer effect associated with topography is important. It is particularly well-suited for modelling flows over the continental shelf and slope, but remains unproven in a global coupled climate modelling context. Progress is being made with some hopes that it will be of use for climate modelling in the near future.
- Most of the codes are written in Fortran, with HIM being the only C ocean model discussed here. Most have also run on both vector and parallel supercomputer platforms.

3. Horizontal coordinates, horizontal grids, and time stepping

3.1. Horizontal coordinates

Spherical coordinates are a natural set of orthogonal curvilinear coordinates for representing geophysical flow. However, the convergence of the meridians and the associated polar singularity [2] leads to numerous numerical problems with the CFL condition. [3] Hence, spherical coordinates require one to either take globally small time steps based on the very small zonal grid spacing near the pole, or to use polar filtering such as Fourier (Bryan et al., 1975) or finite impulse

[2] A well known theorem of topology (e.g., Nakahara, 1990) states that there will be at least one singularity when covering the sphere with a single set of coordinates.

[3] For stability purposes with explicit time stepping schemes, the CFL number $c\,\Delta t/\Delta x$ must on the order of unity, or smaller, with details of the time stepping scheme determining the precise value. The velocity c is the fastest wave speed or advective velocity, Δt is the model time step, and Δx is the local grid size.

response filtering (Pacanowski and Griffies, 1999) within some region around the pole, in order to remove small zonal scale structures. The first option is often prohibitively costly. Thus, many have chosen to filter, using filters based largely on those used by atmospheric modellers.

The main computational problem with polar filters in the ocean is related to the complicated land–sea boundaries, thus making each latitude row consist of numerous broken ocean segments, many of which consist of only a few ocean points. In contrast, grid-point atmospheric models, which are commonly based on a σ-coordinate, encounter no meridional boundaries. Filtering each ocean segment separately is the only option, since otherwise water properties could be transported through land–sea boundaries via the action of the filter. This approach leads to some computational inefficiencies. Additionally, filters have been found to introduce significant amounts of noise to fields, such as the vertical velocity, largely because of the effect filtering the prognostic variables has on pressure gradients (see Pacanowski and Griffies, 1999 for discussion). More generally, filtering the dynamic and thermodynamics fields separately can destroy geostrophic and thermodynamic balances, which in turn can lead to "noisy" adjustments. Therefore, polar filtering introduces a very unphysical component to the simulation. Those even remotely interested in polar ocean dynamics find it to be quite unsatisfying.

For these reasons, modellers have chosen to generalize the spherical grid to allow arbitrary orthogonal curvilinear coordinates so that the coordinate singularity can be moved from the ocean domain and placed over land (e.g., Haidvogel et al., 1991; Smith et al., 1995; Mellor, 1996; Madec and Imbard, 1996; Murray, 1996; Murray and Reason, 1999; Bentsen et al., 1999). HIM, MICOM/HYCOM, OPA, POM, POP, POSUM, and ROMS all have generalized orthogonal grids, and MIT and MOM plan to have such available by 2001. OCCAM has addressed the problem in a slightly different manner by using two spherical grids, one with its poles at the Earth's equator, which are matched on the equator in the Atlantic. A one-dimensional channel model is used to link the two grids through the Bering Strait. Table 4 summarizes these coordinates.

Coupling a spherical coordinate atmosphere to a generalized ocean grid requires an interpolation scheme to conservatively pass data between the models. Two algorithms have been developed for this purpose: The Spherical Coordinate Remapping and Interpolation Package (SCRIP) from Los Alamos (Jones, 1999) (`http://climate.acl.lanl.gov/software/SCRIP/`), and the OASIS scheme from the French CERFACS laboratory (`http://www.cerfacs.fr/globc/software.html`). NCAR's climate modelling group uses SCRIP and French coupled models use OASIS. In principle, the packages should allow coupling between component models using arbitrarily different grids, with some care exercised at the boundaries between the component models.

3.2. Horizontal grids

Fig. 2 presents a schematic of the placement of model variables on the staggered horizontal Arakawa (Arakawa, 1966; Mesinger and Arakawa, 1976; Arakawa and Lamb, 1981) grids used in ocean models, and Table 4 presents the choices made by the various ocean models. Most use either the B or C grid (POSEIDON has an option for either). Notable exceptions include the following: CANDIE has both A and C grid versions; HOPE was originally formulated on the E grid but recently converted to C grid (M. Latif, personal communication 2000); and the MIT

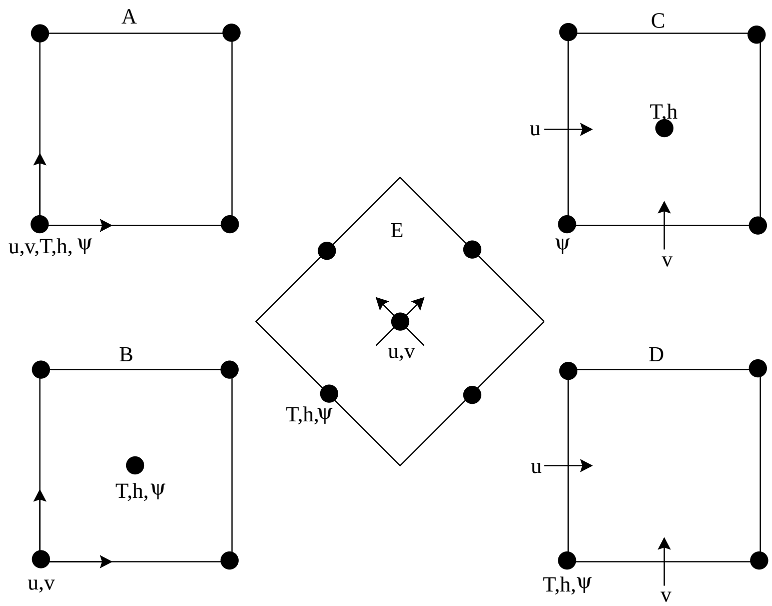

Fig. 2. Schematic of the placement of model variables on the staggered horizontal Arakawa grids used in ocean models. T refers to tracer and density, u, v refer to horizontal velocity components, h refers to layer thickness, and ψ refers to horizontal streamfunction or surface height. This figure is taken from Fig. 3.1 of Haidvogel and Beckmann (1999).

model allows for either the standard C grid or the C/D grid of Adcroft et al. (1999). This section aims to summarize some of the practical properties of the more commonly used B and C grids when used in ocean models (Section 3.1 of Haidvogel and Beckmann (1999) provides a more complete summary).

3.2.1. B and C grid representations

There are many issues which prompt one to choose one sort of a grid over another. This subsection provides a brief account of the relevant topics.

A preference for B grid at coarse resolution and C grid at fine resolution is based on the superior representation of poorly resolved inertia–gravity waves by the B grid, whereas the C grid is superior for well resolved waves (Arakawa and Lamb, 1977; Hsieh et al., 1983). Relatedly, geostrophy is well simulated on the B grid because of the co-location of velocity points, but inviscid gravity wave dynamics can be afflicted with a computational checkerboard mode (e.g., Mesinger, 1973; Janjić, 1974; Killworth et al., 1991; Deleersnijder and Campin, 1995; Pacanowski and Griffies, 1999). In contrast, the C grid handles resolved gravity wave dynamics well, yet must rely on well-resolved features in the velocity field to simulate geostrophy due to the off-set between the horizontal velocity components. This off-set afflicts the C grid with a computational checkerboard mode at low resolution (see Adcroft et al., 1999 for discussion).

The preferred behavior of the B grid for coarsely resolved flows prompted Bryan (1969a,b) to employ the B grid, with direct z-model successors also following this practice. In contrast, iso-

Table 4
Summary of horizontal coordinates, horizontal grids, and time stepping schemes used in the various ocean models[a]

Model	Horz coordinates	Horz grid	Tracer	Baroclinic	Barotropic
CANDIE	Spherical	A and C	LF w/TF	LF w/EB	IFS
COCO	Spherical	B	LF w/EB	LF w/EB	RL–LF
GISS	Spherical	C	LF	LF	EFS
Hadley	Spherical	B	LF w/EB	LF w/EB	RL–LF
HOPE	General	C	IM	IM	IFS
MIT	Spherical	C/D	AB	AB	IFS w/CN or EB
MOM	Spherical	B	LF w/TF	LF w/TF	RL–LF, IFS, EFS–FB
OCCAM	Patched	B	LF w/EB	LF w/EB	EFS–LF
OPA	General	C	LF w/TF	LF w/TF	RL–LF, IFS
POP	General	B	LF w/TA	LF w/TA	IFS
HIM	General	C	F	PC	EFS–FB
MICOM/HYCOM	General	C	LF w/TF	LF w/TF	EFS–FB
POSEIDON	General	B/C	LF w/TF	LF w/TF	EFS–FB
POSUM	General	C	F	FB	EFS–FB

[a] For the horizontal coordinates, "spherical" refers to the traditional spherical coordinates, "general" refers to generalized orthogonal curvilinear coordinates, and "patched" refers to patched spherical coordinates with non-analytic overlapping regions. For the horizontal grids, A, B, C, D, and E refer to Arakawa and Lamb (1977) scheme. The tracer, baroclinic, and barotropic columns distinguish time stepping schemes for these portions of the model. The remaining acronyms represent the following: F = forward, LF = leap-frog, EB = Euler–backward, FB = forward–backward, AB = Adams–Bashforth, PC = predictor–corrector, CN = Crank–Nicholson, TF = Robert–Asselin time filter, TA = time averaging as described by Dukowicz and Smith (1994), EFS = explicit free surface, IFS = implicit free surface, RL = rigid lid streamfunction, RL(sp) = rigid lid/surface pressure, IM = implicit.

pycnal models have traditionally been used under more idealized situations in which the Rossby radius is better resolved. Additionally, many isopycnal models share their fundamental discretizations with the shallow water equations as discussed by Sadourny (1975) who chose a C grid. Thus, most isopycnal models use the C grid.

In addition to the properties of geostrophy and gravity waves, it is useful to consider finite difference Rossby waves. Dukowicz (1995) (see also Wajsowicz, 1986), provides a discussion of the properties of unbounded finite difference Rossby waves, where he shows the B-grid to be superior for both resolved and under-resolved Rossby waves. This behavior is consistent with the preference of the B grid for geostrophic flows mentioned above. From a different perspective, Janjić (1984) points out that as the resolution is refined, the C grid provides a superior handling of the energy cascade associated with baroclinic eddies. More generally, as there will always be unresolved higher baroclinic radii, some argue (e.g., Webb et al., 1998a) that the B grid will remain advantageous for representing fronts and currents with small vertical extent that have a nontrivial projection onto higher baroclinic modes. Equatorial currents are a good example where higher modes are clearly important.

The above comparisons between horizontal grids focus on the representation of waves on unbounded domains. An additional difference between the B and C grid concerns the representation of boundary waves, especially in coarse resolution models (Hsieh et al., 1983; Wajsowicz and Gill, 1986, R. Hallberg, personal communication 2000). Notably, C grid models readily admit a finite difference representation of a Kelvin wave, thus allowing density perturbations to be transmitted parallel to a solid boundary in a realistic manner. In contrast, for the same perturbation, the B grid can also admit a geostrophically balanced flow consisting of a vertical overturning cell in the off-slope direction adjacent to the boundary. Such overturning cells are commonly seen in coarse B grid simulations, such as idealized thermohaline models. For example, Park and Bryan (2000) present a comparison between a B grid z-level model and a C grid ρ-model which illustrates this point (see especially their Fig. 9).

Side boundaries on the B grid are naturally implemented using a no-slip condition, since both velocity points lie on the solid boundary. A general formulation of a free-slip on the B grid does not exist, although idealized channel models have been run with free-slip.

In contrast, side boundary conditions are naturally implemented via the free-slip condition with the C grid. However, no-slip side conditions are also available (e.g., MICOM/HYCOM, OPA), but typically at the cost of losing one degree of formal order of accuracy at the boundary when implementing a Laplacian friction operator (R. Hallberg, personal communication 2000).

Coastlines are typically incorporated via a mask array rather than with the coordinate lines paralleling the coasts. Hence, side boundaries are represented as steps, much like the z-coordinate representation of bottom topography discussed in Section 6. It is conceivable that with a generalized orthogonal curvilinear coordinate system, one can generate coordinate lines that roughly parallel the coasts, but this has proved impractical in large and convoluted ocean basins like the North Atlantic.

Issues of step-wise coastlines were investigated by Adcroft and Marshall (1998) (see also Haidvogel and Beckmann, 1999). They found that on a C grid with a 45° coastline, the no-flow condition provides all the needed values for the zonal and meridional velocities (at least for a Laplacian friction operator), and such is equivalent to a partial slip boundary condition. More generally, the boundary stress is erroneous with piecewise constant coastlines, and in particular the magnitude of the stress is dependent on the coastline's orientation.

As mentioned previously, the presence of spatial computational modes, or null modes, provide ready sources of anguish to developers when trying to discretize the equations of motion. On the B grid, a computational mode exists when discretizing inviscid gravity waves, and this mode often manifests as checkerboard patterns in the surface height or barotropic streamfunction (e.g., Mesinger, 1973; Janjić, 1974; Killworth et al., 1991, Deleersnijder and Campin, 1995; Pacanowski and Griffies, 1999). These papers present methods aimed at suppressing this noise, each of which amounts to adding dissipation. On the C grid, the Coriolis force must be computed via a spatial averaging since the velocity points are not co-located. Such averaging, unfortunately, often results in the presence of a computational mode which manifests again as checkerboard patterns, with the amplitude of the patterns enhanced at coarse resolutions. Adcroft et al. (1999) provide a summary of the C grid problem, discussion of previous approaches for resolving the issue, and a new proposal which involves the use of a combined C/D grid.

3.2.2. Comments on unstructured grids

The Arakawa grids used in ocean models are examples of *structured grids*, which means the grid cells have the same number of sides and same number of neighboring cells. *Unstructured* grids allow one to tile a domain using more general geometrical shapes (e.g., triangles, squares, pentagons, hexagons, etc.) that are pieced together to optimally fit details of the geometry. Because of such generality, the algorithmic details are more complex than with structured grids; for example, the number of neighboring grid cells need not be unique throughout the domain. Nonetheless, the idea of unstructured grids in principle is attractive for ocean modelling since the domain geometry is indeed very complicated.

An example of an ocean model with unstructured grid capabilities is Spectral Element Ocean Model (SEOM) (see Haidvogel and Beckmann, 1999 for discussion). Unstructured grids have proven very useful for coastal and tidal modelling with engineering applications in mind. However, there are two general problems which have arisen when attempting to use unstructured grids in climate models. The first is that it is difficult to represent the geostrophic balance correctly (i.e., represent both the Coriolis term and the pressure gradient without loss of accuracy). The second is that every change in grid spacing provides an opportunity for unphysical wave scattering. Unstructured grids are widely used in engineering to solve the steady-state problem where such scattering is less crucial. It is notable, however, that some ongoing effort by various groups is aimed at dispelling the notion that unstructured grids are impractical for climate models.

3.3. Time stepping schemes

Time stepping schemes used by the various models for the tracer and baroclinic momentum equations are given by Table 4. The treatment of the barotropic dynamics is discussed in Section 4. For more complete presentations of time stepping schemes, the reader is referred to the ocean modelling books by O'Brien (1986) or Haidvogel and Beckmann (1999), the atmospheric modelling book by Haltiner and Williams (1980), or the numerical geophysical fluid dynamics book of Durran (1999).

3.3.1. Standard time stepping methods

Most of the z-models use a three-time level "leap-frog" scheme for both the tracer and baroclinic momentum equations. To remove the time splitting computational mode, the leap-frog scheme must be combined with a Robert–Asselin time filter (Robert, 1966; Asselin, 1972), a periodic Euler backward step, or some other form of time filtering such as the time averaging approach of Dukowicz and Smith (1994). Both time filtering and the periodic use of an Euler backward step reduce the leap-frog time discretization accuracy from second-order to first-order. Additionally, use of the Euler backward step has been found in some cases to cause problems with the representation of sub-grid-scale processes such as convection (Marotzke, 1991). Such difficulties with the Euler backward step have prompted modellers to favor time filtering approaches in which all time steps are treated the same.

Because of the often different numerical time step constraints placed on the baroclinic and tracer equations (see next subsection), use of different time stepping schemes for the tracer and baroclinic schemes have been considered in isopycnal models. For example, HIM uses a two-time level forward scheme for tracers and a predictor–corrector approach (Hallberg, 1997) for the baroclinic momentum equations. MICOM/HYCOM and POSEIDON use a leap-frog with the time filter for both baroclinic and tracers, and POSUM uses the scheme described by Higdon and de Szoeke (1997) and Higdon (1999).

3.3.2. Methods for taking longer time steps

An approach for extending the range of stability for baroclinic time steps with a leap-frog scheme is the pressure gradient averaging approach of Brown and Campana (1978). Pressure gradient averaging is commonly used in POP and is available in MOM and OPA. POP experience indicates that the technique allows for a doubling of the baroclinic time step, provided the time step is controlled by internal gravity waves and not by some other mechanism (John Dukowicz, personal communication 2000).

The barotropic, baroclinic, and thermodynamic adjustment processes in the ocean have quite different characteristic time scales. Barotropic adjustment occurs on the order of days, it takes years for the adjustment of slow planetary waves in the mid-latitude, and it requires centuries to millennia to reach thermodynamic equilibrium. Motivated by this time scale split, Bryan (1969a,b) and Semtner (1974) introduced the idea of differential time stepping of the barotropic, baroclinic, and tracer equations. As described by Bryan (1984) (see also Killworth et al., 1984), to help to reduce the computational cost required to reach thermodynamic equilibrium, it has been found useful to "accelerate" the slower adjustments by using longer time steps for the slower evolving tracers than for the baroclinic components (the barotropic component is discussed in Section 4). For example, tracer time steps of a day and baroclinic time steps of an hour are common in four degree z-coordinate ocean models. [4] At a steady equilibrium, the tendency terms are near zero, so the use of different time steps becomes irrelevant.

So long as the focus is on the steady solution in coarse models, "accelerating" the tracer time step has proven to be quite useful. However, when allowing for a seasonal cycle, coupling to a dynamical atmosphere, or when interested in ocean waves and eddies, the approach can be problematic. For example, the relative times for heat advection versus Rossby wave propagation versus vertical subduction are important for seasonal balances. Therefore, if interested in transients, it is important to use the same tracer and baroclinic time step. In particular, as discussed by Danabasoglu et al. (1996), a period of ocean acceleration must be followed by roughly one to two decades of equal tracer and baroclinic time steps prior to coupling in order to synchronize phases of the seasonal cycle (see also Huang and Pedlosky, 2000).

Further acceleration techniques have been used where the acceleration factor is depth dependent, with the deeper ocean, having even more sluggish velocities, affording much longer effective time steps than the surface (Bryan, 1984). However, this "acceleration with depth" method has become less common due to questions regarding its effects on convection.

As mentioned previously, acceleration "tricks" are problematic when transients are of interest. When moving to high resolution, ocean eddies introduce a new form of transience which typically prompts modellers to avoid splits between the tracer and baroclinic time steps. Pragmatically, this split becomes less feasible as the advective speeds in the model approach the first baroclinic gravity wave speed, thus making the advective CFL constraint comparable to the gravity wave CFL. The resulting expense has resulted in no global eddying model having been spun-up to thermodynamic equilibrium. Systematic and efficient methods for initializing eddying ocean

[4] We emphasize that the tracer time step is simply taken longer than the baroclinic velocity step; there is no sub-cycling of the baroclinic equations. The model remains computationally stable with long tracer time steps due to the sluggish advective speeds present in coarse models.

models for use in coupled climate simulations hence remains an important outstanding problem. Furthermore, to our knowledge, acceleration approaches have not been pursued in ρ-models, even when run at coarse resolution.

3.4. Summary items

The main points from this section include the following:

- Most ocean climate models have, or are presently implementing, generalized orthogonal coordinates. The purpose is to allow for the movement of the coordinate singularity at the North Pole to a more convenient land location.
- Structured grids (e.g., Arakawa grids) remain the norm in ocean modelling. The Arakawa C grid is commonly used in ρ-models, whereas the B grid, with some notable exceptions (see Table 4), is commonly used in z-models. Unstructured grids have proven to be impractical for climate modelling.
- Most z- and ρ-models use a leap-frog time stepping scheme for the baroclinic and tracer equations, with some sort of time filtering or periodic Euler backward to suppress the time splitting mode. Notable exceptions exist (see Table 4), which include fully implicit schemes and two time level explicit schemes.
- Coarse resolution z-models have traditionally employed longer tracer than baroclinic momentum time steps when spinning-up the model to thermodynamic equilibrium.

4. Barotropic dynamics

As discussed by Gill (1982), the orthogonal eigenmodes of a density stratified fluid in a flat bottom ocean determine the simplest examples of what oceanographers call the *barotropic* and infinite number of *baroclinic* gravity wave modes. In the deep ocean, the barotropic gravity wave propagates at roughly two orders of magnitude faster than the fastest baroclinic gravity wave. Additionally, interactions between the barotropic and baroclinic waves are thought to be unimportant from a climate perspective, at least in so far as one needs to explicitly and accurately resolve them. [5] For these reasons, there is strong motivation to exploit the time scale difference when developing algorithms for solving the hydrostatic primitive equations.

For a rotating and stratified ocean with non-trivial topography, the fastest mode resembles the barotropic gravity mode of the flat bottom ocean. However, it is much more difficult to provide an orthogonal decomposition of the fast and slow modes in this general case. Nonetheless, it is possible to approximate the fast mode by fluctuations of the depth averaged fluid, and the slow modes by deviations from the depth average. By analogy to the flat bottom case, these "ocean model modes" are also called the barotropic and baroclinic modes. Although depth averaging provides an approximation to the barotropic mode, its orthogonality from the depth dependent modes is not guaranteed, notably because there has been no eigenvalue problem solved when

[5] The role of tidal and internal gravity waves for ocean mixing is quite important, yet these small scale processes are thought to be parameterizable via a diapycnal mixing scheme. See Toole (1998) for discussion and references.

defining these ocean model modes. For example, in a rigid lid ocean model, vertical averaging does provide a clean split between the fast and slow modes – there is no overlap. In contrast, vertical averaging does not completely separate out the fast dynamics in a free surface model, since in this case the true barotropic gravity mode actually has a weak depth dependence whereas the depth averaged mode is, by definition, depth independent.

The overlap between the fast and slow ocean model modes has proven to be of some practical concern when aiming to provide a numerically stable split between the modes in realistic ocean models. The papers by Killworth et al. (1991), Dukowicz and Smith (1994), Higdon and Bennett (1996), Higdon and de Szoeke (1997), Hallberg (1997), and Dukowicz (1999) provide discussions of these issues. The purpose of this section is to survey developments in this area.

4.1. Rigid lid streamfunction method

Again, the goal is to separately solve the fast and simpler two-dimensional depth averaged dynamics and the slower and more complicated three-dimensional depth dependent dynamics. An early and popular split between fast and slow dynamics was provided by the rigid lid streamfunction method of the Bryan–Cox–Semtner z-model (Bryan, 1969a). In this approach, the ocean surface is held fixed in time, thus eliminating barotropic gravity waves. The residual dynamics includes the baroclinic and slower barotropic modes, which are of central interest for climate modelling purposes. Such models assume that the vertically integrated transport is divergence-free, thus allowing for a two-dimensional scalar streamfunction to specify the transport. Alternatively, a surface pressure formulation has been introduced by Dukowicz et al. (1993), in which the vertically integrated transport remains divergence-free yet the surface pressure is directly solved for instead of the streamfunction.

Although used extensively for ocean climate modelling with z-models over the past three decades, rigid lid models are steadily becoming obsolete, with free surface methods growing in popularity. Notably, free surface methods have been the norm in ρ-modelling (e.g., Bleck and Smith, 1990; Hallberg, 1995; Hallberg, 1997). The advantages of the free surface method are the following.

1. The rigid lid streamfunction method involves an elliptic problem with Dirichlet boundary conditions for the barotropic streamfunction, and the rigid lid surface pressure method involves an elliptic problem with Neumann boundary conditions. In general, elliptic problems in climate modelling are difficult to solve, with the following issues causing the most trouble in practice:
   - In simulations with complicated geometry (e.g., multiple islands), topography, time varying surface forcing, and many space-time scales of variability (i.e., the World Ocean), achieving a good first guess for the iterative elliptic solver is often quite difficult to achieve. This makes it difficult for elliptic solvers to converge to a solution within a reasonable number of iterations. For this reason, many climate modellers limit the number of elliptic solver iterations used, even if the solver has not converged. This approach is very unsatisfying.
   - Rigid lid streamfunction models are prone to numerical instabilities near regions of steep topographic slopes (Killworth, 1987). The cause is a factor of $1/H$ in the elliptic operator which is ill-behaved in these regions (Dukowicz et al., 1993). Such behavior has prompted some modellers to artificially smooth topographic features, especially in the high latitudes. Reformulation into the rigid lid surface pressure approach removes this problem since the elliptic operator is now proportional to H instead of $1/H$.

- Many elliptic solvers with their associated non-local and time dependent boundary conditions (be they Neumann or Dirichlet) do not project well onto parallel computers, which acts to hinder their scaling properties (Dukowicz et al., 1993; Webb, 1996; Webb et al., 1997; Griffies et al., 2000b). However, solvers specially designed for parallel machines, such as the one by Guyon et al. (1999, 2000), have shown some improvements.

2. As traditionally formulated, rigid lid models preclude the introduction of fresh water to the ocean since the total model volume is fixed. Mathematically, one sees this fact via the volume budget within a vertical column of Boussinesq fluid

$$\partial_t \eta = -\nabla \cdot \mathbf{U} + q_w, \tag{3}$$

where $\mathbf{U} = \int_{-H}^{\eta} \mathbf{u}\, \mathrm{d}z$ is the vertically integrated horizontal velocity, $z = \eta$ the ocean surface height relative to a resting ocean at $z = 0$, and q_w is the volume flux per unit area (units of velocity) of fresh water passing across the ocean surface ($q_w > 0$ represents an input of fresh water to the ocean). The rigid lid approximation sets $\partial_t \eta = 0$ in order to eliminate the fast surface gravity waves, and $\nabla \cdot \mathbf{U} = 0$ is necessary in order to determine $\mathbf{U}$ via a single scalar streamfunction $\mathbf{U} = \hat{\mathbf{z}} \wedge \nabla\psi$. With $\partial_t \eta = 0$ and $\nabla \cdot \mathbf{U} = 0$, the ocean volume budget (3) precludes a non-zero fresh water flux q_w, thus keeping the total amount of water in the ocean constant. [6]

   Virtual salt fluxes must then be used in order to indirectly introduce the effects of a hydrological cycle on ocean salinity and seawater density (Huang, 1993; Gordon et al., 2000). This approach assumes the ocean salinity is close to some global averaged value S_0. However, deviations from S_0 are common in climate models including realistic hydrological cycles, especially near river mouths. Such salinity deviations increase upon moving to refined model resolution where grid cells become smaller and fresh water perturbations increase the amplitude of localized salinity deviations.

3. The rigid lid distorts the dispersion relation for barotropic Rossby waves (see e.g., Dukowicz and Smith, 1994).
4. Rigid lid models preclude the direct incorporation of tidal processes. Such processes are important for regional models, and recently have become of interest to climate modellers due to the provocative ideas of Munk and Wuncsh (1998).

Free surface methods can, in principle, resolve each of the above limitations of the rigid lid method. However, in practice there are a number of assumptions which are built into the various free surface methods, and these limit the particular method's range of applicability.

4.2. Implicit free surface methods

The implicit free surface method was introduced into the z-models by Dukowicz and Smith (1994) (used currently in POP) and later employed, with some variations, by the MIT model of

[6] Huang (1993) sets $\partial_t \eta = 0$ yet allows for the balance $\nabla \cdot \mathbf{U} = q_w \neq 0$. In turn, he must solve for both a scalar streamfunction and velocity potential, each of which involve the solution of an elliptic problem.

Marshall et al. (1997a,b) and the HOPE model of Wolff et al. (1997). This approach solves the two-dimensional depth averaged momentum equations implicitly in time, hence allowing for the model's barotropic time step to equal the baroclinic time step. It does so by employing numerical damping to suppress the fast barotropic waves. Limitations of the implicit approach include the following:

1. Because of the large barotropic time step and associated numerical damping, it is not useful for tidal studies. A smaller time step can be used, but then one does not take full advantage of the approach.
2. It involves an elliptic problem with Neumann boundary conditions. The diagonal term in the elliptic operator that comes from the temporal change in surface elevation allows for the operator to be better conditioned than that arising in the rigid lid streamfunction approach (Dukowicz and Smith, 1994). Nevertheless, the remarks on elliptic problems in Section 4.1 apply here as well.
3. As currently implemented, the above mentioned z-models using an implicit free surface method employ a linearized shallow water approximation. In particular, in the barotropic continuity equation (3), undulations of the surface height are assumed small relative to the total ocean depth: $|\eta| \ll H$. Doing so avoids the need to solve a non-linear elliptic problem. This assumption is likely quite good for climate purposes, yet becomes questionable when resolving shallow coastal regions.
4. For purposes of solving the baroclinic velocity and tracer equations, the above mentioned z-models using an implicit free surface assume that the top model grid cell is much thicker than the surface height deviations: $|\eta| \ll \Delta z$. This assumption becomes less accurate as the vertical grid resolution is refined. Furthermore, it generally results in the use of an ocean which has a constant volume in so far as the tracer and baroclinic momentum budgets are concerned. In particular, such models suffer from the same problems with tracer conservation in the presence of a hydrological cycle as described in Section 4.1 for rigid lid models (see Roullet and Madec, 2000 and Griffies et al., 2000b for discussion).

The filtering method of Roullet and Madec (2000), recently implemented in the OPA model, has similar properties to the above implicit approaches, because the filtering operator must be solved implicitly. However, their method does not assume a constant top cell thickness (see Section 4.4). Developers of POP are also implementing a variable top-layer (R. Smith, personal communication 2000).

4.3. Explicit free surface methods

Explicit free surface methods involve a direct integration of the barotropic equations with gravity waves resolved using small time steps. This approach involves the fewest assumptions of the three approaches, and so it has the potential to be of greatest utility. Explicit free surface methods were introduced to the z-models by Killworth et al. (1991) and to ρ-models by Bleck and Smith (1990).

As mentioned earlier, Killworth et al. (1991), Higdon and Bennett (1996), Higdon and de Szoeke (1997), Hallberg (1997), Higdon (1999), and Dukowicz (2000) detail the rather subtle issues involving the difficulty of cleanly separating the fast and slow dynamical modes in a free surface ocean model. In particular, the Higdon and Bennett, Higdon and de Szoeke, and Hallberg papers document a linear instability present in the Bleck and Smith (1990) scheme that is currently used in MICOM and HYCOM. These papers propose new methods which should eliminate the Bleck and Smith instability. HIM uses the Hallberg method and POSUM uses the Higdon et al., method.

For z-models, Webb et al. (1998a) and Griffies et al. (2000b) indicate that the Killworth et al. (1991) method can be unstable under various situations. Both papers provide similar methods to stabilize the scheme via time averaging over the barotropic sub-cycle. Notably, such time averaging is typically used in the ρ-models for stability reasons, although it is not always sufficient to suppress the instabilities noted by the Higdon et al., and Hallberg studies.

Although seemingly less computationally efficient than implicit methods due to the use of short barotropic time steps, explicit methods have actually proven to be competitive for the following reasons.

- The ratio of baroclinic to barotropic time steps is fixed by the ratio of baroclinic to barotropic gravity wave speeds, and this ratio does not change with grid resolution. Hence, for example, a doubling of horizontal model resolution will require an eight-fold increase in computational load (four from the added spatial resolution and two from the smaller time step). However, when solving an elliptic problem, experience has found that the number of elliptic solver scans increases proportional to the largest of the two horizontal grid dimensions (in addition to increases which may arise via the presence of more transients). Doubling the resolution using the implicit free surface method therefore picks up the same factor of eight as for the explicit approach, but this factor is also multiplied by another "elliptic solver factor" that is larger than unity. Furthermore, as mentioned earlier, the question of whether one has converged to the optimal solution of the elliptic problem is absent in the explicit approach; the true solution is always found, by construction.
- The implicit and rigid lid approaches involve non-local boundary conditions via their elliptic problems, whereas the explicit free surface methods do not. Hence, explicit approaches provide enhanced computational performance on parallel computers (see further comments on elliptic problems in Section 4.1).

4.4. Variable top cell thickness in z-models

A natural means to handle undulations of the surface height is to discretize the vertical into pressure layers, or deviation of pressure from the atmospheric pressure. This is the approach used with HYCOM and the new prototype model of Huang et al. (2000). For the traditional z-models, there are two approaches taken. First, the free surface methods of Killworth et al. (1991), Dukowicz and Smith (1994), Wolff et al. (1997) and Marshall et al. (1997a,b) assume that the top model grid cell has a constant thickness for purposes of formulating the tracer and baroclinic velocity equations. This approach strictly precludes conservation of total tracer amount, especially in the presence of surface water fluxes. This limitation may become an issue for century to millenial time-scale integrations (Griffies et al., 2000b; Roullet and Madec, 2000).

A modification to the Killworth et al. (1991) scheme used by OCCAM accounts for the time varying top cell thickness in the tracer and baroclinic equations. Griffies et al. (2000b) detail an implementation of time dependent top cells with a related explicit free surface method in MOM.

Roullet and Madec (2000) have done likewise for the OPA model using their implicit time stepping scheme.

The introduction of variable top cells in z-models generally introduces some subtleties which are important to consider, yet easily handled, when aiming for tracer conservation, energetic consistency, and numerical stability. As shown by Griffies et al. (2000b), the MOM approach has utility for coarse resolution climate models, since the method remains stable upon the use of baroclinic and tracer time steps compatible with those commonly used in rigid lid models (see Section 3.3 for details).

4.5. Summary items

The main points from this section include the following:

- The rigid lid method is becoming obsolete for purposes of ocean climate modelling. The reasons include an inability to directly input fresh water to the ocean model, and difficulties solving elliptic problems with realistic surface forcing, topography, and variability.
- Computationally tractable implicit free surface methods exist which overcome some of the problems with the rigid lid, although they still involve the solution of an elliptic problem.
- Explicit free surface methods are used by all ρ-models and some z-models. They eliminate the elliptic problem and so provide a more straightforward numerical algorithm and added efficiency when implemented on parallel computers as compared to the rigid lid or implicit free surface approaches.
- In z-models, special care must be taken to incorporate the effects of an undulating thickness of the top model grid cell. Such is necessary for conservation of total tracer content in the presence of a hydrological cycle where water is naturally input to the ocean.

5. Surface mixed layer

The surface mixed layer, or oceanic PBL, is that part of the upper ocean which directly interacts with the overlying atmosphere and sea ice. In addition, external sources such as fresh water outflows from rivers are usually input to the surface mixed layer. Complex physical and thermodynamical processes govern the evolution of the surface layer as well as the fluxes of heat, freshwater, and other tracers into the interior via subduction. Accurate surface boundary layer models (for the atmosphere as well as the ocean) are thought to be crucial for coupled ocean–atmosphere models to converge to a realistic mean climate state, and to accurately simulate the variability about this mean state.

A "perfect" surface mixed layer parameterization for ocean climate models must simulate mixing driven by wind stirring at the sea surface, unstable buoyancy forcing, current shear instability, advection of turbulence, and non-local mixing such as the penetration of dense plumes into a stratified fluid and breaking internal gravity waves. All present mixed layer parameterizations assume one-dimensional physics in the vertical, using empirical constants and further parameterizations to represent the three-dimensional structure of the sub-grid-scale processes. The parameterizations are of two basic kinds: the bulk mixed layer models and continuous models. Bulk models assume that the surface mixed layer is fully turbulent and so velocity and tracers in the model are uniform over the mixed layer depth; continuous models allow for vertical structure.

5.1. Bulk oceanic PBLs

As shown in Fig. 1, the mixed layer is naturally represented with z or pressure coordinates. Isopycnal models, therefore, have difficulties in representing well-mixed regions of the ocean such as the surface PBL. Bleck et al. (1989) coupled a bulk mixed layer at the top of the ρ layers with entrainment/detrainment governed by the vertically integrated turbulence kinetic energy balance (Kraus and Turner, 1967; Gaspar, 1988). Although this approach has proven useful (e.g., Bleck et al., 1989; Chassignet et al., 1996; Bleck, 1998), the capability of bulk mixed layer models is limited by their inability to resolve vertical structure within the PBL. Such resolution is critical in subpolar regions where the PBL extends over hundreds of meters, as well as in regions where density is vertically mixed yet momentum is not (see Gnanadesikan and Weller, 1995 for example).

When coupled to ρ models, bulk mixed layers are also prone to numerous difficulties in implementation, with one often forced to introduce unphysical processes such as un-mixing. Extensive experience has proven that seemingly minor differences in how one decides to formulate the coupling between the component models can strongly affect the overall solution (Rainer Bleck, personal communication 1999).

There are two general approaches to address the problems with coupling bulk mixed layers to ρ-interiors. One approach is to insert a variable density "buffer layer" between the bulk mixed layer and the isopycnal interior (Murtugudde et al., 1995). This approach has been adopted by HIM and MICOM. A second more general approach uses a hybrid pressure-ρ coordinate structure with pressure used in regions of low stratification such as the mixed layer. This enables non-bulk, pressure coordinate mixed layer models to be naturally incorporated. This approach has been adopted by HYCOM. POSEIDON's approach is somewhat in between these two, in which a bulk mixed layer and isopycnal interior are matched via the model's generalized vertical coordinate.

Another class of vertical mixing scheme is represented by the quasi-slab model of Price et al. (1986) (PWP). In the PWP model, instantaneous mixing occurs if any of the following three criteria are satisfied: (1) the water column is gravitationally unstable; (2) the bulk Richardson number is <0.65; and (3) the gradient Richardson number is <0.25. Unlike bulk models of the Kraus–Turner type, the depth of the mixed layer base is not a prognostic variable, and the density increase at the mixed layer base is spread out over a finite depth range.

5.2. K theory and turbulence closure approaches

The bulk mixed layer models are deficient in some of the requirements described earlier that are desirable for a perfect mixed layer model. For example, PWP model does not account for the direct effects of wind stirring. The Kraus–Turner bulk models cannot explicitly represent the vertical structure of dynamical (such as velocity shear) and thermodynamical (T, S) variables, as well as of biochemical constituents. None of these schemes account for non-local mixing. Furthermore, the PWP parameterization tends to only work well on a high-resolution vertical grid which limits its usefulness for basin-scale and global ocean models.

In an effort to overcome some of the limitations, Chen et al. (1994) proposed a hybrid mixing scheme. Their approach combines the Kraus–Turner bulk model with the gradient Richardson number mixing criterion from the PWP model. The resulting scheme can therefore account for the joint influence of wind stirring, buoyancy forcing, and shear instability. However, it still lacks a parameterization of non-local mixing.

The most common class of vertical mixing scheme employed in ocean models involves K theory, which parameterizes vertical mixing as a function of eddy diffusivity and viscosity coefficients (K) times the vertical gradients of mean quantities. Some models prescribe these coefficients as functions of the gradient Richardson number (e.g., Munk and Andersan, 1948; Pacanowski and Philander, 1981). Others employ variants of the turbulence work of Mellor and Yamada (MY) (Mellor and Yamada, 1982; see also Mellor, 2000 and Ezer, 2000 for the most recent version of MY). The MY approach introduces a hierarchy of prognostic equations used to solve for various turbulence fields. Turbulent mixing length and velocity scales are computed which are then used to determine the vertical diffusivity and viscosity. Such formulations are effective in regimes with high current shear and/or regimes where advection of turbulence becomes a factor (e.g., coastal models such as Mellor, 1996), tropical ocean models (e.g., Rosati and Miyakoda, 1988; Blanke and Delecluse, 1993), and basin models (e.g., Ezer and Mellor, 1997; Hakkinen, 1999, 2000).

Large et al. (1994) (see also Large, 1998 for a pedagogical review) introduced to the ocean modelling community the K-profile parameterization (KPP) scheme, which is an approach often used in the atmospheric community (Holtslag and Boville, 1993). This development effort was designed to create a mixing scheme that accounts for all important processes, including non-local mixing, and that will perform well on a relatively coarse vertical grid. This approach can be summarized by the equation for vertical diapycnal transport of a tracer or velocity component ϕ

$$\partial_t \phi = \partial_z (\kappa \partial_z \phi - \gamma), \tag{4}$$

where κ is a space-time dependent vertical diffusivity, and γ is a non-local transport term. The means to determine κ are analogous to other approaches. For example, κ is large in regions of small Richardson number to account for shear instability, it reduces to the internal wave background of roughly 0.1–0.2 $cm^2\ s^{-1}$ in the ocean interior, and it allows for double diffusive type effects which can locally result in different salinity and temperature diffusivities (see Schmitt, 1998 for a pedagogical review). Large diffusivities and viscosities in the surface PBL result from surface wind stirring and unstable surface buoyancy forcing. The non-local term is more novel, as it aims to parameterize non-local (or non-diffusive) processes in the PBL which are well known from large-eddy simulations.

Studies such as Large et al. (1997) and Gent et al. (1998) show favorable behavior of KPP, which has prompted it to be implemented in the HYCOM, MIT, MOM, and POP ocean models, amongst others. Further testing of KPP is important in order for it to be used with confidence in global ocean models, and indeed for use in BBL physics (see Section 7).

Simulation of the full range of boundary layer physics is a tall order for any scheme to satisfy, thus prompting some to consider alternatives. One such scheme is that of Canuto and Dubovikov (1996) that has been extensively tested against laboratory data. A group at

NASA Goddard Institute for Space Studies (GISS) in New York, and the HYCOM group have plans to test this approach, though neither have results from large-scale simulations at this time.

5.3. Comments on convective adjustment

Because of the hydrostatic approximation, convective processes must be parameterized in primitive equation models. A method commonly used in ocean climate models for neutralizing gravitationally unstable water columns is the "convective adjustment" scheme. An early method for convective adjustment is that of Cox (1984), whereby a series of iterations act to homogenize vertically adjacent boxes if they are unstable. This scheme converges to a gravitationally stable column only after an uncertain number of iterations (infinite number required in some cases). Furthermore, as vertical resolution is refined, the scheme requires more iterations in order to reach the same level of stability as on the coarser vertical grid. An alternative convective adjustment scheme by Rahmstorf (1993) (similar to that of Marotzke, 1991) completely stabilizes a vertical column in one iteration of the algorithm. [7] Notably, this approach will instantaneously mix a heavy water parcel throughout a column, and so it can be thought of as using an infinite vertical diffusivity.

Another method to stabilize a gravitationally unstable column of water is to employ a large, but finite, vertical diffusivity in regions of gravitational instability. The use of implicit time stepping schemes for the vertical processes affords one the ability to perform such mixing. The study by Klinger et al. (1996) indicates that results of a hydrostatic model using this approach compare well with non-hydrostatic models that explicitly resolve convection.

In general, the use of finite vertical diffusivities is more satisfying computationally than the convective adjustment approach of Cox (1984) due to its lack of dependence on the vertical grid resolution of the diffusion approach. Furthermore, as resolution is refined and time steps reduced, instantaneously mixing a parcel from the surface to the bottom within a single time step, as with the Rahmstorf (1993) scheme, is unphysical. It is for these reasons that most of the newer mixed layer schemes employ a finite vertical diffusivity in regions of vertically unstratified water, instead of relying on convective adjustment.

5.4. Summary items

The main points from this section include the following:

- All mixed layer schemes are based on one-dimensional "column physics" paradigms.
- Bulk mixed layer models are well-suited to z-coordinate configurations and have been adapted to ρ-models. This coupling to ρ-models, however, has proven to be cumbersome and somewhat ad hoc. One approach to overcome the problems is to insert a "buffer layer" between the bulk layer and isopycnal interior. Another is to employ a hybrid pressure–density coordinate.

[7] Rahmstorf's ocean convection method is analogous to the Manabe et al. (1965) moist convective adjustment scheme used in some atmospheric models.

- In either depth or pressure representations of the mixed layer, various continuously formulated surface mixed layer parameterizations are available based either on turbulence closure ideas (e.g., Mellor–Yamada) or "K" profile schemes (e.g., KPP). The KPP scheme has grown in popularity with climate modellers as it provides a ready framework to parameterize mixing driven by wind stirring at the sea surface, unstable buoyancy forcing, current shear instability, and non-local processes, but without the overhead of turbulence closure models.
- Gravitationally stabilizing vertical columns using large, but finite, vertical diffusivities compares well with results from non-hydrostatic models, where convection is explicitly resolved. Ocean climate modellers are tending towards this approach rather than the older convective adjustment schemes.

6. Bottom topography

The representation of bottom topography in ρ and σ models is quite accurate, and neither imposes a distinction between bottom and sides, hence allowing for a faithful representation of f/H contours, in particular. Z-models, in contrast, traditionally impose a distinction due to the use of fixed thickness rectangular bottom cells. Recent improvements with topography in z-models, however, have largely overcome the egregious aspects of this representation, and such is the topic of this section.

6.1. Bottom grid cells in z-models

The most general approach in z-models is that of Adcroft et al. (1997), in which finite volume methods [8] are used to fully contour the bottom cell to conform piecewise linearly to the actual topography (Fig. 3). This *shaved cell* approach brings the bottom cell representation in line with that of the ρ- and σ-models.

A less complete method, but one which is significantly cheaper on memory, is to keep the bottom cell rectangular, yet to allow its thickness to be a function of latitude and longitude as determined by the observed bottom topography. Adcroft et al. (1997) show that this *partial cell* approach achieves much of the shaved cell improvements. An early version of partial cells was developed by Cox and used, for example, by Huppert and Bryan (1976). However, it never was officially released as part of Cox's code.

Prompted by the work of Adcroft et al. (1997), efforts for MOM by Pacanowski and Gnanadesikan (1998) have provided a general implementation of the partial cell ideas for a B grid. The partial cell approach, rather than the shaved cells, is used in practice by the MIT group for their large-scale ocean modelling, as its simulations are nearly as good as the shaved cells, and it is more efficient (A. Adcroft, personal communication 2000). Additionally, the Los Alamos group has recently ported partial cells into POP. Table 5 summarizes the representations available in the various z-models.

[8] Finite volume methods are naturally formulated on a C grid.

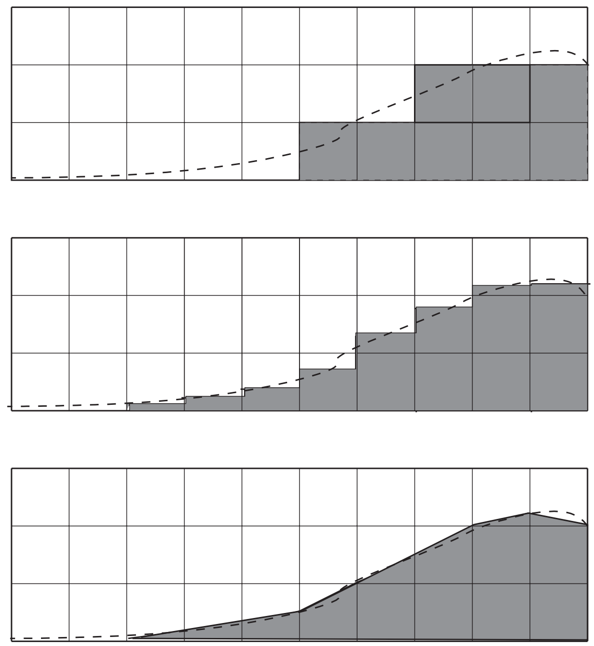

Fig. 3. Example of three representations of the ocean bottom available in z-models. Top: The old-fashioned ‘‘full cell’’ approach in which vertical thicknesses of all cells are independent of latitude and longitude. Middle: The ‘‘partial cell’’ approach in which vertical thicknesses of the bottom cells can vary according to the topographic features. Bottom: The ‘‘shaved cell’’ approach, in which the bottom cell is a piece-wise linear fit to the topography. Both full and partial cells have discontinuous representations of the bottom, whereas the shaved cell has continous depth, but discontinuous gradient. This figure is based on Fig. 4 from Adcroft et al. (1997).

Table 5
Summary of methods available to represent the bottom topography in the various z-models

Z-model	Available bottom representation
CANDIE	Partial & full
COCO	Full
GISS	Full
Hadley	Full
HOPE	Partial
MIT	Shaved, partial, & full
MOM	Partial & full
OCCAM	Full
OPA	Full
POP	Partial & full

There are two characteristics of shaved and/or partial cells which are worth highlighting. First, when refining the horizontal resolution without altering the vertical resolution, a full cell representation of the bottom does not improve, whereas a partial or shaved cell representation does (see Figs. 1 and 2 of Pacanowski and Gnanadesikan, 1998). Second, as the vertical resolution is refined, but the horizontal grid is held fixed, model solutions using partial cells show much less change relative to the full cells (see Fig. 12 of Pacanowski and Gnanadesikan). That is, the partial cell simulation is more robust than those with the full cell, because the representation of the bottom is basically unaltered when only the vertical resolution changes. Such added robustness of the model solution towards refinements in vertical resolution can be quite important, especially given the sensitivity of overflow processes to seemingly small changes in the representation of the bottom (see Roberts and Wood, 1997; Ferron et al., 2000 and Section 7).

Both Adcroft et al. (1997) and Pacanowski and Gnanadesikan (1998) papers provide examples of the changes in simulations realized with the improved representations of topography. Notably, simulations in steep sloped regions show minor differences between the full cells and partial/shaved cells. However, differences are clear in areas of shallow topographic slope, where full cells tend to produce plateaus with abrupt drop-offs, whereas partial or shaved cells more accurately represent the shallow slope. Correspondingly, the propagation of topographic waves is superior with the partial or shaved cell approach relative to the full cells.

Nonetheless, with partial cells the imperfect representation of the kinematic bottom boundary condition can still lead to significant errors in the propagation of topographic waves (Gerdes, 1993a especially Fig. 1 and corresponding discussion). Experience with the CANDIE model indicates a superior representation of coarsely resolved bottom trapped topographic Rossby waves when implementing partial cells on an A grid rather than their original C grid used by Sheng et al. (1998). The results with the revised A grid formulation are similar to those presented by Pacanowski and Gnanadesikan based on the B grid MOM code. These results, and further experience with the DieCAST model have prompted the CANDIE developers to switch from their original C grid as discussed by Sheng et al. (1998) to the A grid (Dan Wright, personal communication 2000).

Because of the "σ-nature" of partial or shaved cells, two terms appear when computing the horizontal pressure gradient in the model's bottom cells (see Eq. (2) and discussion). However, in contrast to σ-coordinate models, difficulties attributed to this term have been found to be minor in z-models. Notably, the extra pressure gradient term occurs *only* in the bottom grid cells. Careful treatments (e.g., Pacanowski and Gnanadesikan, 1998; Song and Wright, 1998a,b,c) have thus resulted in a negligible "pressure gradient error" for partial cell z-coordinate ocean models.

6.2. Summary items

The main points arising from this section include:

- Density coordinate models provide a piecewise linear representation of the ocean topography. They impose no distinction between bottom and sides.
- Depth coordinate models have traditionally employed constant thickness, or "full cells", for representing topography, and so distinguish bottom from sides. Development of shaved cells brings the z-model topography representation in line with ρ-models. The partial cell representation is an abbreviation of the shaved cell, and it garners a great deal of the shaved cell advantages yet with less computational burden. Partial cells impose a distinction between bottom and sides.

7. Overflow representation

The representation of dense outflows from marginal seas has received increased attention in recent years. Outflows play a key role in both the long-term, thermohaline equilibrium structure of the ocean (by setting the properties of much of the ocean's deep water masses) and by affecting the decadal-scale, dynamical response of ocean transport patterns to changes in high-latitude buoyancy forcing. With regard to the latter aspect, the outflow through Denmark Straits of Nordic Sea water, which is the source for the densest component of North Atlantic Deep Water, has been found to be of particular importance (e.g., Döscher and Redler, 1997; Lohmann, 1998).

A realistic simulation of outflow phenomena is faced with a number of delicate physical processes, with the following three of crucial importance. First, the formation of dense water masses in the marginal seas involves, for the case of the Nordic Seas, complex sea ice and shelf dynamics. Second, the sill overflows typically involve passages through the ridge and are under the control of hydraulic effects, each of which are highly dependent on topographic details. Third, the downslope flow of dense water, typically in thin (100 m or less) turbulent layers near the bottom, may strongly entrain ambient waters and are modulated by mesoscale eddies generated near the sill (e.g., Price and Baringer, 1994; Baringer and Price, 1997; Käse and Oschlies, 2000; Junclaus and Mellor, 2000; Ferron et al., 2000).

Development efforts in recent years have primarily concentrated on the downslope flow of dense water, and a summary is given below. In contrast, there has been little progress concerning the question of how to parameterize the physics of throughflows in large-scale ocean models. While process models with very fine resolution have become quite realistic (e.g, Käse and Oschlies, 2000), there is no obvious parameterization of rotating stratified flows over sills for models using grid resolutions practical for climate studies. For references describing such flows, see those listed in the Report of the WOCE/CLIVAR Workshop on Ocean Modelling for Climate Studies, WOCE Report No. 165/99, as well as Pratt and Lundberg (1991), Killworth (1995) and Whitehead (1998).

7.1. The DYNAMO experience

The simulation of downslope flows of dense water differs strongly between ocean models based on different vertical coordinate schemes. A major problem of z-models arises from the stepwise discretization of topography which tends to produce gravitationally unstable water parcels that rapidly mix with the ambient fluid as they flow down the slope. The result is a strong numerically induced mixing of the outflow water downstream of the sill (e.g., Roberts et al., 1996; Winton et al., 1998). This problem is avoided in both σ- and ρ-models. However, σ-models require a large amount of topographic smoothing in order to alleviate pressure gradient errors (see Section 2.3). Such smoothing distorts passage topographies. Additional problems also arise from spurious diapycnic mixing effects depending on the local orientation of the mixing tensor, and from reduced BBL resolution in deep water. In contrast, downslope flows of dense water in ρ-models will not mix with surrounding water masses unless diapycnal mixing is prescribed in regions of strong entrainment (see Hallberg, 2000 for a discussion).

A systematic comparison of model behaviors in the Greenland–Iceland–Scotland ridge regime, and their consequences for the meridional overturning in the North Atlantic, was performed in the European Union project DYNAMO (DYNAMO Group, 1997). The chosen model configuration was an attempt to isolate the performance in the downslope flow regime. All models used horizontal resolution at 1/3° Mercator [9] and specified the northern water masses by a relaxation to a given climatology. In particular, potential densities (in σ_0 units) of 28.00–28.05 and net outflows of 4-5 Sv were set at the Denmark Strait sill. A strong divergence in the outflow characteristics was noted, especially for the first few grid boxes south of the sill. While the ρ-model basically kept the density of the overflow (which resulted in an overly dense North Atlantic Deep Water), both the σ- and z-models exhibited rapid mixing in this region. The result was a much too buoyant (density of about 27.90) outflow compared to observations (density about 27.95) south of Cape Farewell. This relatively localized problem was identified as a leading cause of model deficits in important aspects of the large-scale meridional overturning circulation (Willebrand et al., 2000).

7.2. *Overflow representation in z-models*

During the last few years, parameterizations have emerged that attempt to minimize the often sizable levels of spurious diapycnal mixing associated with flows over stepped topography. As shown by Roberts et al. (1996) and Winton et al. (1998), and as mentioned above, such mixing can result in the premature loss of a dense water signal as it moves down the slope. One means to view the problem is to note that coarse resolution models are unable to produce relative vorticity on the order of the Coriolis parameter. Such large relative vorticity values are experienced in potential vorticity conserving flows undergoing large changes in water column thickness seen in the overflow regions. Instead, potential vorticity in coarse models can be spuriously altered via friction and diapycnal diffusion (Gerdes, 1993b), usually degrading the properties of the overflowing water. The introduction of partial and shaved cells (see Section 6) somewhat reduces the degree of such mixing, yet there are still problems especially in the steep sloped regions. In general, maintaining negligible levels of spurious mixing with downslope flows, along with parameterization of unresolved physics such as entrainment, remains a difficult problem with z-models.

Among the proposed schemes is that of Beckmann and Döscher (1997), with variations suggested by Campin and Goosse (1999), in which they introduce a terrain-following BBL. Horizontal velocity and tracer fields in the boundary layer are taken from the z-coordinate model, while the boundary layer returns modified tracer tendencies to the bottommost and adjacent tracer boxes of the z-coordinate model. These schemes provide a representational framework for getting the dense water down the slope, rather than a physical parameterization. More physically ambitious, yet technically elaborate, schemes are those of Gnanadesikan and Pacanowski (1997) and Gnanadesikan (1999) (implemented in MOM), Killworth and Edwards (1999) and Nurser et al. (2000). Notably, these schemes take account of lateral pressure gradients within the BBL.

[9] With a Mercator grid, the latitudinal grid spacing decreases as the poles are reached so that the grid cells remain square. Since eddies exhibit both strong zonal and meridional gradients, Mercator grids are favored for eddying models.

Doing so, however, necessitates great care in representing these gradients in order to avoid serious problems with pressure gradient errors familiar from σ-models (see Section 2.3). The approaches of Song and Chao (2000) and Nurser et al. (2000) aim to reduce these errors in a manner analogous to the method of Song and Wright (1998a,b,c) used for σ-models.

Early tests with these schemes have usually been run in idealized process configurations (e.g., downslope flow of dense water on a wedge of constant slope). As yet, there are few examples of their performance in more realistic global settings, with the study of Nurser et al. (2000) a recent exception. North Atlantic basin experiments with Beckmann and Döscher (1997) scheme indicate that the properties of Denmark Straits Overflow Water can indeed be improved with this simple parameterization (Dengg et al., 1999). Unfortunately, the optimal parameters setting the details of this scheme will likely require re-tuning for different overflows.

7.3. Overflow representation in ρ-models

Gravity plumes are naturally represented in ρ-coordinates. Additionally, there is no spurious numerical mixing as the dense water flows down a steep slope, nor is there a pressure gradient error problem. Hence, in the absence of a parameterization of the unresolved physics (i.e., entrainment), the overflow water basically keeps its density and does not mix with the surrounding waters. Such was a systematic problem with the MICOM contribution to DYNAMO. In the real ocean, diapcynal mixing becomes large in regions of strong entrainment and so needs to be parameterized. Until recently, diapycnal mixing algorithms in ρ-coordinates were implemented via explicit time stepping schemes (Hu, 1996; McDougall and Dewar, 1998). Unfortunately, numerical stability constraints limit the levels of mixing which can be simulated, often to levels far below those needed to represent the strong and fast mixing observed in such regions.

However, Hallberg (2000) recently proposed an implicit time stepping approach for diapycnal mixing that permits arbitrarily large levels of mixing, thus allowing for the needed rates of water mass transformation. Notably, implicit vertical mixing in an isopycnal model is non-trivial due to the non-linear nature of diapycnal processes in such models. The Hallberg scheme was successfully implemented in HIM and MICOM, and various parameterizations of the entrainment are presently being evaluated with these codes.

7.4. Bottom boundary layer

The BBL is the well-mixed layer (analog of the surface mixed layer) that is present at the ocean bottom (Armi and Millard, 1976). Its thickness is of the order of several tens of meters, depending on the topographic roughness and the velocity of the fluid. It is generally agreed that this layer plays an important role in the entrainment process associated with the dense overflows.

Neither the z- nor the ρ-coordinate models are well suited for an accurate representation of the BBL. Typically, its effects are parameterized via a simple quadratic friction law. In contrast, σ-models can accurately represent this bottom mixed layer through the use of a turbulence closure scheme, such as those used in the surface mixed layer. Unfortunately, high vertical resolution close to a sloping bottom, without relatively high horizontal resolution (Mellor et al., 1994), is prone to large pressure gradient errors in σ-models.

There is currently no compelling evidence that an OGCM needs to *resolve* the BBL everywhere in the World Ocean to address the goals of ocean climate modelling. However, since a correct representation of the overflow is crucial, a good understanding of the BBL's role is of central importance.

7.5. The dynamics of overflow, mixing, and entrainment (DOME) project

Improvements in the representation and parameterization of outflow dynamics are of high priority in ocean model development. In general, simulations have been found to be strongly dependent on choices of vertical coordinate schemes, resolution, entrainment parameterization, and BBL dynamics. Because of this large range of factors, the Workshop on Ocean Modelling for Climate Studies in Boulder, 1998, called for "coordinated studies on the representation of downslope flows [...], first of all in the North Atlantic (especially Denmark Strait outflow and Gulf of Cadiz) where the data coverage is best. Model intercomparisons need to be complemented by exploration of sensitivites to bottom friction, newly developed submodels for the BBL, and mixing schemes."

Prompted by this mandate, an international overflow intercomparison study ("DOME") has been initiated in 1999, under coordination of the GFDL ocean modelling group. The initial focus is on model behaviors in an idealized outflow scenario. This study will be followed by experiments with realistic configurations for the Denmark Strait and Mediterranean Outflow, and finally, quasi-global simulations. Information can be found at the website: `www.gfdl.gov/~rwh/DOME/dome.html`.

7.6. Summary items

The main points from this section include the following:

- Overflow processes are crucial for climate modelling as they set much of the properties of deep water masses of the World Ocean.
- The z-models typically allow too much mixing of dense water masses as they move downslope (large amounts of entrainment produces too light deep waters), whereas ρ-models typically do not mix enough (small amounts of entrainment produces too heavy deep waters).
- Concerted efforts are underway to remedy these problems. In z-coordinates, preliminary approaches have shown some improvements in deep water properties. In ρ-models, a recent method allowing implicit vertical mixing, which permits physically large mixing via entrainment, has also shown much promise.
- Significant effort remains to test the current schemes in realistic climate models, to develop new approaches based on idealized process studies, and to assess the degree to which the variety of overflow and BBL processes are crucial for climate modelling.

8. Equation of state

In the primitive equation system, density is a diagnostic variable. The in situ density is needed to compute pressure gradients, and locally referenced potential density is needed to calculate vertical stability (to parameterize convection) and neutral directions (to parameterize eddy mixing). Density is determined by the equation of state, which for seawater is a complicated non-linear function of pressure, salinity, and temperature, with the UNESCO equation the standard form (e.g., Appendix 3 of Gill, 1982). Notably, this equation encompasses many important physical processes such as cabbeling and thermobaricity (e.g., McDougall, 1987b). Z- and ρ-models handle the equation of state quite differently, prompting separate discussions here.

8.1. Z-models

The treatment of the equation of state in z-models is straightforward and can be quite accurate. Indeed, as the models improve and the simulations reach new levels of realism, some of the traditional approximate approaches may prove to be less than ideal. Eliminating the inaccuracies is not difficult, and viable approaches have been provided.

Z-models based on Bryan–Cox–Semtner lineage have traditionally approximated the UNESCO equation by fitting a separate cubic polynomial at each of the discrete model depths (e.g., Bryan and Cox, 1972 employ cubic polynomials). Webb (1992) advocated such an approach, yet emphasized the importance of an accurate reference equation of state from which approximations are made, especially for purposes of high latitude simulations.

The polynomial approaches are typically useful in models where salinity is close to a depth dependent reference value, as well as cases in which the model's vertical cell thickness is independent of horizontal position. The latter assumption is not satisfied by either the Adcroft et al. (1997) shaved bottom cells, or the Pacanowski and Gnanadesikan (1998) partial cells, since in these cases the center of the bottom cell continuously changes in depth depending on the local topography. As such changes can be many tens to hundreds of meters, it is not accurate to specify a pre-defined vertical depth for computing the polynomial coefficients. Further problems ensue upon allowing model salinity to deviate drastically from a reference value. River discharge, for example, can radically modify the salinity within a grid cell, thus causing it to reach values near zero.

For these reasons, some modellers have chosen to use the full UNESCO equation (e.g., OPA, as discussed in Merle and Morliere, 1988), even though the calculation of density could represent 15–20% of the computational load (Madec et al., 1998). Jackett and McDougall (1995) have introduced a new formulation of the UNESCO equation of state using potential temperature instead of in situ temperature. Because potential temperature is a prognostic model variable, while in situ temperature is diagnosed, their approach was found to save a significant amount of computer time (the cost of the equation of state is now reduced to 3–10% of total model runtime, depending on model configuration). The Jackett and McDougall equation is implemented in MOM and OPA. An alternative, which has been found to be faster and just as accurate (P. Killworth, personal communication 2000), is the equation of state formulated by Wright (1997a).

In general, it is possible that on some computers, the cost of computing the full equation of state can be negligible, so long as the code is organized so that the polynomial coefficients remain in the CPU registers or cache memory while the calculation is repeated for a series of model grid points. Such was the experience with Fine Resolution Antarctic Model (FRAM, The FRAM

Group, 1991), which ran on a Cray YMP. The same has also been found to be true for modern cache based computers such as the Cray-T3E and desktop PCs.

An additional approximation which is often used is to assume the pressure is given by $-\rho_0 g z$ for purposes of computing the in situ density, where ρ_0 is the constant Boussinesq density. Instead, it is a simple matter to compute density at time step τ via $\rho(\tau) = \rho[\theta(\tau), s(\tau), p(\tau - \Delta\tau)]$, where θ is the model's potential temperature, s is salinity, and the hydrostatic pressure is lagged one time step instead of performing an iterative approach (e.g., as done by Dewar et al., 1998). As described by Dewar et al., use of the hydrostatic pressure instead of $-\rho_0 g z$ can result in some improvements in accuracy. The method described here is currently used in MOM and has been found to require trivial added computation.

In MOM 3, neutral directions are still calculated using the Bryan and Cox (1972) approximate equation of state in order to save computation costs. Alternatively, the Jackett and McDougall polynomial expression can be used both for a direct calculation of the Brunt–Väisälä frequency and the neutral directions as a function of salinity and potential temperature (Madec et al., 1998). The added savings with the Wright (1997a) equation are currently being assessed in MOM.

8.2. ρ-models

With a realistic equation of state, there is no materially conserved density coordinate which is also monotonic with depth. For example, $p = 0$ was originally the common choice for a reference pressure used to define the potential density σ_0. Unfortunately, this choice leads to many ocean regions where neutral directions deviate substantially from σ_0 iso-lines (McDougall, 1987a). For example, use of σ_0 leads North Atlantic Deep Water living below Antarctic Bottom Water, and such was a notable problem with the MICOM contribution to DYNAMO. A related problem is the representation of thermal wind balance $f\rho\,\partial_z \mathbf{u} = -g\hat{\mathbf{z}} \wedge \nabla_p \rho$, with $\nabla_p \rho$ the horizontal density gradient along constant pressure surfaces and ρ the in situ density. Straightforward use of potential density leads to an inaccurate thermal wind velocity shear in regions where potential density deviates from in situ density.

Recently, $p = 2000$ db has become the norm for realistic isopycnal models, since this choice leads to fewer regions with coordinate inversions and greatly improves the structure of the simulated deep water masses (Sun et al., 1999). In general, the Sun et al., paper has addressed the above difficulties in an isopycnal model. They describe a method for including the buoyancy anomalies caused by thermobaricity by relaxing the strict correspondence between buoyancy and potential density. Their *virtual potential density* coordinate also reduces dynamical errors associated with the thermal wind balance.

In an isopycnal model with two active tracers and a non-linear equation of state, the question arises how to transport temperature and salinity while maintaining the integrity of the pre-defined density classes. MICOM has chosen to transport salinity and then to invert the equation of state to diagnose temperature. In principle, this inversion can be done by solving the UNESCO equation of state iteratively. The systematic errors inherent in iterative methods will, however, accumulate over time if the iteration is called at each time step. To address this issue, Brydon et al. (1999) generated a polynomial in θ, s, and p representing a best fit to UNESCO. This approach has been incorporated into MICOM, in which potential temperature is diagnosed in the interior [10] isopycnic layers from the prognostic salinity and potential density.

An alternative approach, taken by HIM, HYCOM, POSEIDON, and POSUM, is to explicitly transport and diffuse both thermodynamic variables θ and s. This approach permits modelling of cabbeling effects and helps guarantee global conservation of both heat and salt. As described by Oberhuber (1993), with θ and s prognostic, diapycnal mixing is introduced after the advective transport step in order to correct the layers back towards their pre-defined "target densities".

Much of the current research into generalizations of the isopycnal layer approach has focused on the non-trivial question of how to optimally define a materially conserved quantity whose iso-lines closely approximate neutral directions. As shown by McDougall and Jackett (1988), it is not possible to define a local field which can globally describe the envelope of neutral directions when using the ocean's equation of state. Hence, the goal is to define a conserved field whose iso-lines do not deviate significantly from neutral. Additional considerations arise when aiming to maintain the horizontal pressure force as the gradient of a scalar, which then precludes pressure gradient errors such as described in Section 2.3 for σ-models.

What determines a "significant" deviation from neutral is set by the very small amounts by which tracer transport in the ocean interior occurs across neutral directions (see Section 9 for more details). As coordinate surfaces deviate from neutral, advection and diffusion acting along these surfaces will induce some dianeutral mixing. The impact of dianeutral fluxes from diffusion can be reduced/eliminated by rotating the diffusion operator to act along neutral directions in a manner analogous to that employed in z-models (see Section 11.2). Unfortunately, as described in Section 9.3, such an approach is not readily available for advective transport.

There are two main approaches which have been documented in the literature to address the above issues. The approach taken by Sun et al. (1999) introduces two terms for the pressure force in order to admit a representation of thermobaricity in an isopycnal model. Since the second term is at least an order smaller than the first, their approach engenders negligible pressure gradient errors. de Szoeke (2000) and de Szoeke et al. (2000) propose an alternative in which their thermodynamic variable "orthobaric density" (determined via a fit to ocean climatology) maintains the pressure force as the gradient of a scalar. Since it is determined from climatology, the use of orthobaric density as a coordinate surface provides a better approximation to neutral directions than the σ_2 variable used by Sun et al. It therefore minimizes the amount of dianeutral mixing due to the advection and diffusion of tracer fields along these surfaces. However, basing a thermodynamic variable on ocean climatology may not be as ideal for long term climate change experiments as for simulations of the current ocean.

8.3. Summary items

The main points from this section include the following:

- Recent numerical representations of the full UNESCO equation of state for seawater have acceptable computational expense. Early approximations perform poorly in certain climate relevant situations (e.g., large perturbations to salinity).

[10] Note that both potential temperature and salinity are prognostic variables in MICOM's mixed layer.

- Representing the full equation of state in ρ-models is more cumbersome than z-models. However, recent developments appear to provide a tractable solution using a representation of thermobaricity.
- Research into generalizations of traditional isopycnal models balance the competing interests of maintaining a small pressure gradient error while providing a globally defined coordinate whose isolines are close to neutral directions.

9. Tracer transport in the ocean interior

Large-scale ocean currents and mesoscale eddies are the dominant mechanism for tracer transport in the ocean interior. Transport processes act to mix tracers within constant density layers (more precisely, along neutral directions) in a manner which transfers tracer variance to the small scales, at which point microscale processes act to absorb this cascade of variance. Additionally, the locally referenced potential density is stirred, or adiabatically rearranged, with very small mixing occurring between density classes.

Recent ocean measurements by Ledwell et al. (1993, 1998), Duda and Jacobs (1995), Kelley and Van Scoy (1999) and others, provide direct quantification of the above picture. Their results indicate that the amount of diapycnal mixing in the ocean interior, away from boundary influences, corresponds to a vertical/diapycnal diffusivity of roughly 0.1–0.2 $cm^2\ s^{-1}$, which represents a value some 10^8 times smaller than the epipycnal, or along isopycnal, mixing. Therefore, the representation of tracer transport in ocean models should ideally incur levels of spurious mixing, associated with numerical errors, that are less than the 0.1–0.2 $cm^2\ s^{-1}$ ambient level. Larger values may compromise the physical integrity of the simulated water masses.

9.1. Advection schemes

Over the past decade, ocean modellers have begun to employ more sophisticated advection schemes. The recent paper by Hecht et al. (2000) provides a useful overview with ocean model tests of the various schemes, and Table 6 summarizes the schemes commonly used or available in the various ocean models.

All models employ flux form advection schemes, hence allowing for trivial conservation of total tracer amount. In general, there is a well known and often frustrating tradeoff which exists between centered schemes and dissipative schemes. Centered schemes conserve first (i.e., total tracer) and second (i.e., tracer variance) moments yet admit dispersive errors which tend to result in unacceptably large ripples, overshoots, and extrema. Since the centered schemes conserve second moments, they are often called *conservative* schemes. In contrast, dissipative schemes, such as upwind biased schemes, suppress dispersion errors yet only conserve the first moment. Advection schemes attempt to optimize, in various fashions, the tradeoff between conservation and smoothness.

Until the 1990s, z-models have typically used the second-order centered scheme. However, z-modellers have more recently found schemes admitting some numerical dissipation to be of use for reducing the overall amount of dissipation in the ocean models while maintaining smooth and physically meaningful solutions. That is, in some cases, the net amount of diffusion can be smaller

Table 6
Summary of advection schemes used in the various ocean models[a]

Model	Active	Passive	Thickness
CANDIE	C2, C4, FCT	C2, C4, FCT	NA
COCO	UTOPIA	UTOPIA	NA
GISS	UP	UP	NA
Hadley	C2	C2	NA
HOPE	U3	U3	NA
MIT	C2, U3, C4	C2, U3, C4	NA
MOM	C2, C4, QH, FCT	C2, C4, QH, FCT	NA
OCCAM	QW	QW	NA
OPA	C2	MPDATA	NA
POP	C2, QH	C2, QH	NA
HIM	Easter w/VL or PPM	Easter w/VL or PPM	FCT, MPDATA, Hsu–Arakawa
MICOM	MPDATA	MPDATA	FCT
POSEIDON	C2, QW, C4	C2, QW, C4	Hsu–Arakawa
POSUM	MPDATA	MPDATA	MPDATA

[a] Different columns are provided for schemes transporting thickness (only relevant for isopycnal models), active (temperature and salinity) and passive tracers. Acronyms represent the following: NA = not applicable, C2 = second-order centered differences as used by Bryan (1969a), Cox (1984), and Semtner (1974), C4 = quasi-fourth-order centered differences as documented in the MOM manual, FCT = Flux corrected transport (Boris and Book, 1973; Zalesak, 1979; Gerdes et al., 1991; Thuburn, 1996), QH = Quick scheme (Leonard, 1979) as implemented by Holland et al. (1998), QW = Quick scheme (Leonard, 1979) as implemented by Webb et al. (1998b), MPDATA = Multidimensional Positive Definite Advection Transport Algorithm (Smolarkiewicz, 1984; Smolarkiewicz and Grabowski, 1990), Easter = Easter (1993), VL = Van Leer (1979), PPM = Piece-wise parobolic, UTOPIA = Leonard et al. (1993), Hsu–Arakawa = Hsu and Arakawa (1990), UP = linear upstream of Russell and Lerne (1981), U3 = third-order upstream.

with the dissipative advection scheme than with a centered scheme combined with an explicit diffusion operator (e.g., Farrow and Stevens, 1995). There are two popular dissipative advection schemes used in z-models. One is the Flux Corrected Transport (FCT) scheme of Boris and Book (1973), Zalesak (1979), and Thuburn (1996) as described and tested in MOM by Gerdes et al. (1991). This scheme combines a conservative centered scheme with a dissipative upwind scheme. Alternatively, the Quick scheme of Leonard (1979), as modified for leap-frog time steps by Holland et al. (1998) and Webb et al. (1998b), has been found to be of use since it is less expensive than FCT, yet still reduces dispersion errors relative to the centered schemes. Note that OCCAM uses a scheme known as the modified split Quick scheme (MSQ) which formally has a higher spatial order of accuracy than the scheme described by Leonard (1979).

For ρ-models, it has long been recognized that it is essential to move away from the conservative centered schemes, since layer thickness must maintain positive-definiteness, and centered schemes cannot guarantee such. Consequently, ρ-model developers have traditionally paid close attention to developments in numerical advection schemes and have found the schemes listed in Table 6 to be of use.

Many studies of advection consider the effects of various schemes on the transport of an idealized tracer patch or structure (e.g., Durran, 1999; Hecht et al., 2000). Various schemes do better or worse depending on the particular test problem. Additional considerations arise when allowing the flow to become turbulent, as emphasized by Shchepetkin and McWilliams (1998), Roberts and

Marshall (1998) and Griffies et al. (2000a). In such flows, the cascade of tracer variance to the grid-scale associated with mesoscale eddies must be dissipated. For ρ-models, dissipation can occur within a density layer without incurring any spurious diapycnal mixing. The situation in z-models, however, is much more difficult, and spurious diapycnal mixing typically will occur at non-trivial levels (Roberts and Marshall, 1998; Griffies et al., 2000a). These points are important as the modelling community further develops eddying ocean models. Hence, the remainder of this section aims to expose the key numerical issues.

9.2. ρ-models

By discretizing the vertical according to density classes, ρ-models assume tracer properties to be vertically homogeneous within layers, yet they directly control levels of cross-layer transport. To see how this control is achieved, it is useful to note that under conditions of no diapycnal transport, the isopycnal transport of thickness and tracer occur in ρ-models via separate, yet compatible, discretization of the following equations:

$$\partial_t h = -\nabla_\rho \cdot (h\mathbf{u}), \tag{5}$$

$$\partial_t (hT) = -\nabla_\rho \cdot (hT\mathbf{u}), \tag{6}$$

where $\mathbf{u} = (u, v, 0)$ is the horizontal velocity field, h the vertical thickness between density layers, ∇_ρ and ∂_t are the horizontal gradient and time derivative operators taken along constant density surfaces, and T is the tracer per unit volume (i.e., tracer concentration). The thickness equation Eq. (5) is an expression of volume conservation, and Eq. (6) represents a combination of volume and tracer conservation. The central point is that these equations involve only two spatial dimensions, where the operator ∇_ρ picks out that part of the convergence of horizontal thickness and thickness weighted tracer fluxes which occur along constant density surfaces.

In practice, the thickness and thickness weighted tracer equations must be discretized with some dissipation or mixing in order to absorb numerical noise and variance associated with discretizing the advective stirring operators. Experience has shown that the strong temporal and spatial variability of the h field requires use of positive definite, and preferably monotonicity-preserving transport schemes, not only for h (which has to remain positive by definition), but also for the thermodynamic variables as well. MICOM also finds it effective to add some along isopycnal diffusion to further control small scale noise. HIM employs the monotonic method of Easter (1993) in which the volume and tracer fluxes are constrained to be compatible. In that case, it has been found that no explicit isopycnal tracer diffusion is required for stability.

These issues are crucial in ρ-models since the tracer concentration T is diagnosed from the prognosed thickness weighted tracer hT. Hence, a spuriously small or negative thickness will render the tracer concentration meaningless. Importantly, the above methods which maintain positive thickness also maintain the isopycnal nature of the tracer transport. That is, there is no spurious diapycnal transport engendered. This "smoke screen of isopycnal mixing" [11] lends great utility to ρ-models for simulating transport in the ocean interior.

[11] An expression frequently used by R. Bleck.

9.3. Z-models

Advective stirring of tracer in a volume conserving z-model takes the form

$$\partial_t T = -\nabla \cdot (\mathbf{u} T) - \partial_z (w T), \tag{7}$$

with ∇ the horizontal gradient operator taken along constant z surfaces. The transport equation now involves a three-dimensional convergence. For a stratified fluid, the three-dimensional problem is substantially more difficult to accurately represent numerically than the two-dimensional transport equation considered in ρ-models. In the absence of explicit knowledge of the neutral directions, advection schemes in z-models rely on numerical accuracy to approximate the isopycnal transport processes trivially realized in ρ-models. How accurate is this representation?

The above question was addressed in the study of Griffies et al. (2000a), in which they considered two idealized model configurations, one without eddies and one with eddies, and directly diagnosed a vertically dependent spurious diffusivity associated with numerical realisations of advection. For the laminar model, so long as the flow structures (e.g., boundary currents, fronts, etc.) remain resolved with a nominal number of grid points (e.g., two grid points in the Munk boundary layer region), commonly used advection schemes (e.g., second- and fourth-order centered differences, FCT, Quick) were found to introduce only a negligible amount of spurious diapycnal mixing. This result is consistent with suggestions from numerous coarse resolution z-models in which small diapycnal diffusivity theories were in good agreement with numerical model solutions run at small explicit diapycnal diffusivity (e.g., Toggweiler and Samuels, 1997; Marotzke, 1997; Hirst and McDougall, 1998; Park and Bryan, 2000; Vallis, 2000).

In the presence of mesoscale eddies, the above advection schemes in the Griffies et al. (2000a) study exhibited more than an order of magnitude larger spurious mixing than the 0.1–0.2 $cm^2\ s^{-1}$ ambient background. The experiment in which such high levels were achieved used a grid resolution which was, according to conventional metrics (e.g., spectra), quite adequate to resolve the admitted mesoscale eddies (1/6° in a mid-latitude channel). Upon refining the grid resolution *without* altering the sub-grid scale dissipation parameters (e.g., keeping the viscosity fixed), hence ensuring that no new scales were admitted, the levels of spurious mixing were indeed reduced, roughly as the power of the truncation error in the advection scheme. Yet the resolution needed to reach negligible levels of mixing was roughly an order of magnitude higher than expected according to other metrics (e.g., at 1/9°, the channel model still had about 2–3 times too much mixing).

Besides dissipative advection schemes, modellers have conventionally relied on dissipation operators to absorb the variance cascade, much as mentioned for the case of ρ-models in the previous section. Some choose horizontal Laplacian diffusion (e.g., OCCAM), while others prefer horizontal biharmonic mixing due to its enhanced scale-selective properties (e.g., Semtner and Mintz, 1977; Bryan and Holland, 1989; Böning et al., 1996, the z- and σ-models used in DYNAMO). However, as noted by Roberts and Marshall (1998), horizontally aligned tracer dissipation operators, including biharmonic operators, spuriously mix tracer across neutral directions, even as the grid resolution is refined. There is no convergence to small diapycnal mixing levels as resolution is refined, since higher resolutions simply increase the gradients upon which the horizontal operator acts. The result is the notorious Veronis effect (Veronis, 1975, 1977) at all resolutions. [12]

Roberts and Marshall suggested that instead of horizontally aligned dissipation operators, z-modellers should introduce a new divergence-free velocity field to the Eulerian field, much as done with Gent and McWilliams (1990) (see Section 11) for the purpose of scale selectively suppressing noise, yet without spuriously mixing density classes. They showed compelling results with eddying models that suggest the utility of their "biharmonic GM operator". Work remains, however, to extend their approach to arbitrary tracers (they focused on density alone), where the addition of a biharmonic isopycnal mixing scheme would be necessary for the case of multiple tracers (e.g., Klein et al., 1998).

9.4. Inhomogeneities in the background diapycnal diffusivity

As discussed in Sections 5 and 7, boundaries such as the surface and bottom typically introduce a large amount of diapycnal mixing. Additionally, recent measurements indicate that over rough topography, and extending many hundreds to thousands of meters upwards into the water column, values of diapycnal mixing can be greatly enhanced due to the effects of breaking gravity waves (e.g., Polzin et al., 1997; Toole, 1998). This section focused on the numerical requirements of tracer transport in quiescent regions of the ocean interior where the mixing is very small. Nonetheless, understanding how to parameterize the large inhomogeneities in the background diapycnal diffusivity may play a crucial role in setting the large-scale properties of the ocean (Munk and Wuncsh, 1998).

9.5. Summary items

The main points from this section include the following:

- Eddies and currents transport tracers in the ocean interior in a manner which mixes predominantly along neutral directions, with dianeutral transport roughly 10^8 times smaller than the along, or epineutral, transport.
- Density models are ideally suited for representing interior ocean transport, at least in those regions where isopycnal layers closely parallel neutral directions. These models solve a straightforward two-dimensional transport problem, and by construction trivially maintain zero spurious levels of cross-layer mixing.
- Depth models can represent interior ocean transport quite well at coarse resolution where there is no turbulent cascade of tracer variance to the grid-scale. Unfortunately, when moving into the eddying regime, there is a fundamental problem of how to resolve the conflict of needing to absorb the tracer variance cascade without introducing non-negligible levels of spurious dianeutral mixing. This problem remains largely unsolved.
- Although small in many interior ocean regions, there are notable examples where the diapyncal diffusivity is enhanced many hundreds of meters above rough topography. Understanding how to parameterize this added mixing is an open question (see Toole, 1998 for discussion and references) which could prove to be important for ocean climate models.

[12] In principle, if one resolved the microscale, then convergence could result.

10. Momentum transport

10.1. Horizontal transport

There are two general ways in which the inviscid part of the horizontal momentum equation is written in ocean models. The first consists of an "advective form" used by MIT, MOM, OCCAM, and POP

$$\left[\partial_t + \mathbf{u} \cdot \nabla + (f + u \tan\phi/a)\,\hat{\mathbf{z}} \wedge \right]\mathbf{u} = -\frac{1}{\rho_0}\nabla p, \tag{8}$$

where ρ_0 is the constant Boussinesq density. As written here, this form assumes spherical coordinates in which a is the Earth's radius and ϕ is the latitude. The $u \tan\phi/a$ term is often called the "advective metric term" since it arises from the non-trivial metric on the sphere. Equivalently, via a vector identity (e.g., equation (2.4.1) in Pedlosky, 1987) and within the hydrostatic approximation, this equation can be written in the "vector invariant" form which eliminates the horizontal advection of velocity (e.g., Section 1.3-b of Madec et al., 1998)

$$(\partial_t + w\partial_z + (f + \zeta)\,\hat{\mathbf{z}} \wedge)\,\mathbf{u} = -\nabla[p/\rho_o + \mathbf{u} \cdot \mathbf{u}/2], \tag{9}$$

where $\zeta = \hat{\mathbf{z}} \cdot \nabla \wedge \mathbf{u}$ is the vertical component of the relative vorticity. The vector invariant form is so-called because it remains valid in any horizontal orthogonal coordinate system. In contrast, the advective metric term is dependent on the coordinate system. The vector invariant form is therefore useful for models with generalized orthogonal coordinates, and it is the form chosen by all the isopycnal models, as well as the z-coordinate OPA model.

The advective form is natural on a B grid, where it is commonly used with energy conserving centered difference numerics to advect velocity (Bryan, 1969a). In contrast, the vector invariant form on the B grid requires a larger grid stencil and is not commonly used. [13]

As a complement to the B grid, the vector invariant form is natural on the C grid, and so is the preferred form for many C grid ocean models. Correspondingly, potential enstrophy, rather than energy, is more readily conserved with this formulation. In particular, HIM and POSUM use an energy conserving scheme based on Sadourny (1975), whereas MICOM and OPA use Sadourny's enstrophy conserving scheme. Note that with any enstrophy conserving scheme, special limitations must be applied when layer thicknesses vanish, as they can in isopycnal models (Bleck and Smith, 1990). Furthermore, as detailed by Abramopoulos (1988), energy *and* potential enstrophy conserving schemes (Arakawa and Lamb, 1981) require smaller stencils on the C grid than B grid. POSEIDON is the only ocean model which uses the Arakawa and Lamb energy and potential enstrophy conserving scheme. [14] This scheme is not commonly used in ocean models, largely due to its relatively large grid stencils which are cumbersome with complicated boundaries.

---

[13] POSEIDON is an exception, in which its vector-invariant momentum equations can be solved on either the B or C grids.

[14] POSEIDON also uses Hollingsworth et al. (1983) correction for the energy gradient term.

10.2. Vertical momentum advection in B grid z-models

In B grid z-models, there are well known problems with up/down slope momentum advection as originally coded by Cox (1984). In particular, the Bryan–Cox–Semtner code has a vertical velocity which is calculated to advect the horizontal momentum, and this velocity is different from that advecting temperature and salinity. Webb (1995), Bell (1998) and Ishizaki and Motoi (1999) demonstrated that mishandling of the momentum advection induces grid-scale noise near topography. Webb noted that it is preferable to have a vertical velocity for momentum advection defined consistent with that for tracer advection in order to better represent marginally resolved phenomena. This method is standard in COCO, MOM (see Pacanowski and Griffies, 1999 for further discussion), OCCAM, and POP.

10.3. Summary items

The main points from this section include the following:

- Most z-coordinate models employ the energy conserving "advective" form of the momentum equation (there is one exception), whereas ρ-coordinate models (except OPYC) employ the "vector invariant" form in which either energy or enstrophy are readily conserved.
- Schemes conserving both energy and enstrophy are not commonly used in ocean models (there is one exception), largely due to the increased size of the grid stencil which becomes cumbersome with complicated land–sea boundaries. In contrast, either energy conservation alone or enstrophy conservation alone are more commonly chosen.
- Vertical momentum advection in B grid z-models requires some care to ensure compatibility between vertical advection of tracers and momentum.

11. Parameterization of mesoscale eddies

Over the past decade, there has been a flurry of activity aimed at parameterizing mesoscale eddies for use in coarse resolution climate models. Arguably it will be at least another decade before eddying climate models can be routinely used for large-scale climate modelling purposes, hence motivating continued investigations of eddy parameterizations. The field of mesoscale eddy parameterization has been dominated by two main ideas: the eddy–topography interaction ideas of Holloway (1992), and the eddy-induced velocity ideas of Gent and McWilliams (1990) and Gent et al. (1995) (both referred to as GM90 in the following). A brief overview of their impacts is provided in this section.

11.1. Eddy–topography interaction

A closed physical system will equilibrate to a state which maximizes entropy. Kraichnan (1975) applied this notion to inviscid two-dimensional flows, and he was soon followed by the study of Salmon et al. (1976) (SHH) who extended Kraichnan's work to one and two layered quasi-geostrophic (QG) turbulence in the presence of bottom topography. What emerged from the SHH study is a striking correlation between the equilibrium flow and the topography, with cyclonic mean currents around topographic depressions and anti-cyclonic currents around domes. That is, the maximum entropy solution, which can also be interpreted as the one possessing the least bias or the most likelihood, is one which has non-trivial structure rather than zero motion. A physical mechanism which provides a pathway to realize this solution is eddy–topographic form stress, as studied by Holloway (1987).

The ocean is neither a closed system, nor is it in a state of equilibrium. Instead, it is a forced and dissipative system. Nevertheless, when querying how relevant equilibrium statistical mechanical ideas are to the ocean, one must ask whether the time scales determining the rate at which a system reaches its maximum entropy state are faster or slower than the time scales which act to keep it out of that state (see Dukowicz and Greatbatch, 1999 for a discussion in the context of ocean gyre flows). This question is at the heart of non-equilibrium statistical mechanics.

Working under the hypothesis that eddy–topography interactions are able to systematically and relatively rapidly force the ocean towards its maximum entropy state, or a suitable approximation to this state, Holloway (1992, 1999) conjectured that it is relevant, and important, to include such non-equilibrium forcing in ocean models. In linear irreversible thermodynamics (e.g., DeGroot and Mazur, 1962), this forcing takes the form of a linear damping with empirically determined damping coefficients. Holloway's approach is similar, with the simplest form being that of a scale dependent damping towards a barotropic circulation determined by topography: $H\,\mathbf{u}^{\rm nep} = \hat{\mathbf{z}} \times \nabla\psi^{\rm nep}$, where $\psi^{\rm nep} = -f\,L^2 H$, L is a length scale largely acting as a tuning parameter, and $z = -H(x, y)$ is the ocean bottom. This parameterization, colloquially known as the "Neptune effect" (Holloway, 1986b) has been shown to improve coarse resolution primitive equation simulations via enhancements to boundary currents (e.g., Alvarez et al., 1994; Eby and Holloway, 1994; Fyfe and Marinone, 1995; Holloway et al., 1995; Sou et al., 1995; Pal and Holloway, 1996; Nazarenko et al., 1997; Marinone, 1998; England and Holloway, 1998).

During the past few years, there has been an increasing body of research aiming to further employ equilibrium and non-equilibrium statistical mechanics for ocean modelling. Notably, Merryfield (1998) has extended SHH to continuously stratified quasi-geostrophy, and Merryfield et al. (2000) have considered barotropic flow over finite amplitude topography. Frederiksen (1999) aims to provide a parameterization using turbulent closure theories. The statistical theories of Kraichnan–SHH incorporate only the energy and enstrophy invariants. A more general theory which brings in all invariants [15] has been proposed by Miller (1990), Miller et al. (1992) and Robert (1991) (see also Turkington, 1999 for an alternative perspective which is not in agreement with the Miller–Robert theory). Kazantsev et al. (1998) have considered the relevance of the Miller–Robert theory for ocean modelling, and in addition employed the "Maximum Entropy Production" ideas of Robert and Sommeria (1992) and Chavanis and Sommeria (1997) to propose a form for a vorticity diffusive flux which relaxes the system towards the maximum entropy state. Quite recently, Chavanis and Sommeria (2000) and Weichman and Petrich (2000) have independently extended the infinite invariant theory for the Euler equations to the shallow water equations. Two notable pedagogical review articles are those of Alvarez and Tintoré (1998) and Sommeria (1998). Finally, an intriguing application of statistical mechanical ideas to studies of

[15] Recall that potential vorticity is materially conserved for inviscid adiabatic fluids. Hence, global integrals of *all* products of potential vorticity are held constant by the ideal flow.

convection has been given by DiBattista and Majda (2000) and DiBattista et al. (2000), whose methods are motivated by Turkington (1999) study.

Although there have been global ocean model studies using "Neptune" (e.g., Eby and Holloway, 1994; England and Holloway, 1998), it is notable that currently no published global climate model uses a statistical mechanical motivated parameterization of eddy–topography interaction. One thing which is missing is a convincing theory for the amplitude of the parameterized stress. The stress may depend on the level of eddy kinetic energy, as well as the amplitude of barotropic tides since rectified currents from the tides may be as large as mesoscale eddy generated currents on some continental slopes. Notably, when used with a constant eddy parameter, the scheme adds energy to the mean flow in the presence of non-trivial topography. Given the very active research addressing many of these issues, one may guess that statistical mechanical parameterizations may soon be more common-place in climate models as the theories and process oriented numerical investigations mature.

11.2. Eddy-induced transport

Motivated by the property of baroclinic instability to adiabatically feed off the available potential energy (APE) in the mean flow, GM90 suggested a form for such a sink in coarse models. In z-models, the sink takes the form of a divergence-free eddy-induced velocity field $\mathbf{v}^*$, whereas in ρ-models the corresponding sink arises via downgradient diffusion of layer thickness or interface depth. In addition to such a sink, GM90 prescribed that an arbitrary tracer should be stirred by this eddy-induced velocity and mixed via a diffusion operator oriented according to the neutral directions, as described by various authors (Iselin, 1939; Montgomery, 1940; Solomon, 1971; Redi, 1982; Olbers et al., 1985; McDougall and Church, 1986; McDougall, 1987a; Gent and McWilliams, 1990; Griffies et al., 1998).

Notably, both thickness/depth interface diffusion and isopycnal tracer diffusion are natural in ρ-models, and have been standard practice in models such as MICOM since the early 1990s. [16] Hence, the direct influence of GM90 on the manner by which the ρ-modelling community integrates their models has been relatively minimal. In contrast, tests over the last decade have generally pointed to an improved physical integrity of z-models employing both isopycnal diffusion of tracers and GM90. Consequently, climate modellers running z-models have almost universally adopted some form of isopycnal diffusion with GM90 as standard practice. The following discussion thus focuses on these impacts on z-models.

11.2.1. Algorithmic considerations

Cox (1987) developed a means to rotate the diffusion tensor in z-models according to the locally referenced potential density. Unfortunately, his isopycnal diffusion algorithm was unstable, which made it necessary to add a non-trivial horizontal background diffusion to stabilize the scheme. Such horizontal diffusion largely counteracted the benefits of the rotated diffusion in that it introduced a large unphysical source of diapycnal diffusion in regions of non-zero isopycnal slope. A method used in OPA to remove the need for horizontal background diffusion is to pre-filter the

[16] See Holloway (1997) for a discussion of the history of thickness diffusion in ρ-models.

isopycnal slope prior to performing the rotation (Madec et al., 1998). A more general approach is provided by the algorithm of Griffies et al. (1998), who removed the Cox instability via a reformulation of the discretized diffusion operator. [17] Even without these fixes to the rotated diffusion schemes, some researchers using MOM-based code (although not all) have found that adding GM90 eddy advection stabilizes the Cox scheme so that horizontal diffusion can be removed. In general, removing horizontal background diffusion, and hence the associated Veronis effect (Veronis, 1975, 1977), has proven to be a key improvement to the z-model simulations.

As proposed by Gent et al. (1995), the GM90 eddy-induced velocity is given by

$$\mathbf{v}^* = -\partial_z(\kappa \mathbf{S}) + \hat{\mathbf{z}} \nabla \cdot (\kappa \mathbf{S}) \tag{10}$$

with κ a diffusivity and $\mathbf{S} = \nabla_\rho z = -\nabla\rho/\partial_z\rho$ the projection of the neutral slope into the two horizontal directions. [18] When advecting tracers, this eddy-induced velocity is added to the model's resolved scale velocity $\mathbf{v}$ to produce a divergence-free effective transport velocity $\widehat{\mathbf{v}} = \mathbf{v} + \mathbf{v}^*$. As an outgrowth of the isopycnal diffusion work of Griffies et al. (1998), Griffies (1998) suggested an alternative form of GM90, in which the eddy-induced velocity $\mathbf{v}^*$ is represented in terms of its vector streamfunction. The result is a transformation of the GM90 advective tracer flux into a skew tracer flux. It has been found that the combination of isopycnal diffusion plus GM90 skew-diffusion is generally much more efficient and numerically accurate to realize than the alternative isopycnal diffusion plus GM90 eddy-advection approach. In particular, the problems with noise introduced by realisations of $\mathbf{v}^*$, as pointed out by Weaver and Eby (1997), are largely overcome via the skew-diffusion approach. Additionally, the common choice of equal isopycnal diffusion and GM90 thickness diffusivities (e.g., Danabasoglu and McWilliams, 1995; England, 1995; Robitaille and Weaver, 1995; Duffy et al., 1995, 1997; Hirst and McDougall, 1996, 1998; Hirst et al., 2000) renders the following flux for isopycnal diffusion plus GM90 skew-diffusion:

$$\mathbf{F} = -\kappa \nabla T - \hat{\mathbf{z}} \kappa (S^2 \partial_z T + 2\mathbf{S} \cdot \nabla T). \tag{11}$$

Notably, the horizontal flux component is downgradient horizontal diffusion. No analogous simplification of the horizontal flux component results when implementing GM90 via the eddy-advection approach. As horizontal diffusion is trivial to implement in z-models, such a simplification greatly adds to the model's efficiency as well as its numerical integrity. The skew-flux approach is the standard form of GM90 in the MIT, MOM, and POP codes.

11.2.2. General effects on climate model solutions

There are many studies which have investigated the sensitivity of various ocean model simulations to the choice of lateral tracer mixing schemes. The early studies were quite encouraging as they showed a strong improvement of the solutions with isopycnal diffusion and GM90 as compared to the use of horizontal diffusion. However, there are many details which can affect the solution's integrity and hence numerous studies show some advantages are combined with disadvantages. The following provides a sample.

[17] Beckers et al. (2000) present alternatives to Griffies et al. (1998) scheme. Their approaches may be more appropriate especially passive tracer diffusion.

[18] This expression omits the surface and floor delta-functions created by setting the diffusivity to zero there, and such can cause strong flows as described by Killworth (1997).

Inclusion of GM90 in global ocean models results in generally improved stratification leading to a major reduction in convection at high southern latitudes (e.g., Danabasoglu and McWilliams, 1995; England, 1995; Robitaille and Weaver, 1995; Duffy et al., 1995, 1997; Hirst and McDougall, 1996, 1998). Notably, however, England and Holloway (1998) and England and Rahmstorf (1999) find that GM90 using a constant diffusivity can degrade the model performance in the North Atlantic where simulations were evaluated against observed chloroflurocarbon (CFC) uptake. They suggest that further GM90 studies are warranted which employ spatially variable diffusivities as deduced from the theory of Visbeck et al. (1997).

The above studies were performed with codes that employ the unstable Cox (1987) isopycnal diffusion scheme. It is therefore difficult to distinguish between improvements brought by GM90 and those arising from the use of smaller horizontal background diffusion. The paper by Gnanadesikan and Toggweiler (1999) provides one exception. They compared the distribution of silica in a coarse resolution global climate model run with the Griffies et al. (1998) isopycnal diffusion scheme, using no horizontal background diffusion, to a run with isopycnal diffusion plus GM90. The results with GM90 were clearly preferable to those without. Guilyardi et al. (2000) investigate the sensitivity of the upper ocean thermal balances to the choice of lateral mixing. They conclude that GM90 plus isopycnal diffusion (with a large uniform coefficient) is less preferable than isopycnal diffusion alone. Finally, Raynaud et al. (2000) investigate the impacts of lateral mixing on El Niño/Southern Oscillation (ENSO) variability. They find that ENSO characteristics differ in simulations using either horizontal diffusion, isopycnal diffusion, or isopycnal diffusion plus GM90. However, they do not conclude which choice is superior.

In general, as noted in the coupled model study of Hirst et al. (2000), the inclusion of GM90 in the ocean component of a coupled model might lead to at least three practical advantages. First, Rahmstorf (1995) has suggested that a coupled model that includes GM90 and is run with flux adjustment may display less residual drift as a result of reduced oceanic convection. Second, the heat flux adjustments required at high southern latitudes may be significantly smaller in a coupled model that includes GM90 than one that does not. This is because ocean models with GM90 tend to have surface heat fluxes at such latitudes that are relatively small and markedly less noisy than models without GM90, as a consequence of the reduced poleward heat transport (in the absence of horizontal diffusive flux) and subdued convection (Danabasoglu and McWilliams, 1995; Böning et al., 1995; Hirst and McDougall, 1996).

Third, biases in the pattern of global warming resulting from the unrealistic convective mixing in the Southern Ocean may be eliminated. Tests of CFC uptake in ocean models reveal that CFC penetration at high southern latitudes is much reduced, and generally more realistic, when the GM90 scheme is used (Robitaille and Weaver, 1995; England, 1995; England and Hirst, 1997). The reduced CFC penetration in ocean models using this scheme implies slower oceanic ventilation and possibly a reduced effective thermal inertia of the Southern Ocean (e.g., McDougall et al., 1996).

The first two of these anticipated results have been seen in the coupled model study of Hirst et al. (2000), who carefully compare two control (constant CO_2) integrations, one with GM90 and the other with more traditional isopycnal diffusion with horizontal background. Although the simulations with GM90 are far from perfect, they do represent improvements over the traditional approaches, hence verifying the hopes suggested by ocean-only studies.

The third anticipated result, namely the expected changes in Southern Ocean warming rates under increased atmospheric CO_2, is in practice sometimes complicated by differences in the control integration climatology (e.g., different sea ice extent) which may lead to changes in a range of feedback sensitivities (Hirst et al., 1996; Wiebe and Weaver, 1999; Lohmann and Gerdes, 1998). It appears that some similarity in the surface control climatologies for the versions with and without the GM90 scheme is required in order for the anticipated differences in warming rates to be realized (G. Flato, personal communication 1999; A. Hirst, personal communication 2000).

11.3. Current research into eddy-induced transport

In general, the coarse resolution z-model tests indicate the utility of GM90. This success has prompted a large body of studies whose aim is largely to clarify the theoretical foundation upon which GM90, or its related extensions, are based. Should one diffuse thickness or potential vorticity (PV)? Should the GM diffusivity be a constant, be flow dependent, and/or have a depth dependence? How is the isopycnal diffusivity related to the GM diffusivity? Should a closure provide just a sink of potential energy as in GM90, or allow for a transfer of APE to mean kinetic energy? Are local closures sufficient, or should non-local closures be considered as well? How should the boundary conditions be applied to the eddy-induced transport? Should a mesoscale eddy closure involve the momentum equations, via inter-facial form-drag, instead of, or in addition to, the tracer equations? These are just a few of the questions debated in the literature, with the following providing a brief, and very incomplete, account.

11.3.1. Attempts at refined diffusive theories

Several studies prompted by GM90 are based on the idea that diffusion of QG PV should form the basis of a closure, rather than layer thickness or interface depth (e.g., Marshall, 1981; McWilliams and Chow, 1981; Rhines and Young, 1982; Treguier et al., 1997; Killworth, 1997; Greatbatch, 1998; Wardle and Marshall, 1999). It is not obvious how to implement such an idea in a global primitive equation model, where QG is not generally valid and PV is not a prognostic field. Nevertheless, diagnosis of certain high resolution process simulations have indicated the validity of this idea (e.g., Lee et al., 1997; Marshall et al., 1999; Treguier, 1999), although a recent study by Drijfhout and Hazeleger (2000) counter by proposing that thickness diffusion is actually preferable in practice. On the other hand, the distinction between thickness and PV mixing may not be very significant. Notably, Smith (1999) shows using a QG scale analysis that the ensemble-mean adiabatic primitive equations can be formulated such that the eddy-induced transport velocity is associated with either a turbulent thickness flux or a turbulent PV flux, and that the two formulations are equivalent in the QG regime.

In general, downgradient diffusive parameterizations of turbulent fluxes are ultimately based on stochastic or random-walk models of turbulent diffusion. Dukowicz and Smith (1997) (see also Smith, 1999) showed that a stochastic theory appropriate for adiabatic stratified turbulence predicts, in its simplest form, a generalized form of the GM90 parameterization. While this analysis provides an underlying small scale theory for the GM90 parameterization, it remains to be seen to what extent the assumptions underlying the stochastic theory, and hence the assumptions of downgradient fluxes, apply to the real ocean.

Large-scale PV is a combination of three terms: isopycnal thickness, topographic height, and planetary vorticity. The Neptune parameterization represents the topographic part by adding a stress in the momentum equations. Some studies suggest that other pieces of the parameterization for PV mixing could be represented in the momentum equations, such as through the use of a large vertical viscosity (Olbers et al., 1985; Greatbatch and Lamb, 1990; Greatbatch, 1998; Greatbatch and Li, 2000; Gent et al., 1995; Smith, 1999). The work of Adcock and Marshall (2000), in which they study the effects of topography in a shallow water model, also provides some insight into these issues. In general, there currently has been no large-scale coarse resolution ocean model run to test the utility of PV-based closures over thickness-based closures.

Besides trying to understand whether it is thickness or PV which serves best as the basis of a closure, there are studies which aim to deduce a flow dependence of the mixing coefficient used to diffuse either thickness or PV. The papers by Held and Larichev (1996) and Visbeck et al. (1997) each propose methods for computing a mixing coefficient in terms of a length and time scale determined by properties of the coarse fields. The time scale is proportional to the Eady growth rate $f/\sqrt{Ri}$ for baroclinic instability, whereas the length scale is proportional to the Rossby radius NH/f (Visbeck et al.) or the Rhines length $(U/\beta)^{1/2}$ (Held and Larichev). [19] The study by Bryan et al. (1999) suggests that the Visbeck et al. scaling agrees better with high resolution model output than the Held and Larichev scaling. An additional study by Killworth (1997) is notable for providing a theory which deduces a depth dependent diffusivity, whereas Visbeck et al., and Held and Larichev studies do not directly address this issue. Results from the high resolution channel model study by Treguier (1999) are consistent with Killworth's idea.

There remains a dearth of large-scale coarse resolution studies to investigate the utility of a flow dependent thickness diffusivity. The only documented account is that of Wright (1997b), in which he compared a suite of constant coefficient GM90 experiments with a single run with the Visbeck et al. diffusivity. The tests were run with the Hadley Centre's 1.25° ocean model, and the results were generally favorable towards the Visbeck et al. diffusivity, hence prompting the Hadley Centre to employ this scheme in their climate simulations. Unpublished studies in coarser simulations (e.g., coarser than 2°) suggest that non-constant diffusivities may not be so advantageous at such modest to coarse resolutions (A. Adcroft, personal communication 2000; M. Roberts, personal communication 1998; report of the WOCE/CLIVAR Workshop on Ocean Modelling for Climate Studies, WOCE Report No. 165/99). Further study in this area is clearly needed.

11.3.2. Two additional conceptual issues

We offer here further comments which have some general applicability to the issues of parameterizing eddy-induced transport.

First, an important kinematic point has been raised by McDougall and McIntosh (1996, 2000), McIntosh and McDougall (1996) and McDougall (1998), in which they note the need to be careful when transforming between isopycnal (Lagrangian) and depth (Eulerian) coordinates (see Andrews and McIntyre, 1978 for a general discussion). In particular, this transformation

[19] Ri is the large-scale Richardson number based on thermal wind shears, f is the Coriolis parameter, and $\beta = \partial f/\partial y$ is its meridional gradient. A summary of how to implement Held and Larichev (1996) and Visbeck et al. (1997) length and time scales in a model can be found in the MOM Manual of Pacanowski and Griffies (1999).

directly affects how one interprets the variables carried by a coarse resolution ocean model. Their studies provide some caveats which may prove to be important when testing the validity of parameterization schemes within a z-coordinate framework.

Second, as intimated at various times in the discussion above, it is useful to note the distinction between layer thickness and interface depth. The distinction arises, in particular, when considering what GM90 means in practice in a ρ-model in the presence of sloping side boundaries. Notably, downgradient diffusion of layer thickness will cause interfaces to migrate up sloping topography (see Holloway, 1997), thus increasing APE and so acting counter to the GM90 goal of always reducing APE. However, downgradient diffusion of interface depth will move dense water down a slope, thus reducing APE. It turns out that the latter effect is what happens in practice when GM90 is implemented in its simplest form in z-models in the presence of topography (e.g., see Fig. 3 of Hirst and McDougall, 1996). When implementing GM90 in ρ-models, the distinction between the downgradient diffusion of layer thickness and diffusion of interface depth become more crucial and care must be exercised. MICOM diffuses interface depth rather than thickness just for this reason. Note that this distinction was not part of the original GM90 study as they focused on areas away from boundaries.

11.4. Testing theories with data

Problems related to parameterizing the ocean mesoscale eddy field, both in the open ocean and their interaction with topography, are conceptually and computationally very difficult. The problem is compounded by the lack of direct observational data which could help develop and test theories and applications.

Resolving the mesoscale eddy field synoptically is only practical with remote sensing (e.g., satellite altimetry and SST). For example, Le Traon and Dibarbouree (1999) demonstrate that mesoscale mapping is feasible using multiple altimeters. However, without complementary subsurface data, even such a capacity has limitations since we know from the previous discussions that it is the detail of the eddy transports along density surfaces which is critical. The global array of floats which are part of the *Argo* program presents the potential to address this key scientific need (Argo Science Team, 2000).

Creative and promising ideas of how to exploit satellite data for eddy parameterizations have been proposed by Holloway (1986a) and Stammer (1998) based on analysis of sea surface topography data from satellites. The study by Kushner and Held (1998) provides a compelling test of these ideas using atmospheric reanalysis data. It is hoped that further exploitation of satellite data will find use for parameterizing, and generally simulating (e.g., see Fu and Smith, 1996), ocean mesoscale eddies.

11.5. Summary items

The main points from this section include the following:

- Statistical mechanically based eddy–topography parameterizations (e.g., Neptune) have shown some improvements in the simulations of boundary currents. These methods are based on relaxing non-equilibrium flows to their maximum entropy states, and as such are quite distinct in principle from downgradient diffusive closures. Research into this area is active and shows some promise of providing general methods of parameterization. Currently, there are no global climate models which use such parameterizations.

- The GM90 scheme provides an eddy-induced advection, or equivalently a skew component to the tracer mixing tensor, motivated by the desire to adiabatically release potential energy from baroclinic flow. When combined with isoneutral diffusion, GM90 has been seen to enhance the physical integrity of most z-coordinate climate model simulations. GM90 in its simplest form is based on downgradient diffusion of layer thickness (or interface depth). Some form of GM90 has become ubiquitous in both z and ρ ocean climate models.
- Many studies motivated by GM90 have pursued extensions to the original ideas, with nearly all studies based on the assumption of local downgradient diffusion of either thickness or potential vorticity.

12. Horizontal momentum friction

Ocean models require frictional dissipation in order to suppress instabilities such as those associated with the grid Reynolds number, to provide a vorticity sink at western boundaries, and to generally suppress power at unresolved scales. In the presence of geostrophic-turbulence, friction must be sufficient to absorb enstrophy upon cascading towards the smallest resolved scales. Finally, frictional dissipation can be included as a physical parameterization of the effect of unresolved scales on the resolved scales. Currently, however, there is no generally agreed upon form of a physically motivated closure for linear momentum in ocean models. Notably, Laplacian momentum friction *has not* been motivated from first principles at the scales resolved in large-scale ocean models, even those admitting mesoscale eddies. As a result, the bulk of large-scale ocean models employ friction as small as feasible so long as it maintains the above numerical constraints. Such is the perspective taken in this section.

12.1. Constant viscosity friction

The simplest form of friction is constant viscosity Laplacian friction (e.g., OCCAM) or constant viscosity biharmonic friction (e.g., Semtner and Mintz, 1977; Bryan and Holland, 1989; DYNAMO, Böning et al., 1996). A biharmonic operator provides enhanced scale-selectivity over the Laplacian, and so allows for less dissipation at the resolved scales while concentrating it at the grid-scale. Even more scale selectivity can be achieved with an eighth-order Shapiro filter, which is the choice of POSEIDON. The biharmonic or higher order Shapiro filters are notable for their utility with eddying models, since it is here that one aims to achieve simulations in which the natural tendency for oceanic flows to exhibit hydrodynamic instabilities and turbulence is not handicapped by overly strong frictional dissipation.

12.2. Non-constant viscosity friction

Choosing a constant viscosity over the globe constrains the value to be large enough to control the most vigorous anticipated motions and to resolve all boundary currents. Unfortunately, there will generally be regions that contain an overly large level of friction than that needed to satisfy local numerical constraints. Hence, modellers have tried various approaches to reducing the local levels of frictional dissipation via the use of non-constant viscosities.

12.2.1. Form of the friction operator

Upon allowing non-constant viscosity on a non-flat geometry, such as the sphere, it is important to employ a form of the friction operator which both dissipates kinetic energy and conserves angular momentum. The naive use of the Laplacian operator with the non-constant viscosity is insufficient. These points were emphasized by Wajsowicz (1993), who provides a means for satisfying the desired constraints (see Smith et al., 1995; Murray and Reason, 1999 for a related implementation of friction with arbitrary orthogonal coordinates). These approaches are based on expanding in the continuum the covariant divergence of the symmetric stress tensor, and discretizing the resulting expression for the friction operator. Alternatively, one can implement horizontal friction as the discrete covariant divergence of the discretized stress tensor, as discussed by Smagorinsky (1963, 1993), Williams (1972), Rosati and Miyakoda (1988), Sadourny and Maynard (1997) and Griffies and Hallberg (2000).

Ocean current stresses and strains are not horizontally isotropic. Such has motivated recent research into the implementation of anisotropic stress tensors. A first test of such has been performed by Large et al. (2000). They introduce two horizontal viscosities, instead of the single value used in the conventional isotropic stress approach. Their results are intriguing and have been shown to improve their simulation, especially their equatorial currents. In the Large et al. formulation, the directions which break the transverse isotropy are aligned with the grid directions. A more general formulation has been developed for general curvilinear coordinates (R. Smith, personal communication 2000), where the direction which breaks the anisotropy can be chosen arbitrarily (e.g., in the direction of the local mean flow). This is the form of the friction operator currently implemented in POP.

12.2.2. A priori choices for the viscosity

Upon reaching the high latitudes with spherical coordinates, the convergence of the meridians means that the zonal grid spacing gets quite small. A viscosity which may be appropriate for lower latitudes may become too large for the high latitudes, and so violate the diffusion stability constraint. More generally, variable grid spacing imposes different numerical constraints on the viscosity. Without altering the viscosity according to the grid spacing, one is forced to either use a globally smaller viscosity, which is undesirable for purposes of resolving boundary currents, or a globally smaller time step, which will make the model less efficient.

A simple approach to overcome this problem is to rapidly taper the viscosity to smaller values as the pole is reached (e.g., Gent et al., 1998 tapered viscosity poleward of 84°N). A related approach is to make the viscosity vary like a power of the grid spacing Δ. For Laplacian friction, one may consider a viscosity varying as Δ^2, which leads to a constant momentum diffusion time scale, or as Δ, which leads to a constant diffusion velocity scale. The second choice was made in the DYNAMO models, with Δ^3 dependence for biharmonic friction (see also Maltrud et al., 2000). Generally, some care must be taken in these approaches not to reduce the viscosity so much as to allow grid noise.

12.2.3. Smagorinsky viscosity

Another approach, recently surveyed by Griffies and Hallberg (2000), is motivated by ideas of Smagorinsky (1963, 1993). The Smagorinsky viscosity is a function of the local horizontal rate of deformation times the local grid spacing

$$A_{\mathrm{smag}} = (C\Delta/\pi)^2|D|, \tag{12}$$

where C is a dimensionless scaling parameter, Δ a measure of the local grid spacing, and $D^2 = D_{\mathrm{T}}^2 + D_{\mathrm{S}}^2$ is the squared horizontal deformation rate. In Cartesian coordinates, the horizontal tension $D_{\mathrm{T}} = u_x - v_y$ and the horizontal shearing strain $D_{\mathrm{S}} = u_y + v_x$. The Smagorinsky viscosity is enhanced in regions of large horizontal shear, such as near boundaries, and reduced in quiescent regions, such as the ocean interior, as well as regions of smaller grid spacing, such as near the poles. Typically, this approach produces enough viscosity in those regions with vigorous currents, yet it can have a tendency to under-dissipate in the more quiet regions. Setting a minimum viscosity, such as that prescribed by the constraint that Munk (1950) boundary layer must be resolved by some two or more grid points, is an effective means to remedy this problem.

The overall strength of the Smagorinsky viscosity is set via a single non-dimensional number C, and this parameter is empirically determined in ocean models (see Smagorinsky, 1993 for a survey of theories setting C for three-dimensional homogeneous and isotropic turbulence). One advantage of this approach is that upon setting C for one model resolution, it is typically appropriate when resolution is changed. Griffies and Hallberg (2000) provide a discussion of this point.

The Smagorinsky scheme is a physically plausible parameterization of the effects of three-dimensional isotropic turbulence, and it has inspired many schemes commonly used in large-eddy simulations (e.g., see Galperin and Orszag, 1993 for a compendium). For large-scale geophysical fluid simulations, however, it has little physical justification since the unresolved scales are dominated by quasi-two-dimensional geostrophic turbulence. For this reason, Leith (1968, 1996) proposed an alternative approach based on two-dimensional turbulence. Leith's viscosity is proportional to the horizontal gradient of the relative vorticity times the cubed grid spacing. The Leith approach has found some use in atmospheric models (e.g., Boer and Shepherd, 1983), but it is not commonly used in ocean models for the following reasons. First, the Smagorinsky viscosity is more convenient to compute than the Leith viscosity due to the smaller required grid stencil, and because the deformation rate used to compute the Smagorinsky viscosity is furthermore needed to compute the stress tensor. Second, tests comparing the Leith and Smagorinsky schemes show little difference (G. Williams, personal communication 1998).

Various ocean modellers, such as Bleck and Boudra (1981), Rosati and Miyakoda (1988), Bleck et al. (1992), Sadourny and Maynard (1997) and Griffies and Hallberg (2000) have argued for the utility of the Smagorinsky approach with either a Laplacian or biharmonic friction operator. Hence, some form of the Smagorinsky scheme is the preferred approach for friction in MICOM, MOM, and HIM.

12.3. Summary items

The main points from this section include the following:

- Horizontal momentum friction in ocean models is employed for practical computational reasons. That is, there is currently no plausible first principles theory which motivates either the

Laplacian or biharmonic operators at the scales relevant for climate models. Both operators are used to suppress grid noise, maintain resolution of boundary currents, and provide a sink for enstrophy cascading to the grid-scale.
- The traditional approach to friction in ocean models is to employ a single horizontal viscosity, which arises from assuming horizontally isotropic frictional stresses. However, some new research suggests that two horizontal viscosities, which arise from an anisotropic stress tensor, provide enhanced simulation integrity.
- Either a priori specified and/or flow dependent Smagorinsky viscosities have been used, each to varying degrees of success.

13. Towards more realistic simulations

The early pioneering efforts in numerical ocean modelling of the 1960s–1980s, which were largely restricted to a few select laboratories possessing large computers, have led to today's quite diverse field where numerous investigators, as well as researchers in the larger labs, all play significant parts in trying to understand the ocean's role in the climate system. The environmental challenges of the 21st century, most notably those related to anthropogenic climate change (e.g., IPCC, 1995), lend a great deal of importance and relevance to such research. These issues, as well as a general drive to scientifically understand the ocean more deeply, prompt numerical ocean modellers to expend a large part of their efforts to improving the physical and numerical integrity of their simulations. The many areas touched upon in this paper, and the numerous areas omitted due to limitations of time and energy, provide some evidence that this field, which is admittedly part science and part art, has entered an era of healthy adolescence. It is probably a conservative prediction to say that numerical ocean modelling will continue to mature rapidly over the course of the next decades.

Much of the current research in ocean modelling, including the present discussion, is conducted in the context of coupled climate model development. The "tuning" required to make all the parts work well together and to produce physically relevant simulations often requires many years of work by teams of researchers. Because of this, advances made in algorithm development and process studies can take some 5–10 years to become mature in the coupled climate models. [20] It is difficult to see how to speed up this process, especially when atmosphere, ice, land, biogeochemical, ecological, etc. model developments are also involved. Like their meteorological relatives, ocean climate modellers are continually challenged to balance the scientific urge to enhance the physical integrity and accuracy of the simulations with the pragmatism needed to produce a computationally efficient coupled climate model. Maintaining this balance amongst the rich complexity of the climate system tends to make climate modellers a patient, yet persistent, sort of folk.

[20] For example, Gent and McWilliams (1990) ideas have perhaps only now reached a level of maturity in the z-coordinate climate models, some 10 years after the initial paper. Even so, some major climate centers have yet to publish research with a fully coupled climate model using this scheme.

13.1. Fewer approximations

There is a steady trend in ocean model development towards a discretization of more fundamental equations, and hence to the use of fewer a priori assumptions. The movement away from the rigid lid approximation towards a free surface is one example. Another is the use of refined grid resolution which improves the representation of the domain geometry and dynamics (see below for more on resolution). A third is the move towards the use of a full equation of state. This trend has occurred in parallel with the growth in computer power. Quite simply, in many cases we can afford a more faithful representation without needing to introduce many of the approximations that were essential some decades ago. Furthermore, as modellers aim to bring their simulations towards improved levels of physical realism for purposes of rationalizing ocean measurements and making predictions, it is important that the underlying equations of motion do not hinder their ability to do so.

Another approximation which has been re-examined over the past few years is Boussinesq approximation. Is it warranted to continue using its approximate form for the pressure gradient $\rho^{-1}\nabla p \approx \rho_0^{-1}\nabla p$ as well as its associated assumption of a volume instead of mass conserving fluid? The studies by Greatbatch (1994), Greatbatch et al. (2000), Mellor and Ezer (1995), Dukowicz (1997), Huang (1998, 1999), Huang et al. (2000), and McDougall et al. (2000), each raise these questions. The initial studies which concluded the Boussinesq approximation was accurate enough when compared to the state of ocean measurements. However, a new generation of remote sensing techniques holds the potential to measure bottom pressure to an accuracy of 10^{-3} m of equivalent depth on scales of several hundred kilometres (Wunsch and Zlotnicki, 1999; Hughes et al., 2000). Additionally, a non-Boussinesq model will allow for unambiguous interpretations of tide gauge and satellite altimeter measurements, without needing the adjustments described by Greatbatch (1994), Mellor and Ezer (1995) and Dukowicz (1997). For these reasons, Huang et al. (2000) and Greatbatch et al. (2000) argue that it is important to develop fully non-Boussinesq ocean models. They also provide some suggestions for how to proceed in this direction.

13.2. Grid resolution for ocean climate models

Most ocean modellers (at least the authors) are in agreement that higher resolution than currently common-place is crucial for simulating large-scale climate variations and change. The movement towards refined grid resolution is prompted by the goal of reducing dependence on frequently ad hoc sub-grid-scale parameterizations. Strictly, this goal is fleeting since there are potentially important dynamical degrees of freedom which will always remain unresolved, at least until we can perform molecular dynamical simulations for climate! Nonetheless, admitting newly resolved scales, no matter how modest, ideally allows the solution added room in phase space to explicitly manifest more of the underlying dynamical degrees of freedom which may be important for ocean circulation. Higher resolution also allows for a more faithful representation of ocean basin geometry (e.g., sills, passages, coastlines) and associated multiple flow regimes which are a key characteristic of ocean fluid dynamics.

There are two points worth noting in this regard. First, and most directly related to the content of this paper, higher resolution often exposes problems with the underlying numerical framework which may have been hidden at the coarse resolution. That is, the often held belief that resolution is the "cure to all model ills" is far from reality. Instead, as the simulated flows become more advectively dominant at refined resolution, the need to solidify the numerical, mathematical, and physical foundations upon which the models are based becomes even more important. Furthermore, we should be aware of the lessons learned in meteorology, where tuning models to parameterizations with strong dependence on resolution can create a burdensome overhead for long-term model development.

Second, as one pushes the resolution envelope, be it in process, regional, basin, or global studies, the question arises: Just what is a sufficient resolution? The answer clearly depends on the phenomena of interest. From an idealized computational physics perspective, systematic studies of numerical convergence of geophysical flow regimes are few (a notable exception is the ultra-high resolution QG study of Siegel et al., 1999). However, from a pragmatic perspective of one studying coupled ocean–atmosphere interactions, the focus is typically on determining a resolution adequate to accurately simulate, say, the large-scale sea surface temperature patterns which affect the atmospheric circulation.

There are some guide-posts which provide hints for what may be necessary. For example, studies of the El Niño-Southern Oscillation (ENSO) phenomenon indicate the need to resolve the equatorial Rossby radius in order to represent the rich wave and current structures along the equator (e.g., Philander, 1990). Meridional resolution better than 1/2° has been found to be necessary for this purpose (e.g., Rosati and Miyakoda, 1988; Philander et al., 1992; Roeckner et al., 1996; Yukimoto et al., 1996). Given the importance of ENSO for interannual climate variability, we believe that the next generation of global ocean climate models should, as a minimum, aim to realize such resolution.

The mesoscale is an unique and key threshold since the kinetic energy of the middle to high latitude ocean is concentrated at these scales. Do we need mesoscale eddy resolution to accurately represent the ocean's role in climate or will a parameterization, such as those discussed in Section 11, prove sufficient? Systematically answering this question requires a careful examination of what determines *full* resolution of mesoscale eddies as well as their effects on the ocean's large-scale properties (e.g., mean state, variability, and stability). Recent Atlantic simulations indicate that upwards of 1/10°–1/12° Mercator resolution may be necessary for Gulf Stream modelling (Bryan and Smith, 1999; Smith et al., 2000; Chassignet et al., 2000; Paiva et al., 2000).

Questions such as these, and innumerable others of similar character, are difficult to fully answer both computationally and intellectually. Nonetheless, studies addressing these questions are necessary to test the robustness of climate simulations. Therefore, we firmly believe that a focused examination and testing of ocean model resolution must be a prime goal of ocean climate model development over the next decades.

Acknowledgements

This paper grew from a meeting of the authors in Miami during March, 2000. We thank the University of Miami's Rosenstiel School of Marine and Atmospheric Science for their hospitality. The paper has benefited greatly from comments and suggestions by Alistair Adcroft, Aike

Beckmann, Mike Bell, Rainer Bleck, Kirk Bryan, John Dukowicz, Tal Ezer, Jorgen Frederiksen, Ichiro Fukumori, Richard Greatbatch, Bob Hallberg, George Halliwell, Greg Holloway, Xin Huang, Peter Killworth, Youyou Lu, David Marshall, John McGreggor, Igor Polyakov, Michele Rienecker, Joachim Ribbe, Andreas Schiller, Paul Schopf, Robert Scott, Jinyu Sheng, Neville Smith, Rick Smith, Shafer Smith, Ron Stouffer, and Dan Wright. Lennart Bengtsson and two additional anonymous reviewers also helped to improve the manuscript. All of their contributions are sincerely appreciated. We also thank Peter Killworth and the publishers of *Ocean Modelling* for their encouragement and willingness to publish this paper.

References

Abramopoulos, F., 1988. Generalized energy and potential enstrophy conserving finite difference schemes for the shallow water equations. Monthly Weather Review 116, 650–662.

Adcock, S.T., Marshall, D.P., 2000. Interactions between geostrophic eddies and the mean circulation over large-scale bottom topography. Journal of Physical Oceanography, in press.

Adcroft, A., Hill, C., Marshall, J., 1997. Representation of topography by shaved cells in a height coordinate ocean model. Monthly Weather Review 125, 2293–2315.

Adcroft, A., Marshall, D., 1998. How slippery are piecewise-constant coastlines in numerical ocean models?. Tellus 50A, 95–108.

Adcroft, A.J., Hill, C.N., Marshall, J.C., 1999. A new treatment of the coriolis terms in C-grid models at both high and low resolutions. Monthly Weather Review 127, 1928–1936.

Alvarez, A., Tintoré, J., 1998. Topographic stress: importance and parameterization. In: Chassignet, E.P., Verron, J. (Eds.), Ocean Modelling and Parameterization. NATO Advanced Study Institute, Kluwer Academic Publishers, Dordrecht, p. 451.

Alvarez, A., Tintoré, J., Holloway, G., Eby, M., Beckers, J.M., 1994. The effect of the topographic stress on the Western Mediterranean circulation. Journal of Geophysical Research 99, 16053–16064.

Andrews, D.G., McIntyre, M.E., 1978. An exact theory of nonlinear waves on a Lagrangian-mean flow. Journal of Fluid Mechanics 89, 609–646.

Arakawa, A., 1966. Computational design for long-term numerical integration of the equation of fluid motion: two-dimensional incompressible flow. Part I. Journal of Computational Physics 1, 119–143.

Arakawa, A., Lamb, V.R., 1977. Computational design of the basic dynamical process of the UCLA general circulation model. Methods in Computational Physics vol. 17. Academic Press, New York, pp. 173–265.

Arakawa, A., Lamb, V.R., 1981. A potential enstrophy and energy conserving scheme for the shallow water equations. Monthly Weather Review 109, 18–36.

Argo Science Team, 2000. Argo, the global array of profiling floats. In: Smith, N.R., Koblinsky, C.J. (Eds.), Observing the Ocean in the 21st Century. Bureau of Meteorology, Melbourne, Australia, submitted.

Armi, L., Millard, R.C., 1976. The bottom boundary layer of the deep ocean. Journal of Geophysical Research 81, 4983–4990.

Asselin, R.A., 1972. Frequency filter for time integrations. Monthly Weather Review 100, 487–490.

Barnier, B., Marchesiello, P., De Miranda, A.P., Molines, J.-M., Coulibaly, M.A., 1998. A sigma-coordinate primitive equation model for studying the circulation in the South Atlantic. Part I: Model configuration with error estimates. Deep-Sea Research (1 Oceanography Research Paper) 45, 543–572.

Baringer, M.O., Price, J.F., 1997. Mixing and spreading of the Mediterranean outflow. Journal of Physical Oceanography 27, 1654–1676.

Beckers, J.M., Burchard, H., Deleersnijder, E., Mathieu, P.P., 2000. Numerical discretization of rotated diffusion operators in ocean models. Monthly Weather Review 128, 2711–2733.

Beckmann, A., Haidvogel, D.B., 1993. Numerical simulation of flow around a tall isolated seamount. Part I: Problem formulation and model accuracy. Journal of Physical Oceanography 23, 1736–1753.

Beckmann, A., Döscher, R., 1997. A method for improved representation of dense water spreading over topography in geopotential – coordinate models. Journal of Physical Oceanography 27, 581–591.
Beckmann, A., Hellmer, H.H., Timmermann, R., 1999. A numerical model of the weddell sea: large scale circulation and water mass distribution. Journal of Geophysical Research 104, 23375–23391.
Bell, M., 1998. Momentum fluxes in the Bryan–Cox ocean circulation model. Journal of Atmospheric and Oceanic Technology 15, 1400–1413.
Bentsen, M., Evensen, G., Drange, H., Jenkins, A.D., 1999. Coordinate transformation on a sphere using conformal mapping. Monthly Weather Review 127, 2733–2740.
Blanke, B., Delecluse, P., 1993. Variability of the tropical atlantic ocean simulated by a general circulation model with two different mixed-layer physics. Journal of Physical Oceanography 23, 1363–1388.
Bleck, R., 1978. Finite difference equations in generalized vertical coordinates. Part I: total energy conservation. Contributions to Atmospheric Physics 51, 360–372.
Bleck, R., Boudra, D.B., 1981. Initial testing of a numerical ocean circulation model using a hybrid-(quasi-isopycnic) vertical coordinate. Journal of Physical Oceanography 11, 755–770.
Bleck, R., Hanson, H.P., Hu, D., Kraus, E.B., 1989. Mixed layer-thermocline interaction in a three-dimensional isopycnal coordinate model. Journal of Physical Oceanography 19, 1417–1439.
Bleck, R., Smith, L.T., 1990. A wind-driven isopycnic coordinate model of the north and equatorial Atlantic Ocean. 1. Model development and supporting experiments. Journal of Geophysical Research 95 (C3), 3273–3285.
Bleck, R., Rooth, C., Hu, D., Smith, L.T., 1992. Ventilation patterns and mode water formation in a wind- and thermodynamically driven isopycnic coordinate model of the North Atlantic. Journal of Physical Oceanography 22, 1486–1505.
Bleck, R., 1998. Isopycnic modelling. In: Chassignet, E.P., Verron, J. (Eds.), Ocean Modelling and Parameterization. NATO Advanced Study Institute, Kluwer Academic Publishers, Dordrecht, p. 451.
Blumberg, A.F., Mellor, G.L., 1987. A description of a three-dimensional coastal ocean circulation model. In: Heaps, N. (Ed.), Three-Dimensional Coastal Ocean Models. American Geophysical Union, 208 pp.
Boer, G.J., Shepherd, T.G., 1983. Large-scale two-dimensional turbulence in the atmosphere. Journal of Atmospheric Sciences 40, 164–184.
Böning, C.W., Holland, W.R., Bryan, F.O., Danabasoglu, G., McWilliams, J.C., 1995. An overlooked problem in model simulations of the thermohaline circulation and heat transport in the Atlantic Ocean. Journal of Climate 8, 515–523.
Böning, C.W., Bryan, F.O., Holland, W.R., Döcher, R., 1996. Deep-water formation and meridional overturning in a high-resolution model of the North Atlantic. Journal of Physical Oceanography 26, 1142–1164.
Boris, J.P., Book, D.L., 1973. Flux-corrected transport, I. SHASTA: A fluid transport algorithm that works. Journal of Computational Physics 11, 38–69.
Brown, J.A., Campana, K.A., 1978. An economical time-differencing system for numerical weather prediction. Monthly Weather Review 106, 1125–1136.
Bryan, F.O., Holland, W.R., 1989. A high resolution simulation of the wind- and thermohaline-driven circulation in the North Atlantic Ocean. In: Parameterization of Small-Scale Processes in the Ocean, Proceedings of the Hawaiian Winter Workshop, 'Aha Huiliko'a. University of Hawaii, pp. 99–115.
Bryan, F.O., Smith, R.D., 1999. Modelling the North Atlantic circulation: from eddy-permitting to eddy-resolving. WOCE Newsletter 33, 12–14.
Bryan, K., 1969a. A numerical method for the study of the circulation of the world ocean. Journal of Computational Physics 4, 347–376.
Bryan, K., 1969b. Climate and the ocean circulation. III. The ocean model. Monthly Weather Review 97, 806–827.
Bryan, K., 1984. Accelerating the convergence to equilibrium of ocean-climate models. Journal of Physical Oceanography 14, 666–673.
Bryan, K., Cox, M.D., 1972. An approximate equation of state for numerical models of the ocean circulation. Journal of Physical Oceanography 2, 510–514.
Bryan, K., Manabe, S., Pacanowski, R.C., 1975. A global ocean-atmosphere climate model. II. The oceanic circulation. Journal of Physical Oceanography 5, 30–46.

Bryan, K., Dukowicz, J.K., Smith, R.D., 1999. On the mixing coefficient in the parameterization of Bolus velocity. Journal of Physical Oceanography 29, 2442–2456.

Brydon, D., Sun, S., Bleck, R., 1999. A new approximation of the equation of state for seawater, suitable for numerical ocean models. Journal of Geophysical Research 104, 1537–1540.

Campin, J.-M., Goosse, H., 1999. Parameterization of density-driven downsloping flow for a coarse-resolution ocean model in z-coordinate. Tellus, Series A-B, 51A, 412–430.

Canuto, V.M., Dubovikov, M.S., 1996. A dynamical model for turbulence. I. General formalism. Physics of Fluids 8, 571–586.

Chassignet, E.P., Verron, J. (Eds.), 1998. Ocean Modelling and Parameterization. NATO Advanced Study Institute, Kluwer Academic Publishers, Dordrecht, p. 451.

Chassignet, E.P., Smith, L.T., Bleck, R., Bryan, F.O., 1996. A model comparison: numerical simulations of the North and Equatorial Atlantic oceanic circulation in depth and isopycnic coordinates. Journal of Physical Oceanography 26, 1849–1867.

Chassignet, E.P., Garraffo, Z.D., Smith, R.D., Hurlburt, H.E., 2000. High resolution gulf stream modelling. Geophysical Research Letters, submitted.

Chassignet, E.P., Malanotte-Rizzoli, P. (Eds.), 2000. Ocean Circulation Model Evaluation Experiments for the North Atlantic Basin. Elsevier Science, Amsterdam. Dynamics of Atmospheres and Oceans (special issue) 32, 155–432.

Chassignet, E.P., Arango, H., Dietrich, D., Ezer, T., Ghil, M., Haidvogel, D.B., Ma, C.-C., Mehra, A., Paiva, A.M., Sirkes, Z., 2000. DAMÉE-NAB: The base experiments. Dynamics of Atmospheres and Oceans 32, 155–184.

Chavanis, P.-H., Sommeria, J., 1997. Theromdynamical approach for small-scale parametrization in 2D turbulence. Physical Review Letters 78, 3302–3305.

Chavanis, P.-H., Sommeria, J., 2000. Statistical mechanics of the shallow water system. Preprint available from `http://xxx.lanl.gov/abs/physics/0004056`.

Chen, D., Rothstein, L.M., Busalacchi, A.J., 1994. A hybrid vertical mixing scheme and its application to tropical ocean models. Journal of Physical Oceanography 24, 2156–2179.

Chu, P.C., Fan, C., 1997. Sixth-order difference scheme for sigma coordinate ocean models. Journal of Physical Oceanography 27, 2064–2071.

Cox, M.D., 1984. A primitive equation, 3-dimensional model of the ocean. GFDL Ocean Group Technical Report No. 1. Available from Geophysical Fluid Dynamics Laboratory, P.O. Box 308, Princeton, New Jersey, 08542.

Cox, M.D., 1987. Isopycnal diffusion in a z-coordinate ocean model. Ocean Modelling 74, 1–5.

Danabasoglu, G., McWilliams, J.C., 1995. Sensitivity of the global ocean circulation to parameterizations of mesoscale tracer transports. Journal of Climate 8, 2967–2987.

Danabasoglu, G., McWilliams, J.C., Large, W.G., 1996. Approach to equilibrium in accelerated global oceanic models. Journal of Climate 9, 1092–1110.

DeGroot, S.R., Mazur, P. (Ed.), 1962. Non-equilibrium Thermodynamics. Interscience, New York, pp. 510.

Deleersnijder, E., Campin, J.M., 1995. On the computation of the barotropic mode of a free-surface world ocean model. Annales Geophysicae 13, 675–688.

Dengg, J., Böning, C., Ernst, U., Redler, R., Beckmann, A., 1999. Effects of an improved model represntation of overflow water on the subpolar North Atlantic. International WOCE Newsletter 37, pp. 10–15, unpublished manuscript.

de Szoeke, R.A., 2000. Equations of motion using thermodynamic coordinates. Journal of Physical Oceanography 30, 2814–2829.

de Szoeke, R.A., Springer, S.R., Oxilia, D.M., 2000. Orthobaric density: A thermodynamic variable for ocean circulation studies. Journal of Physical Oceanography 30, 2830–2852.

Dewar, W.K., Hsueh, Y., McDougall, T.J., Yuan, D., 1998. Calculation of pressure in ocean simulations. Journal of Physical Oceanography 28, 577–588.

DiBattista, M.T., Majda, A.J., 2000. An equilibrium statistical theory for large-scale features of open-ocean convection. Journal of Physical Oceanography 30, 1325–1353.

DiBattista, M.T., Majda, A.J., Marshall, J., 2000. A statistical theory for the patchiness of open-ocean deep convection: the effect of preconditioning. Journal of Physical Oceanography, in press.

Dietrich, D.E., Marietta, M.G., Roach, P.J., 1987. A ocean modelling system with turbulent boundary layers and topography: numerical description. International Journal of Numerical Methods in Fluids 7, 833–855.
Döscher, R., Redler, R., 1997. The relative importance of northern overflow and subpolar deep convection for the North Atlantic thermohaline circulation. Journal of Physical Oceanography 27, 1894–1902.
Drijfhout, S.S., Hazeleger, W., 2000. Eddy mixing of potential vorticity versus thickness in an isopycnic ocean model. Preprint submitted to Journal of Physical Oceanography.
Duda, T.F., Jacobs, D.C., 1995. Comparison of shear measurements and mixing predictions with a direct observation of diapycnal mixing in the Atlantic thermocline. Journal of Geophysics Research 100 (C7), 13481–13498.
Duffy, P.B., Eliason, D., Bourgeois, A.J., Covey, C., 1995. Simulation of bomb radiocarbon in two ocean general circulation models. Journal of Geophysical Research 100, 22545–22565.
Duffy, P.B., Caldeira, K., Selevaggi, J., Hoffert, M.I., 1997. Effects of subgrid-scale mixing parameterizations on simulated distributions of natural 14C, temperature, and salinity in a three-dimensional ocean general circulation model. Journal of Physical Oceanography 27, 498–523.
Dukowicz, J.K., 1997. Steric sea level in the Los Alamos POP code-non Boussinesq effects. In: Lin, C.A., Laprise, R., Ritchie, H. (Eds.), Numerical Methods in Atmospheric and Oceanic Modelling. NRC Research Press, Ottawa.
Dukowicz, J.K., 1995. Mesh effects for Rossby waves. Journal of Computational Physics 119, 188–194.
Dukowicz, J.K., 1999. The theory of baroclinic/barotropic modal decomposition in a layered ocean model. Preprint.
Dukowicz, J.K., 2000. The theory of baroclinic/barotropic modal decomposition in a layered ocean model. Journal of Physical Oceanography, submitted.
Dukowicz, J.K., Smith, R.D., Malone, R.C., 1993. A reformulation and implementation of the Bryan–Cox–Semtner ocean model on the connection machine. Journal of Atmospheric and Oceanic Technology 10, 195–208.
Dukowicz, J.K., Smith, R.D., 1994. Implicit free-surface method for the Bryan–Cox–Semtner ocean model. Journal of Geophysical Research 99, 7991–8014.
Dukowicz, J.K., Smith, R.D., 1997. Stochastic theory of compressible turbulent fluid transport. Physics of Fluids 9, 3523–3529.
Dukowicz, J.K., Greatbatch, R.J., 1999. Evolution of mean flow Fofonoff gyres in barotropic quasi-geostrophic turbulence. Journal of Physical Oceanography 29, 1832–1852.
Durran, D.R. (Ed.), 1999. Numerical Methods for Wave Equations in Geophysical Fluid Dynamics. Springer, Berlin, pp. 470.
DYNAMO Group, 1997. Dynamics of North Atlantic models: simulation and assimilation with high resolution models. Ber. Inst. f. Meereskunde Kiel, vol. 294, p. 333. Report available at www.ifm.uni-kiel.de/to/dynamo/dyn_m.html.
Easter, R.C., 1993. Two modified versions of Bott's positive-definite numerical advection scheme. Monthly Weather Review 121, 297–304.
Eby, M., Holloway, G., 1994. Sensitivity of a large-scale ocean model to a parameterization of topographic stress. Journal of Physical Oceanography 24, 2577–2588.
England, M.H., 1995. Using chlorofluorocarbons to assess ocean climate models. Geophysical Research Letters 22, 3051–3054.
England, M.H., Hirst, A.C., 1997. Chloroflurocarbon uptake in a world ocean model 2: sensitivity to surface thermohaline forcing and subsurface mixing parameterization. Journal of eophysical Research 102, 15709–15731.
England, M.H., Holloway, G., 1998. Simulations of CFC content and water-mass age in the deep North Atlantic. Journal of Geophysical Research 103, 15885–15902.
England, M.H., Rahmstorf, S., 1999. Sensitivity of ventilation rates and radiocarbon uptake to subgrid-scale mixing in ocean models. Journal of Geophysical Research 29, 2802–2828.
Ezer, T., Mellor, G.L., 1997. Simulations of the Atlantic Ocean with a free surface sigma coordinate ocean model. Journal of Geophysical Research 102 (C7), 15647–15657.
Ezer, T., 1999. Decadal variabilities of the upper layers of the subtropical North Atlantic: an ocean model study. Journal of Physical Oceanography 29, 3111–3124.
Ezer, T., 2000. On the seasonal mixed layer simulated by a basin-scale ocean model and the Mellor–Yamada turbulence scheme. Journal of Geophysical Research 105, 16843–16855.

Farrow, D.E., Stevens, D.P., 1995. A new tracer advection scheme for Bryan and Cox type ocean general circulation models. Journal of Physical Oceanography 25, 1731–1741.
Ferron, B., Mercier, H., Treguier, A.M., 2000. Modelisation of the flow of bottom water through the Romanche fracture zone with a primitive equation model. Part 1: dynamics. Journal of Marine Research.
FRAM Group, 1991. Initial results from a fine resolution model of the Southern Ocean. EOS Transactions of the American Geophysical Union 72, 174–175.
Frederiksen, J.S., 1999. Subgrid-scale parameterizations of eddy-topographic force, eddy viscosity, and stochastic backscatter for flow over topography. Journal of Atmospheric Sciences 56, 1481–1494.
Fu, L.-L., Smith, R.D., 1996. Global ocean circulation from satellite altimetry and high-resolution computer simulation. Bulletin of the American Meteorological Society, 2625–2636.
Fyfe, J., Marinone, G., 1995. On the role of unresolved eddies in a model of the residual currents in the central Strait of Georgia, B.C. Atmospheres and Oceans 33, 613–619.
Galperin, B., Orszag, S.A. (Eds.), 1993. Large Eddy Simulation of Complex Engineering and Geophysical Flows. Cambridge University Press, Cambridge, pp. 600.
Gaspar, P., 1988. Modelling the seasonal cycle of the upper ocean. Journal of Physical Oceanography 18, 161–180.
Gent, P.R., McWilliams, J.C., 1990. Isopycnal mixing in ocean circulation models. Journal of Physical Oceanography 20, 150–155.
Gent, P.R., Willebrand, J., McDougall, T., McWilliams, J.C., 1995. Parameterizing eddy-induced tracer transports in ocean circulation models. Journal of Physical Oceanography 25, 463–474.
Gent, P.R., Bryan, F.O., Danabasoglu, G., Doney, S.C., Holland, W.R., Large, W.G., McWilliams, J.C., 1998. The NCAR Climate System Model Global Ocean Component. Journal of Climate 11, 1287–1306.
Gerdes, R., 1993a. A primitive equation ocean circulation model using a general vertical coordinate transformation. Description and testing of the model 1. Journal of Geophysical Research 98, 14683–14701.
Gerdes, R., 1993b. A primitive equation ocean circulation model using a general vertical coordinate transformation 2. Application to an overflow problem. Journal of Geophysical Research 98, 14703–14726.
Gerdes, R., Köberle, C., Willebrand, J., 1991. The influence of numerical advection schemes on the results of ocean general circulation models. Climate Dynamics 5, 211–226.
Gill, A.E. (Ed.), 1982. Atmosphere-Ocean Dynamics. Academic Press, New York, pp. 662.
Gnanadesikan, A., Pacanowski, R.C., 1997. Improved representation of flow around topography in the GFDL modular ocean model MOM2. International WOCE Newsletter 27, 23–35, unpublished manuscript.
Gnanadesikan, A., 1999. Representing the bottom boundary layer in the GFDL ocean model. Unpublished manuscript available at `http://www.gfdl.gov/~alg/bbl.html`.
Gnanadesikan, A., Weller, R.A., 1995. Structure and instability of the Ekman spiral in the presence of surface gravity waves. Journal of Physical Oceanography 25, 3148–3171.
Gnanadesikan, A., Toggweiler, J.R., 1999. Constraints placed by silicon cycling on vertical exchange in general circulation models. Geophysical Research Letters 26, 1865–1868.
Gordon, C., Cooper, C., Senior, C.A., Banks, H., Gregory, J.M., Johns, T.C., Mitchell, J.F.B., Wood, R.A., 2000. The simulation of SST, sea ice extents and ocean heat transports in a version of the Hadley centre coupled model without flux adjustments. Climate Dynamics 16, 147–168.
Greatbatch, R.J., Lamb, K.G., 1990. On parameterizing vertical mixing of momentum in non-eddy resolving ocean models. Journal of Physical Oceanography 20, 1634–1637.
Greatbatch, R.J., 1994. A note on the representation of steric sea level in models that conserve volume rather than mass. Journal of Geophysical Research 99, 12767–12771.
Greatbatch, R.J., 1998. Exploring the relationship between eddy-induced transport velocity, vertical momentum transfer, and the isopycnal flux of potential vorticity. Journal of Physical Oceanography 28, 422–432.
Greatbatch, R.J., Mellor, G.L., 1999. An overview of coastal ocean models. In: Mooers, C.N.K. (Ed.), Coastal Ocean Prediction. American Geophysical Union, Washington, DC, pp. 31–57.
Greatbatch, R.J., Lu, Y., Cai, Y., 2000. Relaxing the Boussinesq approximation in ocean circulation models. Journal of Atmospheric and Oceanic Technology, submitted.
Greatbatch, R.J., Li, G., 2000. Along slope mean flow and an associated upslope bolus flux of tracer in a parameterization of mesoscale turbulence. Deep Sea Research, in press.

Griffies, S.M., 1998. The Gent–McWilliams skew-flux. Journal of Physical Oceanography 28, 831–841.
Griffies, S.M., Gnanadesikan, A., Pacanowski, R.C., Larichev, V., Dukowicz, J.K., Smith, R.D., 1998. Isoneutral diffusion in a z-coordinate ocean model. Journal of Physical Oceanography 28, 805–830.
Griffies, S.M., Hallberg, R.W., 2000. Biharmonic friction with a Smagorinsky viscosity for use in large-scale eddy-permitting ocean models. Monthly Weather Review 128, 2935–2946.
Griffies, S.M., Pacanowski, R.C., Hallberg, R.W., 2000a. Spurious diapycnal mixing associated with advection in a z-coordinate ocean model. Monthly Weather Review 128, 538–564.
Griffies, S.M., Pacanowski, R.C., Schmidt, R.M., Balaji, V., 2000b. Improved tracer conservation with a new explicit free surface method for z-coordinate ocean models. Monthly Weather Review, accepted.
Guilyardi, E., Madec, G., Terray, L., 2000. The role of lateral ocean physics in the upper ocean thermal balance of a coupled ocean-atmosphere GCM. Climate Dynamics, in press.
Guyon, M., Madec, G., Roux, F.X., Imbard, M., 1999. A parallel ocean model for high resolution studies. In: Amestoy, P., et al. (Eds.), Euro-Par'99, LNCS 1685, pp. 603–607.
Guyon, M., Madec, G., Roux, F.X., Imbard, M., Herbaut, C., Fronier, P., 2000. Parallelization of the OPA ocean model. Calculateurs Paralleles, in press.
Haidvogel, D.B., Beckmann, A., 1999. Numerical Ocean Circulation Modelling. Imperial College Press, p. 318.
Haidvogel, D.B., Wilkin, J.L., Young, R.E., 1991. A semi-spectral primitive equation ocean circulation model using vertical sigma and orthogonal curvilinear horizontal coordinates. Journal of Computational Physics 94, 151–185.
Haidvogel, D.B., Arango, H.G., Hedström, K.S., Beckmann, A., Malanotte-Rizzoli, P., Shcheptkin, A.F., 2000. Model evaluation experiments in the North Atlantic basin: simulations in nonlinear terrain-following coordinates. Dynamics of Atmospheres and Oceans 32, 239–281.
Hakkinen, S., 1999. Variability of the simulated meridional heat transport in the North Atlantic for the period 1951–1993. Journal of Geophysical Research 104 (C5), 10991–11007.
Hakkinen, S., 2000. Decadal air–sea interaction in the North Atlantic based on observations and modelling results. Journal of Climate 13, 1195–1219.
Hallberg, R.W., 1995. Some aspects of the circulation in ocean basins with isopycnals intersecting the sloping boundaries, Ph.D. thesis, University of Washington, Seattle, p. 244.
Hallberg, R.W., 1997. Stable split time stepping schemes for large-scale ocean modelling. Journal of Computational Physics 135, 54–65.
Hallberg, R.W., 2000. Time integration of diapycnal diffusion and Richardson number dependent mixing in isopycnal coordinate ocean models. Monthly Weather Review 128, 1402–1419.
Haltiner, G.J., Williams, R.T., 1980. Numerical Prediction and Dynamic Meteorology. Wiley, New York, pp. 477.
Hasumi, H., 2000. CCSR Ocean Component Model (COCO) Version 2.1, CCSR Report No.13.
Hecht, M.W., Wingate, B.A., Kassis, P., 2000. A better, more discriminating test problem for ocean tracer transport. Ocean Modelling, in press.
Held, I.M., Larichev, V.D., 1996. A scaling theory for horizontally homogeneous baroclinically unstable flow on a beta plane. Journal of Atmospheric Sciences 53, 946–952.
Higdon, R.L., 1999. Implementation of a barotropic–baroclinic time splitting for isopycnic coordinate ocean modelling. Journal of Computational Physics 148, 579–604.
Higdon, R.L., Bennett, A.F., 1996. Stability analysis of operator splitting for large-scale ocean modelling. Journal of Computational Physics 123, 311–329.
Higdon, R.L., de Szoeke, R.A., 1997. Barotropic–baroclinic time splitting for ocean circulation modelling. Journal of Computational Physics 135, 30–53.
Hirst, A.C., McDougall, T.J., 1996. Deep-water properties and surface buoyancy flux as simulated by a z-coordinate model including eddy-induced advection. Journal of Physical Oceanography 26, 1320–1343.
Hirst, A.C., McDougall, T.J., 1998. Meridional overturning and dianeutral transport in a z-coordinate ocean model including eddy-induced advection. Journal of Physical Oceanography 28, 1205–1223.
Hirst, A.C., Gordon, H.B., O'Farrell, S.P., 1996. Global warming in a coupled climate model including oceanic eddy-induced advection. Geophysical Research Letters 23, 3361–3364.
Hirst, A.C., O'Farrell, S.P., Gordon, H.B., 2000. Comparison of a coupled ocean-atmosphere model with and without oceanic eddy-induced advection. Part I: ocean spinup and control integrations. Journal of Climate 13, 139–163.

Hogg, N., 1973. On the stratified Taylor column. Journal of Fluid Mechanics 58, 517–537.
Holland, W.R., Chow, J.C., Bryan, F.O., 1998. Application of a third-order upwind scheme in the NCAR ocean model. Journal of Climate 11, 1487–1493.
Hollingsworth, A., Kalbers, P., Renner, V., Burridge, D.M., 1983. An internal symmetric computational instability. Quarterly Journal of the Royal Meteorological Society 109, 417–428.
Holloway, G., 1986a. Estimation of oceanic eddy transports from satellite altimetry. Nature 323, 243–244.
Holloway, G., 1986b. A shelf wave/topographic pump drives mean coastal circulation. Parts 1 & 2. Ocean Modelling 68, 69.
Holloway, G., 1987. Systematic forcing of large-scale geophysical flows by eddy–topography interactions. Journal of Fluid Mechanics 184, 463–476.
Holloway, G., 1992. Representing topographic stress for large-scale ocean models. Journal of Physical Oceanography 22, 1033–1046.
Holloway, G., 1997. Eddy transport of thickness and momentum in layer and level models. Journal of Physical Oceanography 27, 1153–1157.
Holloway, G., 1999. Moments of probable seas: statistical dynamics of planet ocean. Physica D 133, 199–214.
Holloway, G., Sou, T., Eby, M., 1995. Dynamics of the circulation of the Japan Sea. Journal of Marine Research 53, 539–569.
Holtslag, A.A., Boville, B.A., 1993. Local versus nonlocal boundary-layer diffusion in global climate model. Journal of Climate 6, 1825–1842.
Hsieh, W.W., Davey, M.K., Wajsowicz, R.C., 1983. The free Kelvin wave in finite-difference numerical models. Journal of Physical Oceanography 13, 1383–1397.
Hsu, Y.-J.G., Arakawa, A., 1990. Numerical modelling of the atmosphere with an isentropic vertical coordinate. Monthly Weather Review 118, 1933–1959.
Hu, D., 1996. On the sensitivity of thermocline depth and meridional heat transport to vertical diffusivity in OGCMS. Journal of Physical Oceanography 26, 1480–1494.
Huang, R.X., 1993. Real freshwater flux as a natural boundary condition for the salinity balance and thermohaline circulation forced by evaporation and precipitation. Journal of Physical Oceanography 23, 2428–2446.
Huang, R.X., 1998. Mixing and available potential energy in a Boussinesq ocean. Journal of Physical Oceanography 28, 669–678.
Huang, R.X., 1999. Mixing and energetics of the oceanic thermohaline circulation. Journal of Physical Oceanography 29, 727–746.
Huang, R.X., Jin, X., Zhang, X., 2000. An oceanic general circulation model in pressure coordinates. Advances in Atmospheric Sciences, accepted.
Huang, R.X., Pedlosky, J., 2000. On aliasing Rossby waves induced by asynchronous time stepping. Journal of Physical Oceanography, submitted.
Hughes, C.W., Wunsch, C., Zlotnicki, V., 2000. Satellite peers through the oceans from space. EOS 81, 68.
Huppert, H.E., Bryan, K., 1976. Topographically generated eddies. Deep-Sea Research 23, 655–679.
Intergovernmental Panel on Climate Change (IPCC), Climate Change 1995. In: Houghton, J.T., MeiraFilho, L.G., Callander, B.A., Harris, N., Kattenberg, A., Maskell, K (Eds.), The Science of Climate Change. Cambridge University Press, Cambridge, p. 572.
Iselin, C.O., 1939. The influence of vertical and lateral turbulence on the characteristics of the waters at mid-depth. EOS Transactions of AGU 20, 414–417.
Ishizaki, H., Motoi, T., 1999. Reevaluation of the Takano–Oonishi scheme for momentum advection on bottom relief in ocean models. Journal of Atmospheric and Oceanic Technology 16, 1994–2010.
Jackett, D.R., McDougall, T.J., 1995. Minimal adjustment of hydrographic profiles to achieve static stablilty. Journal of Atmospheric and Oceanic Technology 12, 381–389.
Janjić, Z.I., 1974. A stable centered difference scheme free of two-grid-interval noise. Monthly Weather Review 102, 319–323.
Janjić, Z.I., 1977. Pressure gradient force and advection scheme used for forecasting with steep and small scale topography. Contributions in Atmospheric Physics 50, 186–199.

Janjić, Z.I., 1984. Non-linear advection schemes and energy cascade on semi-staggered grids. Monthly Weather Review 112, 1234–1245.

Jones, P.W., 1999. First- and second-order conservative remapping schemes for grids in spherical coordinates. Monthly Weather Review 127, 2204–2210.

Junclaus, J.H., Mellor, G., 2000. A three-dimensional model study of the Mediterranean outflow. Journal of Marine Systesms 24, 41–66.

Kantha, L.H., Clayson, C.A., 2000a. Numerical Models of Oceans and Oceanic Processes. International Geophysics Series, vol. 66. Academic Press, New York, p. 936.

Kantha, L.H., Clayson, C.A., 2000b. Small Scale Processes in Geophysical Fluid Flows. International Geophysics Series, vol. 67. Academic Press, New York, p. 883.

Käse, R.H., Oschlies, A., 2000. Flow through Denmark Strait. Journal of Geophysical Research, in press.

Kazantsev, E., Sommeria, J., Verron, J., 1998. Subgrid-scale eddy parameterization by statistical mechanics in a barotropic ocean model. Journal of Physical Oceanography 28, 1017–1042.

Kelley, D.E., Van Scoy, K.A., 1999. A basinwide estimate of vertical mixing in the upper pycnocline: spreading of bomb tritium in the North Pacific Ocean. Journal of Physical Oceanography 29, 1759–1771.

Killworth, P.D., 1987. Topographic instabilities in level model OGCM's. Ocean Modelling 75, 9–12.

Killworth, P.D., 1995. Hydraulic control and maximal flow in rotating stratified hydraulics. Deep-Sea Research 42, 859–876.

Killworth, P.D., 1997. On the parameterization of eddy transfer Part I: theory. Journal of Marine Research 55, 1171–1197.

Killworth, P.D., Smith, J.M., Gill, A.E., 1984. Speeding up ocean circulation models. Ocean Modelling 56, 1–5.

Killworth, P.D., Stainforth, D., Webb, D.J., Paerson, S.M., 1991. The development of a free-surface Bryan–Cox–Semtner ocean model. Journal of Physical Oceanography 21, 1333–1348.

Killworth, P.D., Edwards, N.R., 1999. A turbulent bottom boundary layer code for use in numerical models. Journal of Physical Oceanography 29, 1221–1238.

Klein, P., Treguier, A.M., Hua, B.L., 1998. Quasi-geostrophic stirring of thermohaline fronts. Journal of Marine Research 56, 589–612.

Klinger, B.A., Marshall, J., Send, U., 1996. Representation of convective plumes by vertical adjustment. Journal of Geophysical Research 101, 18175–18182.

Kowalik, Z., Murty, T.S. (Eds.), 1993. Numerical Modelling of Ocean Dynamics: Ocean Models (Advances Series on Ocean Engineering). World Scientific, Singapore, pp. 481.

Kraichnan, R.H., 1975. Statistical dynamics of two-dimensional flow. Journal of Fluid Dynamics 67, 1555–1575.

Kraus, E.G., Turner, J.S., 1967. A one-dimensional model of the seasonal thermocline, II. The general theory and its consequences. Tellus 19, 98–105.

Kushner, P.J., Held, I.M., 1998. A test, using atmospheric data, of a method for estimating oceanic eddy diffusivity. Geophysical Research Letters 25, 4213–4216.

Large, W.G., 1998. Modelling and parameterizing oceanic planetary boundary layers. In: Chassignet, E.P., Verron, J. (Eds.), Ocean Modelling and Parameterization. NATO Advanced Study Institute, Kluwer Academic Publishers, Dordrecht, p. 451.

Large, W.G., McWilliams, J.C., Doney, S.C., 1994. Oceanic vertical mixing: a review and a model with a nonlocal boundary layer parameterization. Reviews of Geophysics 32, 363–403.

Large, W.G., Danabasoglu, G., Doney, S.C., McWilliams, J.C., 1997. Sensitivity to surface forcing and boundary layer mixing in a global ocean model: annual-mean climatology. Journal of Physical Oceanography 27, 2418–2447.

Large, W.G., Danabasoglu, G., McWilliams, J.C., Gent, P.R., Byran, F.O., 2000. Equatorial circulation of a global ocean climate model with anisotropic horizontal viscosity. Journal of Physical Oceanography, submitted.

Ledwell, J.R., Watson, A.J., Law, C.S., 1993. Evidence for slow mixing across the pycnocline from an open-ocean tracer-release experiment. Nature 364, 701–703.

Ledwell, J.R., Watson, A.J., 1998. Mixing of a tracer in the pycnocline. Journal of Geophysical Research 103 (C10), 21499–21529.

Lee, M.-M, Marshall, D.P., Williams, R.G., 1997. On the eddy transfer of tracers: advective or diffusive?. Journal of Marine Research 55, 483–505.

Leith, C.E., 1968. Diffusion approximation for two-dimensional turbulence. Physics of Fluids 10, 1409–1416.
Leith, C.E., 1996. Stochastic models of chaotic systems. In: Holm, D.D., Malone, R.C., Margolin, Len, G. (Eds.), Nonlinear Phenomena in Ocean Dynamics, Physica D 98, 481–491.
Leonard, B.P., 1979. A stable and accurate convective modelling procedure based on quadratic upstream interpolation. Computer Methods in Applied Mechanics and Engineering 19, 59–98.
Leonard, B.P., MacVean, M.K., Lock, A.P., 1993. Positivity-preserving numerical schemes for multidimensional advection, NASA Technical Memorandum, 106055, ICOMP-93-05.
Le Traon, P.Y., Dibarbouree, G., 1999. Mesoscale mapping capabilities from multiple altimeter missions. Journal of Atmospheric and Oceanic Technology 16, 1208–1223.
Lohmann, G., 1998. The influence of a near-bottom transport parameterization on the sensitivity of the thermohaline circulation. Journal of Physical Oceanography 28, 2095–2103.
Lohmann, G., Gerdes, R., 1998. Sea ice effects on the sensitivity of the thermohaline circulation. Journal of Climate 11, 2789–2803.
Lu, Y., Wright, D.G., Brickman, D., 2000. Internal tide generation over topography: experiments with a free-surface z-level model. Journal of Atmospheric and Oceanic Technology, submitted.
Lunkeit, F., Sausen, R., Oberhuber, J.M., 1996. Climate simulations with the global coupled atmosphere–ocean model ECHAM2/OPYC. Climate Dynamics 12, 195–212.
Madec, G., Imbard, M., 1996. A global ocean mesh to overcome the North Pole singularity. Climate Dynamics 12, 381–388.
Madec, G., Delecluse, P., Imbard, M., Lévy, C., 1998. OPA 8.1 Ocean General Circulation Model reference manual. Note du Pôle de modélisation, Institut Pierre-Simon Laplace (IPSL), France, No. XX, p. 91.
Maltrud, M.E., Smith, R.D., Semtner, A.J., Malone, R.C., 2000. Global eddy-resolving ocean simulations driven by 1984–1995 atmospheric winds. Journal of Geophysical Research.
Manabe, S., Smagorinsky, J., Strickler, R.F., 1965. Simulated climatology of a general circulation model with a hydrologic cycle. Monthly Weather Review 93, 769–798.
Marchesiello, P., Barnier, B., De Miranda, A.P., 1998. A sigma-coordinate primitive equation model for studying the circulation in the South Atlantic Part I: Meridional transports and seasonal variability. Deep-Sea Research (1 Oceanography Research Paper) 45, 573–608.
Marinone, S.G., 1998. Effect of the topographic stress on the tidal and wind induced residual currents in the Gulf of California. Journal of Geophysical Research 103, 18437–18446.
Marotzke, J., 1991. Influence of convective adjustment on the stability of the thermohaline circulation. Journal of Physical Oceanography 21, 903–907.
Marotzke, J., 1997. Boundary mixing and the dynamics of three-dimensional thermohaline circulations. Journal of Physical Oceanography 27, 1713–1728.
Marshall, D.P., Williams, R.G., Lee, M.-M., 1999. The relation between eddy-induced transport and isopycnic gradients of potential vorticity. Journal of Physical Oceanography 29, 1571–1578.
Marshall, J., 1981. On the parameterization of geostrophic eddies in the ocean. Journal of Physical Oceanography 11, 257–271.
Marshall, J., Hill, C., Perelman, L., Adcroft, A., 1997a. Hydrostatic, quasi-hydrostatic, and nonhydrostatic ocean modelling. Journal of Geophysical Research 102, 5733–5752.
Marshall, J., Adcroft, A., Hill, C., Perelman, L., Heisey, C., 1997b. A finite-volume, incompressible Navier Stores model for studies of the ocean on parallel computers. Journal of Geophysical Research 102, 5753–5766.
McDougall, T.J., 1987a. Neutral surfaces. Journal of Physical Oceanography 17, 1950–1967.
McDougall, T.J., 1987b. Thermobaricity, cabbeling, and water-mass conversion. Journal of Geophysical Research 92, 5448–5464.
McDougall, T.J., 1995. The influence of ocean mixing on the absolute velocity vector. Journal of Physical Oceanography 25, 705–725.
McDougall, T.J., 1998. Three-dimensional residual mean theory. In: Chassignet, E.P., Verron, J. (Eds.), Ocean Modelling and Parameterization. NATO Advanced Study Institute, Kluwer Academic Publishers, Dordrecht, p. 451.
McDougall, T.J., Church, J.A., 1986. Pitfalls with numerical representations of isopycnal and diapycnal mixing. Journal of Physical Oceanography 16, 196–199.

McDougall, T.J., Dewar, W.K., 1998. Vertical mixing and cabbeling in layered models. Journal of Physical Oceanography 28, 1458–1480.
McDougall, T.J., Jackett, D.R., 1988. On the helical nature of neutral trajectories in the ocean. Progress in Oceanography 20, 153–183.
McDougall, T.J., McIntosh, P.C., 1996. The temporal-residual-mean velocity. Part I: derivation and scalar conservation equation. Journal of Physical Oceanography 26, 2653–2665.
McDougall, T.J., McIntosh, P.C., 2000. The temporal-residual-mean velocity. Part II: Isopycnal interpretation and the tracer and momentum equations. Journal of Physical Oceanography, accepted.
McDougall, T.J., Hirst, A.C., England, M.H., McIntosh, P.C., 1996. Implications of a new eddy parameterization for ocean models. Geophysical Research Letters 23, 2085–2088.
McDougall, T.J., Greatbatch, R.J., Lu, Y., 2000. On conservation equations in oceanography: how accurate are Boussinesq ocean models? Journal of Physical Oceanography, submitted.
McIntosh, P.C., McDougall, T.J., 1996. Isopycnal averaging and the residual mean circulation. Journal of Physical Oceanography 26, 1655–1660.
McWilliams, J.C., Chow, J., 1981. Equilibrium geostrophic turbulence: I. A reference solution in a β-plane channel. Journal of Physical Oceanography 11, 921–949.
Mellor, G.L., 1996. User's Guide for a Three-Dimensional, Primitive Equation, Numerical Ocean Model. June 1996 ed. Available from Princeton University Program in Atmospheric and Oceanic Sciences.
Mellor, G.L., 2000. One dimensional ocean surface layer modelling, a problem and a solution. Journal of Physical Oceanography, in press.
Mellor, G.L., Yamada, T., 1982. Development of a turbulence closure model for geophysical fluid problems. Reviews of Geophysics and Space Physics 20, 851–875.
Mellor, G.L., Ezer, T., 1995. Sea level variations induced by heating and cooling: An evaluation of the Boussinesq approximation in ocean models. Journal of Geophysical Research 100 (C10), 20565–20577.
Mellor, G.L., Ezer, T., Oey, L.-Y., 1994. The pressure gradient conundrum of sigma coordinate ocean models. Journal of Atmospheric and Oceanic Technology 11, 1126–1134.
Mellor, G.L., Ezer, T., Oey, L.-Y., 1998. Sigma coordinate pressure gradient errors and the seamount problem. Journal of Atmospheric and Oceanic Technology 15, 1122–1131.
Mellor, G.L., Hakkinen, S., Ezer, T., 2000. A generalization of a sigma coordinate ocean model and an inter-comparison of model vertical grids. In: Pinari, N. (Ed.), Ocean Forecasting: Theory and Practice. Springer, New York.
Merle, J., Morliere, A., 1988. Towards a 3-dimensional simulation of the Tropical Atlantic. Geophysical Research Letters 15, 653–656.
Merryfield, W.J., 1998. Effects of stratification on quasi-geostrophic inviscid equilibria. Journal of Fluid Mechanics 354, 345–356.
Merryfield, W.J., Cummins, P.F., Holloway, G., 2000. Equilibrium statistical mechanics of barotropic flow over finite topography. Journal of Physical Oceanography, submitted.
Mesinger, F., 1973. A method for construction of second-order accurate difference schemes permitting no false two-grid-interval waves in the height field. Tellus 25, 444–457.
Mesinger, F., 1982. On the convergence and error problems of the calculation of the pressure gradient force in sigma coordinate models. Geophysical and Astrophysical Fluid Dynamics 19, 105–117.
Mesinger, F., Arakawa, A., 1976. Numerical Methods used in Atmospheric Models. vol. I. JOC, GARP Publication Series, No. 17. Geneva, World Meteorological Organization, C.P. No. 5, CH-1211, Geneva, p. 64.
Miller, J., 1990. Statistical mechanics of Euler equations in two-dimensions. Physical Review Letters 22, 2137–2140.
Miller, J., Weichman, P.B., Cross, M.C., 1992. Statistical mechanics, Euler's equation, and Jupiter's Red Spot. Physical Review A 45, 2238–2359.
Montgomery, R.B., 1940. The present evidence on the importance of lateral mixing processes in the ocean. Bulletin of the AMS 21, 87–94.
Munk, W.H., Andersan, E.R., 1948. Notes on a theory of the thermocline. Journal of Marine Research 7, 276–295.
Munk, W.H., 1950. On the wind-driven ocean circulation. Journal of Meteorology 7, 3–29.

Munk, W., Wuncsh, C., 1998. Abyssal recipes II: energetics of tidal and wind mixing. Deep-Sea Research 45, 1977–2010.
Murray, R., 1996. Explicit generation of orthogonal grids for ocean models. Journal of Computational Physics 126, 251–273.
Murray, R., Reason, C.J.C., 2000. A curvilinear version of the Bryan–Cox ocean model. Journal of Computational Physics, submitted.
Murtugudde, R., Cane, M., Prasad, V., 1995. A reduced-gravity, primitive equation, isopycnal ocean GCM: formulation and simulations. Monthly Weather Review 123, 2864–2887.
Nakahara, M., 1990. Geometry, Topology, and Physics. Graduate Student Series in Physics, Adam Hilder Publisher, Bristol, England, p. 505.
Nazarenko, L., Sou, T., Eby, M., Holloway, G., 1997. The Arctic ocean/ice system, studied by contaminant modelling. Annals of Glaciology 25, 17–21.
Nurser, A.G., Killworth, P.D., Alderson, S.G., 2000. A new approach to the sigma-coordinate pressure gradient problem in a terrain-following bottom boundary layer model. International WOCE Newsletter, in press.
Oberhuber, J.M., 1993. Simulation of the atlantic circulation with a coupled sea ice-mixed layer-isopycnal general circulation model. Part I: model description. Journal of Physical Oceanography 23, 808–829.
O'Brien, J.J. (Ed.), 1986. Advanced Physical Oceanographic Numerical Modelling. NATO ASI Series. Reidel, Dortrecht, p. 607.
Olbers, D.J., Wenzel, M., Willebrand, J., 1985. The inference of North Atlantic circulation patterns from climatological hydrographic data. Reviews of Geophysics 23, 313–356.
Pacanowski, R.C., Gnanadesikan, A., 1998. Transient response in a *z*-level ocean model that resolves topography with partial-cells. Monthly Weather Review 126, 3248–3270.
Pacanowski, R.C., Griffies, S.M., 1999. The MOM 3 Manual. Geophysical Fluid Dynamics Laboratory/NOAA, Princeton, USA, p. 680.
Pacanowski, R.C., Philander, G., 1981. Parametrization of vertical mixing in numerical models of the tropical ocean. Journal of Physical Oceanography 11, 1442–1451.
Paiva, A.M., Chassignet, E.P., Mariano, A.J., 2000. Numerical simulations of the North Atlantic subtropical gyre: Sensitivity to boundary conditions and horizontal resolution. Deep-Sea Research, in press.
Pal, B.K., Holloway, G., 1996. Dynamics of circulation off the westcoast of Vancouver island. Continental Shelf Research 16, 1591–1607.
Park, Y.-G., Bryan, K., 2000. Comparison of thermally driven circulations from a depth-coordinate model and an isopycnal-layer model. Part I: Scaling-law sensitivity to vertical diffusivity. Journal of Physical Oceanography 30, 590–605.
Pedlosky, J., 1987. Geophysical Fluid Dynamics, second ed. Springer, New York, p. 710.
Philander, S.G., 1990. El Niño, La NiÑorth Atlantic, and the Southern Oscillation. International Geophysics Series vol. 46. Academic Press, New York, p. 289.
Philander, S.G.H., Pacanowski, R.C., Lau, N.-C., Nath, M.J., 1992. Simulation of ENSO with a global atmospheric GCM coupled to a high-resolution, tropical Pacific Ocean GCM. Journal of Climate 5, 308–329.
Phillips, N.A., 1957. A coordinate system having some special advantages for numerical forecasting. Journal of Meteorology 14, 184–185.
Polzin, K.L., Toole, J.M., Ledwell, G.R., Schmitt, R.W., 1997. Spatial variability of turbulent mixing in the abyssal ocean. Science 276, 93–96.
Pratt, L.J., Lundberg, P.A., 1991. Hydraulics of rotating strait and sill flow. Annual Review of Fluid Mechanics 23, 81–106.
Price, J.F., Weller, R.A., Pinkel, R., 1986. Diurnal cycling: observations and models of the upper ocean response to diurnal heating, cooling, and wind mixing. Journal of Geophysical Research 91, 8411–8427.
Price, J.F., Baringer, M., 1994. Outflows and deep water production by marginal seas. Progress in Oceanography 33, 161–2000.
Rahmstorf, S., 1993. A fast and complete convection scheme for ocean models. Ocean Modelling 101, 9–11.
Rahmstorf, S., 1995. Climate drift in an ocean model coupled to a simple, perfectly matched atmosphere. Climate Dynamics 11, 447–458.

Raynaud, S., Speich, S., Guilyardi, E., Madec, G., 2000. Impacts of the ocean lateral diffusion on the El Niño/southern oscillation-like variability of a global coupled general circulation model. Geophysical Research Letters 27, 3041.

Redi, M.H., 1982. Oceanic isopycnal mixing by coordinate rotation. Journal of Physical Oceanography 12, 1154–1158.

Rhines, P.B., Young, W.R., 1982. Homogenization of potential vorticity in planetary gyres. Journal of Fluid Mechanics 122, 347–367.

Robert, A.J., 1966. The integration of a low order spectral form of the primitive meteorological equations. Journal of the Meteorological Society of Japan, Series 2, 44, 237–245.

Robert, R., 1991. A maximum-entropy principle for two-dimensional perfect fluid dynamics. Journal of Statistical Physics 65, 531–553.

Robert, R., Sommeria, J., 1992. Relaxation towards a statistical equilibrium state in two-dimensional perfect fluid dynamics. Physical Review Letters 69, 2776–2779.

Roberts, M.J., Wood, R.A., Marsh, R., New, A.L., 1996. An intercomparison of a Bryan–Cox-type ocean model and an isopycnic ocean model. Part I: The Subpolar gyre and high-latitude processes. Journal of Physical Oceanography 26, 1495–1527.

Roberts, M.J., Wood, R.A., 1997. Topographic sensitivity studies with a Bryan–Cox-type ocean model. Journal of Physical Oceanography 27, 823–836.

Roberts, M.J., Marshall, D., 1998. Do we require adiabatic dissipation schemes in eddy-resolving ocean models?. Journal of Physical Oceanography 28, 2050–2063.

Robitaille, D.Y., Weaver, A.J., 1995. Validation of sub-grid-scale mixing schemes using CFCs in a global ocean model. Geophysical Research Letters 22, 2917–2920.

Roeckner, E., Oberhuber, J.M., Bacher, A., Christoph, M., Kirchner, I., 1996. ENSO variability and atmospheric response in a global coupled atmosphere–ocean GCM. Climate Dynamics 12, 737–754.

Rosati, A., Miyakoda, K., 1988. A general circulation model for upper ocean simulation. Journal of Physical Oceanography 18, 1601–1626.

Roullet, G., Madec, G., 2000. A variable volume formulation conserving salt content for a level OGCM: a fully nonlinear free surface. Journal of Geophysical Research, in press.

Russell, G.L., Lerner, J.A., 1981. A new finite differencing scheme for the tracer transport equation. Journal of Applied Meteorology 20, 1483–1498.

Russell, G.L., Miller, J.R., Rind, D., 1995. A coupled atmosphere–ocean model for transient climate change studies. Atmosphere–Ocean 33, 683–730.

Sadourny, R., Maynard, K., 1997. Formulations of lateral diffusion in geophysical fluid dynamics models. In: Lin, C.A., Laprise, R., Ritchie, H. (Eds.), Numerical Methods in Atmospheric and Oceanic Modelling. NRC Research Press, Toronto, pp. 547–556.

Sadourny, R., 1975. The dynamics of finite-difference models of the shallow water equations. Journal of Atmospheric Sciences 32, 680–689.

Salmon, R., Holloway, G., Hendershot, M.C., 1976. The equilibrium statistical-mechanics of simple quasi-geostrophic models. Journal of Fluid Mechanics 75, 691–703.

Schmitt, R., 1998. Double-diffusive convection. In: Chassignet, E.P., Verron, J. (Eds.), Ocean Modelling and Parameterization. NATO Advanced Study Institute, Kluwer Academic Publishers, Dordrecht, p. 451.

Schopf, P.S., Loughe, A., 1995. A reduced gravity isopycnal ocean model: Hindcasts of El Nio. Monthly Weather Review 123, 2839–2863.

Shchepetkin, A.F., McWilliams, J.C., 1998. Quasi-monotone advection schemes based on explicit locally adaptive dissipation. Monthly Weather Review 126, 1541–1580.

Semtner, A.J., 1974. An oceanic general circulation model with bottom topography. In: Numerical Simulation of Weather and Climate, Technical Report No. 9, UCLA Department of Meteorology.

Semtner, A.J., Mintz, Y., 1977. Numerical simulation of the gulf stream and mid-ocean eddies. Journal of Physical Oceanography 7, 208–230.

Sheng, J., Wright, D.G., Greatbatch, R.J., Dietrich, D.E., 1998. CANDIE: A new version of the DieCAST ocean circulation model. Journal of Atmospheric and Oceanic Technology 15, 1414–1432.

Siegel, A., Weiss, J.B., Toomre, J., McWilliams, J.C., Berloff, P.S., Yavneh, I., 1999. Eddies and vortices in ocean basin dynamics. Geophysical Research Letters, accepted.

Smagorinsky, J., 1963. General circulation experiments with the primitive equations: I. The basic experiment. Monthly Weather Review 91, 99–164.
Smagorinsky, J., 1993. Some historical remarks on the use of nonlinear viscosities. In: Galperin, B., Orszag, S.A. (Eds.), Large Eddy Simulation of Complex Engineering and Geophysical Flows. Cambridge University Press, Cambridge.
Smith, R.D., 1999. The primitive equations in the stochastic theory of adiabatic stratified turbulence. Journal of Physical Oceanography 29, 1865–1880.
Smith, R.D., Dukowicz, J.K., Malone, R.C., 1992. Parallel ocean general circulation modelling. Physica D 60, 38–61.
Smith, R.D., Kortas, S., Meltz, B., 1995. Curvilinear coordinates for global ocean models. Los Alamos Report LA-UR-95-1146.
Smith, R.D., Maltrud, F.O., Bryan, M.E., Hecht, M.W., 2000. Numerical simulation of the North Atlantic Ocean at 1/10°. Journal of Physical Oceanography 30, 1532–1561.
Smolarkiewicz, P.K., 1984. A fully multidimensional positive definite advection transport algorithm with small implicit diffusion. Journal of Computational Physics 54, 325–362.
Smolarkiewicz, P.K., Grabowski, W.W., 1990. The multidimensional positive definite advection transport algorithm: nonoscillatory option. Journal of Computational Physics 86, 355–375.
Solomon, H., 1971. On the representation of isentropic mixing in ocean models. Journal of Physical Oceanography 1, 233–234.
Sommeria, J., 1998. Statistical mechanics of potential vorticity. In: Chassignet, E.P., Verron, J. (Eds.), Ocean Modelling and Parameterization. NATO Advanced Study Institute, Kluwer Academic Publishers, Dordrecht, p. 451.
Song, Y.T., Haidvogel, D.B., 1994. A semi-implicit ocean circulation model using a generalized topography-following coordinate system. Journal of Computational Physics 115, 228–244.
Song, Y.T., Chao, Y., 2000. An embedded bottom boundary layer formulation for z-coordinate ocean models. Journal of Atmospheric and Oceanic Technology 17, 546–560.
Song, Y.T., Wright, D.G., 1998a. A general pressure gradient formulation for ocean models. Part I: scheme design and diagnostic analysis. Monthly Weather Review 126, 3213–3230.
Song, Y.T., Wright, D.G., 1998b. A general pressure gradient formulation for ocean models. Part I: scheme design and diagnostic analysis. Corrigentum. Monthly Weather Review 128, 2608–2609.
Song, Y.T., Wright, D.G., 1998c. A general pressure gradient formulation for ocean models. Part II: energy, momentum, and bottom torque consistency. Monthly Weather Review 126, 3231–3247.
Sou, T., Holloway, G., Eby, M., 1995. Topographic stress and Carribean Sea circulation. Journal of Geophysical Research 101, 16449–16453.
Stammer, D., 1998. On eddy characteristics, eddy transports, and mean flow properties. Journal of Physical Oceanography 28, 727–739.
Starr, V., 1945. A quasi-Lagrangian system of hydrodynamical equations. Journal of Meteorology 2, 227–237.
Sun, S., Bleck, R., Rooth, C.G.H., Dukowicz, J., Chassignet, E.P., Killworth, P., 1999. Inclusion of thermobaricity in isopycnic-coordinate ocean models. Journal of Physical Oceanography 29, 2719–2729.
Sutcliffe, R.C.A., 1947. A contribution to the problem of development. Quarterly Journal of the Royal Meteorological Society 73, 370–383.
Thuburn, J., 1996. Multidimensional flux-limited advection schemes. Journal of Computational Physics 123, 74–83.
Timmermann, A., Oberhuber, J.M., Backer, A., Esch, M., Latif, M., Roeckner, E., 1999. ENSO response to greenhouse warming. Nature 398, 694–696.
Toggweiler, J.R., Samuels, B., 1997. On the ocean's large-scale circulation near the limit of no vertical mixing. Journal of Physical Oceanography 28, 1832–1852.
Toole, J., 1998. Turbulent mixing in the ocean. In: Chassignet, E.P., Verron, J. (Eds.), Ocean Modelling and Parameterization. NATO Advanced Study Institute, Kluwer Academic Publishers, Dordrecht, p. 451.
Treguier, A.M., Held, I.M., Larichev, V.D., 1997. On the parameterization of quasi-geostrophic eddies in primitive equation ocean models. Journal of Physical Oceanography 27, 567–580.
Treguier, A.M., 1999. Evaluating eddy mixing coefficients from eddy-resolving ocean models: a case study. Journal of Marine Research 57, 89–108.
Turkington, B., 1999. Statistical equilibrium measures and coherent states in two-dimensional turbulence. Communications in Pure and Applied Mathematics LII, 781–809.

Vallis, G.K., 2000. Large-scale circulation and production of stratification: effects of winds, geometry, and diffusion. Journal of Physical Oceanography 30, 933–954.
Van Leer, B., 1979. Towards the ultimate conservative difference scheme. V. A second-order sequel to Godunov's method. Journal of Computational Physics 32, 101–136.
Veronis, G., 1975. The role of models in tracer studies. In: Numerical Models of Ocean Circulation. National Academy of Sciences, Washington, D.C.
Veronis, G., 1977. Use of tracers in circulation studies. In: Goldberg, E.D., McCasve, I.N., O'Brien, J.J., Steele, J.H. (Eds.), The Sea. Wiley-Interscience, New York.
Visbeck, M., Marshall, J., Haine, T., Spall, M., 1997. Specification of eddy transfer coefficients in coarse resolution ocean circulation models. Journal of Physical Oceanography 27, 381–402.
Wajsowicz, R.C., 1986. Free planetary waves in finite-difference numerical models. Journal of Physical Oceanography 16, 773–789.
Wajsowicz, R.C., 1993. A consistent formulation of the anisotropic stress tensor for use in models of the large-scale ocean circulation. Journal of Computational Physics 105, 333–338.
Wajsowicz, R.C., Gill, A.E., 1986. Adjustment of the ocean under buoyancy forces, Part I, The role of Kelvin waves. Journal of Physical Oceanography 16, 2097–2114.
Wardle, R., Marshall, J., 1999. Representation of eddies in primitive equation models by a PV flux. Preprint.
Weaver, A.J., Eby, M., 1997. On the numerical implementation of advection schemes for use in conjunction with various mixing parameterizations in the GFDL ocean model. Journal of Physical Oceanography 27, 369–377.
Webb, D.J., 1992. The equation of state algorithms used by the FRAM model. Internal Document No. 313, Institute of Oceanographic Sciences, Deacon Laboratory.
Webb, D.J., 1995. The vertical advection of momentum in Bryan–Cox–Semtner ocean general circulation models. Journal of Physical Oceanography 25, 3186–3195.
Webb, D.J., 1996. An ocean model code for array processor computers. Computers and Geophysics 22, 569–578.
Webb, D.J., Coward, A.C., de Cuevas, B.A., Gwilliam, C.S., 1997. A multiprocessor ocean general circulation model using message passing. Journal of Atmospheric and Oceanic Technology 14, 175–183.
Webb, D.J., de Cuevas, B.A., Coward, A.C., 1998a. The first main run of the OCCAM global ocean model. Southampton Oceanography Centre, Internal Document No. 34.
Webb, D.J., de Cuevas, B.A., Richmond, C.S., 1998b. Improved advection schemes for ocean models. Journal of Atmospheric and Oceanic Technology 15, 1171–1187.
Weichman, P.B., Petrich, D.M., 2000. Shallow water equilibria. Preprint available from `http://xxx.lanl.gov/abs/physics/0008236`.
Whitehead, J.A., 1998. Topographic control of ocean flows in deep passages and straits. Reviews of Geophysics and Space Physics 36, 423–440.
Wiebe, E.C., Weaver, A.J., 1999. On the sensitivity of global warming experiments to the parameterisation of sub-grid-scale ocean mixing. Climate Dynamics 15, 875–893.
Willebrand, J., Barnier, B., Böning, C., Dieterich, C., Killworth, P.D., LeProvost, C., Jia, Y., Molines, J.-M., New, A.L., 2000. Circulation characteristics in three eddy – permitting models of the North Atlantic. Progress in Oceanography, in press.
Williams, G.P., 1972. Friction term formulation and convective instability in a shallow atmosphere. Journal of Atmospheric Sciences 29, 870–876.
Winton, M., Hallberg, R.W., Gnanadesikan, A., 1998. Simulation of density-driven frictional downslope flow in z-coordinate ocean models. Journal of Physical Oceanography 28, 2163–2174.
Wolff, J.-O., Maier-Reimer, E., Legutke, S., 1997. The Hamburg Ocean Primitive Equation Model HOPE. DKRZ Technical Report No. 13.
Wright, D.G., 1997a. An equation of state for use in ocean models: Eckart's formula revisited. Journal of Atmospheric and Oceanic Technology 14, 735–740.
Wright, D.K., 1997b. A new eddy mixing parameterization in an ocean general circulation model. International WOCE Newsletter 26, 27–29.
Wunsch, C., Zlotnicki, V., 1999. Measuring ocean bottom pressure changes from space. Report of a meeting. Available from `http://puddle.mit.edu/~cwunsch/lndmtgwithfig/lndmtgwithfig.html`.

Yukimoto, S., Endoh, M., Kitamura, Y., Kitoh, A., Motoi, T., Noda, A., Tokioka, T., 1996. Interannual and interdecadal variabilities in the Pacific in an MRI coupled GCM. Climate Dynamics 12, 667–683.

Zalesak, S.T., 1979. Fully multidimensional flux-corrected transport algorithms for fluids. Journal of Computational Physics 31, 335–362.